

University of Montana

ScholarWorks at University of Montana

Graduate Student Theses, Dissertations, &
Professional Papers

Graduate School

1998

A novel methodology for functionalizing heterocycles using electron-deficient bonding to triosmium clusters

Brian R. Bergman

The University of Montana

Follow this and additional works at: <https://scholarworks.umt.edu/etd>

Let us know how access to this document benefits you.

Recommended Citation

Bergman, Brian R., "A novel methodology for functionalizing heterocycles using electron-deficient bonding to triosmium clusters" (1998). *Graduate Student Theses, Dissertations, & Professional Papers*. 10545.
<https://scholarworks.umt.edu/etd/10545>

This Dissertation is brought to you for free and open access by the Graduate School at ScholarWorks at University of Montana. It has been accepted for inclusion in Graduate Student Theses, Dissertations, & Professional Papers by an authorized administrator of ScholarWorks at University of Montana. For more information, please contact scholarworks@mso.umt.edu.

INFORMATION TO USERS

This manuscript has been reproduced from the microfilm master. UMI films the text directly from the original or copy submitted. Thus, some thesis and dissertation copies are in typewriter face, while others may be from any type of computer printer.

The quality of this reproduction is dependent upon the quality of the copy submitted. Broken or indistinct print, colored or poor quality illustrations and photographs, print bleedthrough, substandard margins, and improper alignment can adversely affect reproduction.

In the unlikely event that the author did not send UMI a complete manuscript and there are missing pages, these will be noted. Also, if unauthorized copyright material had to be removed, a note will indicate the deletion.

Oversize materials (e.g., maps, drawings, charts) are reproduced by sectioning the original, beginning at the upper left-hand corner and continuing from left to right in equal sections with small overlaps. Each original is also photographed in one exposure and is included in reduced form at the back of the book.

Photographs included in the original manuscript have been reproduced xerographically in this copy. Higher quality 6" x 9" black and white photographic prints are available for any photographs or illustrations appearing in this copy for an additional charge. Contact UMI directly to order.

UMI

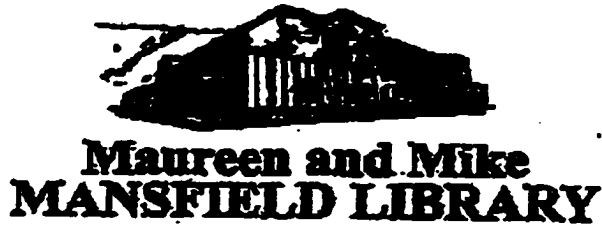
A Bell & Howell Information Company
300 North Zeeb Road, Ann Arbor MI 48106-1346 USA
313/761-4700 800/521-0600

NOTE TO USERS

The original manuscript received by UMI contains pages with slanted print. Pages were microfilmed as received.

This reproduction is the best copy available

UMI



The University of
Montana

Permission is granted by the author to reproduce this material in its entirety, provided that this material is used for scholarly purposes and is properly cited in published works and reports.

****Please check "Yes" or "No" and provide signature****

Yes, I grant permission

No, I do not grant permission

Author's Signature:

Raymond Bugman

Date:

10-16-98

Any copying for commercial purposes or financial gain may be undertaken only with the author's explicit consent.

**A Novel Methodology for Functionalizing Heterocycles Using
Electron Deficient Bonding to Triosmium Clusters.**

By

Brian R. Bergman

B.Sc., University of Wisconsin-Stevens Point, Stevens Point, Wisconsin

Presented in partial fulfillment of the requirements

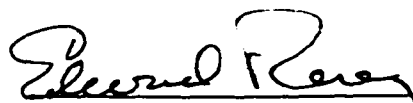
for the degree of


Doctor of Philosophy

University of Montana

1998

Approved by


Chairman, Board of Examiners


Dean, Graduate School

10-20-98
Date

UMI Number: 9914169

**Copyright 1999 by
Bergman, Brian Richard**

All rights reserved.

**UMI Microform 9914169
Copyright 1999, by UMI Company. All rights reserved.**

**This microform edition is protected against unauthorized
copying under Title 17, United States Code.**

UMI
300 North Zeeb Road
Ann Arbor, MI 48103

A Novel Methodology for Functionalizing Heterocycles Using Electron Deficient Bonding to Triosmium Clusters (p151)

Director: Edward Rosenberg

ER

A new synthetic methodology for the addition of carbon-based nucleophiles to the carbocyclic ring of quinolines has been developed which is based on the electron deficient bonding of the C(8) carbon and the protective coordination of the nitrogen atom to the metal core in the complexes $\text{Os}_3(\text{CO})_9(\mu_3-\eta^2\text{-C}_9\text{H}_5(\text{R})\text{N})(\mu\text{-H})(\mathbf{35a}, \text{R}=\text{H}; \mathbf{35b}, \text{R}=3\text{-CO}_2\text{CH}_3; \mathbf{35c}, \text{R}=3\text{-NH}_2; \mathbf{35d}, \text{R}=4\text{-CH}_3; \mathbf{35e}, \text{R}=4\text{-Cl}; \mathbf{35f}, \text{R}=4\text{-OCH}_3; \mathbf{35g}, \text{R}=4\text{-NH}_2; \mathbf{35h}, \text{R}=4\text{-CO}_2\text{CH}_3; \mathbf{35i}, \text{R}=5\text{-F}; \mathbf{35j}, \text{R}=5\text{-Cl}; \mathbf{35k}, \text{R}=5\text{-Br}; \mathbf{35l}, \text{R}=5\text{-NH}_2; \mathbf{35m}, \text{R}=6\text{-CH}_3; \mathbf{35n}, \text{R}=6\text{-Cl}; \mathbf{35o}, \text{R}=6\text{-OCH}_3; \mathbf{35p}, \text{R}=6\text{-CO}_2\text{CH}_3; \mathbf{35q}, \text{R}=6\text{-NH}_2; \mathbf{35r}, \text{R}=6\text{-OH})$. Compound $\mathbf{35a}$ reacts with a wide range of carbanions ($\text{R}'\text{Li}$: $\text{R}'=\text{Me}, ^t\text{Bu}, ^i\text{Bu}, \text{Bz}, \text{Ph}, \text{CH}=\text{CH}_2, \text{C}_2(\text{CH}_2)_3\text{CH}_3, \text{CH}_2\text{CN}, (\text{CH}_3)_2\text{CCN}, \text{-CHS}(\text{CH}_2)_2\text{S}^-; \text{CH}_2\text{CO}_2^i\text{Bu}, \text{R}'\text{MgBr}, \text{CH}_2\text{CH}=\text{CH}_2$) to give the nucleophilic addition products $\text{Os}_3(\text{CO})_9(\mu_3-\eta^3\text{-C}_9\text{H}_7(5\text{-R}')\text{N})(\mu\text{-H})(\mathbf{37a-37l})$, after quenching with trifluoroacetic acid, in isolated yields of 25-86%. Substitution at the 3- or 4-position is well tolerated with $\mathbf{35b-35h}$ giving the expected nucleophilic addition products $\text{Os}_3(\text{CO})_9(\mu_3-\eta^3\text{-C}_9\text{H}_6(3 \text{ or } 4\text{-R})(5\text{-R}')\text{N})(\mu\text{-H})(\mathbf{38b}, \text{R}=3\text{-CO}_2\text{CH}_3, \text{R}'=\text{CH}_2\text{CO}_2^i\text{Bu}; \mathbf{38c}, \text{R}=3\text{-NH}_2, \text{R}'=\text{C}(\text{CH}_3)_2\text{CN}; \mathbf{38d}, \text{R}=4\text{-CH}_3, \text{R}'=\text{C}(\text{CH}_3)_2\text{CN}; \mathbf{38e}, \text{R}=4\text{-Cl}, \text{R}'=\text{CH}_2\text{CO}_2^i\text{Bu}; \mathbf{38e}, \text{R}=4\text{-Cl}, \text{R}'=\text{C}(\text{CH}_3)_2\text{CN}; \mathbf{38f}, \text{R}=4\text{-OCH}_3, \text{R}'=\text{CH}_2\text{CO}_2^i\text{Bu}; \mathbf{38g}, \text{R}=4\text{-NH}_2, \text{R}'=\text{C}(\text{CH}_3)_2\text{CN}; \mathbf{38h}, \text{R}=4\text{-CO}_2\text{CH}_3, \text{R}'=\text{C}(\text{CH}_3)_2\text{CN}; \mathbf{38i}, \text{R}=4\text{-CO}_2\text{CH}_3, \text{R}'=\text{C}(\text{CH}_3)_2\text{CN})$. The 6-substituted derivatives $\mathbf{35m}$ and $\mathbf{35n}$ give >95% of the *cis*-diastereomer, ($\text{Os}_3(\text{CO})_9(\mu_3-\eta^3\text{-C}_9\text{H}_6(5\text{-R}')(6\text{-R})\text{N})(\mu\text{-H})(\mathbf{38n}, \text{R}=\text{Cl}, \text{R}'=\text{C}(\text{CH}_3)_2\text{CN}; \mathbf{38m}, \text{R}=\text{CH}_3, \text{R}'=\text{C}(\text{CH}_3)_2\text{CN})$. The stereochemistry was verified by a solid state structure in the case of *cis* $\mathbf{38m}$. The stereochemistry is preserved even in the case of less bulky carbanions (*cis*- $\mathbf{38m}'$, $\text{R}=\text{CH}_3, \text{R}'=\text{CH}_3$). In the case of $\mathbf{38n}$, a second product is obtained $\text{Os}_3(\text{CO})_9(\mu_3-\eta^2\text{-C}_9\text{H}_5(6\text{-Cl})(5\text{-C}(\text{CH}_3)_2\text{CN})\text{N})(\mu\text{-H})_2(\mathbf{39n})$ which is the result of protonation at the metal core and rearrangement of the carbocyclic ring. The solid state structure of $\mathbf{39n}$ is reported. The *trans*-diastereomer of the addition products $\mathbf{38m}$ and $\mathbf{38m}'$ is obtained when compound $\mathbf{1a}$ is reacted with $\text{R}'\text{Li}(\text{R}'=\text{C}(\text{CH}_3)_2\text{CN}, \text{CH}_3)$ and then quenched with $(\text{CH}_3\text{O})_2\text{SO}_2$. A solid state structure *trans*- $\mathbf{38m}$ is reported. Acetic anhydride can also be used as the quenching electrophile for the intermediate anions generated from $\text{R}'\text{Li}(\text{R}'=\text{CH}_3)$, yielding *trans*- $\text{Os}_3(\text{CO})_9(\mu_3-\eta^3\text{-C}_9\text{H}_6(6\text{-CH}_3\text{CO})(5\text{-CH}_3)\text{N})(\mu\text{-H})(\mathbf{38z})$. Nucleophilic addition occurs across the 3-4 bond in the case of $\mathbf{35i-35l}$ where the 5-position is blocked. The addition products, type $\mathbf{37}$ and $\mathbf{38}$ can be rearomatized by reaction with DBU/DDQ or by reaction of the intermediate anion with trityl cation or DDQ. The resulting rearomatized complexes can be cleanly cleaved from the cluster by reflux in acetonitrile under a CO atmosphere yielding the functionalized quinoline and $\text{Os}_3(\text{CO})_{12}$ as the only two products. Unlike the π -bound metal arene complexes which undergo nucleophilic attack at the ring with heteroatom nucleophiles, the triosmium clusters coordinate these nucleophiles to the metal core, but at the ring with carbanions. This amphiphilic behavior could prove very useful. The structural features of the compounds reported and the mechanistic implications of the reported transformations are discussed and compared with the previously reported activation of aromatic systems towards nucleophiles by π -complexation.

ACKNOWLEDGMENTS

I would like to thank Dr. Edward Rosenberg for his guidance, friendship, and support during the course of this work. I would also like to thank Dr. Charles Thompson for being a valuable member of my committee, and for the many stimulating discussions related to this project. A special thanks goes to Dr. Kenneth Hardcastle and his group at California State University Northridge, for their excellent work determining all the solid state structures.

To my parents Edward and Carolyn Bergman, I extend the deepest appreciation and gratitude for their love and support. To my wife Christy, I am very grateful you have become a part of my life, and I thank you for your patience and understanding during the preparation of this thesis.

I would also like to thank the University of Montana and the National Science Foundation for supporting this research project.

**To my wife Christy and my parents
Edward and Carolyn Bergman for their love
and support.**

Table of Contents

	page
Authorization to Submit Dissertation	i
Abstract.....	ii
Acknowledgements.....	iii
Dedication.....	iv
Table of Contents.....	v
Lists of Compounds.....	xi
List of Figures.....	xvi
List of Tables.....	xvii
Chapter One: Introduction	
1.1 General Background for Transition Metal-Arene Complexes.....	1
1.2 Arene-Metal Complexes as Substrates for Nucleophiles.....	3
1.2.1 Nucleophilic Addition / Oxidation on Metal Arene Complexes....	4
1.2.2 Nucleophilic Addition / Protonation on Metal Arene Complexes..	5
1.2.3 Nucleophilic Addition / Elimination on Metal Arene Complexes	5
1.3 Effects of Metal Complexation on Arenes.....	6
1.3.1 Preparation of (Arene)-Cr(CO) ₃ Complexes.....	7
1.3.2 Preparation of (Arene)-FeCp ⁺ Complexes.....	7
1.3.3 Preparation of (Arene)-Mn(CO) ₃ Complexes.....	9
1.4 Nucleophilic Reactivity of η^6 -(Benzene)-Cr(CO) ₃	10
1.5 Nucleophilic Substitution with Heteroatom Nucleophiles.....	12

1.6	Regioselective Nucleophilic Addition on Metal Arene Complexes.....	13
1.6.1	Regioselectivity on (benzene)-Cr(CO) ₃ Complexes.....	13
1.6.2	Regioselectivity on (indole)-Cr(CO) ₃ Complexes.....	13
1.7	Ring Lithiation on (arene)-Cr(CO) ₃ Complexes.....	15
1.8	Stereoselective Carbon-Carbon Bond Formation to η^6 -C ₆ H ₆ -Cr(CO) ₃	16
1.9	Asymmetric Synthesis Using Homo <i>o</i> -Anisaldehyde-Cr(CO) ₃ as a Chiral Auxiliary.....	18
1.10	References	19

Chapter Two: The Synthesis of Electron Deficient Quinoline Triosmium

	Clusters.....	23
2.1	Introduction and Background of Quinolines Complexed to Transition Metals.....	23
2.2	Results and Discussion.....	29
2.2.1	The Synthesis of Electron Deficient Monosubstituted Analogs of 35a (Os) ₃ (CO) ₉ (μ_3 - η^2 -C ₉ H ₆ N)(μ -H)	29
2.3	Experimental Section	38
2.3.1	Materials and General Considerations	38
2.3.2	Preparation of Electron Deficient Monosubstituted Quinoline Complexes (Os) ₃ (CO) ₉ (μ_3 - η^2 -C ₉ H ₅ (R)N)(μ -H) 35a-35r	39
2.3.3	Analytical and Spectroscopic Data for 35a-35r	40
2.4	X-Ray Structure Determination	44
2.5	References	46

Chapter Three:	Reactivity of Carbanions with $(Os)_3(CO)_9(\mu_3-\eta^2-C_9H_6N)(\mu-H)$ and its Analogs	49
3.1	Results and Discussion.....	49
3.1.1	Reactivity of Carbanions with $Os_3(CO)_9(\mu_3-\eta^2-C_9H_6N)(\mu-H)$ 35a	49
3.2	Reactions of 3-, and 4- Monosubstituted Quinoline Complexes	56
3.3	Stereospecific Nucleophilic Addition Across the C(5)-C(6) bond.....	58
3.3.1	The Reaction of $[(Os)_3(CO)_9(\mu_3-\eta^2-C_9H_5N)(6-Cl)(\mu-H)]$ 35n with LiR ($R=C(CH_3)_2CN$)	58
3.3.2	The Reaction of $[(Os)_3(CO)_9(\mu_3-\eta^2-C_9H_5N)(6-CH_3)(\mu-H)]$ 35m with LiR ($R=C(CH_3)_2CN, CH_3$)	63
3.3.3	Synthesis of $[(Os)_3(CO)_9(\mu_3-\eta^3-C_9H_6(5-R)(6-CH_3)N)(\mu-H)]$ trans-38m, trans-38m', trans-38z , ($R=C(CH_3)_2CN, CH_3, CH_3CO$)	67
3.4	Reactivity of 5-Substituted Complexes: Addition Across the C(3)-C(4) Quinoline Bond	71
3.5	Rearomatization of the Nucleophilic Addition Products	75
3.6	Cleavage of the Functionalized Quinoline from the Cluster	78
3.7	Conclusions	81
3.8	Experimental Section	83
3.8.1	Materials and General Considerations	83
3.8.2	Preparation of complexes $[(Os)_3(CO)_9(\mu_3-\eta^3-C_9H_7(R')N)(\mu-H)]$ (37a-37l), and $[(Os)_3(CO)_9(\mu_3-\eta^2-C_9H_6(R)(R')N)(\mu-H)]$ (38b,	

	38c, 38d, 38e, 38e', 38f, 38f', 38g, 38h, 38i, cis-38n, 39n, cis-38m, cis-38m', cis-38p, 35s, 35t, 39l, 39l', 39j, 39j', 39k, 39k', 39l, and 39l')	84
3.8.3	Preparation of $[(Os)_3(CO)_9(\mu_3-\eta^3-C_9H_6(6-R)(5-R')N)(\mu-H)]$ (trans-38m, trans-38m', trans-38z)	95
3.8.4	Rearomatization of Nucleophilic addition Products with Ph_3CBF_4 : Preparation of $[(Os)_3(CO)_9(\mu_3-\eta^2-C_9H_5(R')N)(\mu-H)]$ (R'=n-Bu, 35u ; R'=CH ₂ CO ₂ ^t Bu, 35v)	97
3.8.5	Rearomatization of Nucleophilic Addition Products with 2,2-dichloro-3,3-dicyanoquinone (DDQ): Preparation of $[(Os)_3(CO)_9(\mu_3-\eta^2-C_9H_4(5-CH_3)(6-CH_3)N)(\mu-H)]$ 35w	98
3.8.6	The Reaction of $[(Os)_3(CO)_9(\mu_3-\eta^3-C_9H_7(5-CH_3)N)(\mu-H)]$ 37a with 1,8-Diazabicyclo[5.4.0]undec-7-ene (DBU) / 2,2-dichloro-3,3-dicyanoquinone (DDQ)	99
3.8.7	Cleavage of the Quinoline Ligand from the Triosmium Cluster...99	
3.9	X-Ray Structure Determination of cis-38m, trans-38m, 39n, and 39j	100
3.10	References	101

Chapter Four:	Reaction of $(Os)_3(CO)_9(\mu_3-\eta^2-C_9H_6N)(\mu-H)$ with Heteroatom Nucleophiles and Protic Acids	104
4.1	Introduction	104

4.2	Results and Discussion	106
4.2.1	Reactions with Amines	107
4.2.2	Reaction with Protic Acids	115
4.3	Conclusions	117
4.4	Experimental Section	120
4.4.1	Materials and General Considerations	120
4.5	Evaluation of Isomer Ratios and Equilibrium Constants	121
4.6	References	122
Chapter Five: Unresolved Problems and Future Work.....		123
5.1	Reaction of $\text{Os}_3(\text{CO})_9(\mu^3-\eta^2-\text{C}_9\text{H}_5(4\text{-Cl})\text{N})(\mu\text{-H})$ with Excess Lithium t-Butyl Acetate to Form Complex 53	123
5.2	Reaction of $\text{Os}_3(\text{CO})_9(\mu^3-\eta^2-\text{C}_9\text{H}_5(5\text{-F})\text{N})(\mu\text{-H})$ 35i with Lithium n- Butoxide	129
5.3	Carbon C(6) Hydroxylation of Complex 35m : Preparation of the Phenolic Complex $\text{Os}_3(\text{CO})_9(\mu^3-\eta^3-\text{C}_9\text{H}_5(5\text{-}^t\text{Bu})(6\text{-CH}_3)(6\text{-OH})\text{N})(\mu\text{-H})$ 55	133
5.4	The Restricted σ - π -Vinyl Interchange on Complexes $\text{Os}_3(\text{CO})_9(\mu^3-\eta^2\text{-}$ $\text{C}_9\text{H}_5(5\text{-}^t\text{BuOAc})(6\text{-Cl})\text{N})(\mu\text{-H})$ <i>cis</i> - 56	138
5.5	Attempted Two-Step Lithiation Followed by Electrophilic Trapping ...	141
5.6	Double Alkylation at Carbon C(5) and the Ester Carbonyl: Reaction of 35h with Excess Carbanion	143
5.7	Experimental Section	145
5.7.1	Materials and General Considerations	145

5.8	Preparation of Complexes 53-57	146
5.9	Analytical and Spectroscopic Data for 53-57	147
5.10	X-Ray Structure Determination of 53-55	149
5.11	References	150

List of Compounds

		Page
1	$\eta^6\text{-}(\text{C}_6\text{H}_5\text{X})\text{-M}(\text{CO})_3$	4
2	$\eta^5\text{-}(\text{C}_6\text{H}_5\text{XR})\text{-M}^-(\text{CO})_3$	4
3	$\eta^6\text{-}(\text{C}_6\text{H}_5\text{R})\text{-M}(\text{CO})_3$	4
4	$\eta^4\text{-}2,4\text{-cyclohexadiene-M}(\text{CO})_3$	4
5	$\eta^4\text{-}1,3\text{-cyclohexadiene-M}(\text{CO})_3$	4
6	$[\text{C}_6\text{H}_5\text{-R}]$	4
7	$\eta^6\text{-}(\text{C}_6\text{H}_5\text{-R})\text{-Cr}(\text{CO})_3$	7
8	$\eta^6\text{-}(\text{C}_6\text{H}_5\text{-R})\text{-Mn}^+(\text{CO})_3$	7
9	$(\eta^6\text{-C}_6\text{H}_6)\text{-Fe}^+(\eta^5\text{-C}_5\text{H}_5)$	7
10	$\eta^6\text{-}(\text{C}_6\text{H}_5\text{-Cl})\text{-Cr}(\text{CO})_3$	10
11	$\eta^6\text{-}(\text{C}_6\text{H}_5\text{-OCH}_3)\text{-Cr}(\text{CO})_3$	11
12	$\eta^6\text{-}(\text{C}_6\text{H}_5\text{-Cl})\text{-Mn}^+(\text{CO})_3$	12
13	$\eta^6\text{-}(\text{C}_6\text{H}_5\text{-R})\text{-Mn}^+(\text{CO})_3$	12
14	$\eta^6\text{-}(\text{C}_6\text{H}_5\text{-Cl})\text{-Fe}(\text{C}_5\text{H}_5)$	12
15	$\eta^6\text{-}(\text{C}_6\text{H}_5\text{-R,Cl})\text{-Fe}(\text{C}_5\text{H}_5)$	12
16	$\eta^6\text{-}(\text{C}_6\text{H}_5\text{-R})\text{-Fe}^+(\text{C}_5\text{H}_5)$	12
17	$\eta^6\text{-}(\text{C}_6\text{H}_5\text{-X})\text{-Cr}(\text{CO})_3$	13
18	$\eta^6\text{-}(\text{indole})\text{-Cr}(\text{CO})_3$	14
19	$\eta^6\text{-}(\text{C}_6\text{H}_6)\text{-Cr}^-(\text{R})(\text{CO})_3$	15
20	$\eta^6\text{-}(\text{C}_6\text{H}_5\text{-Li})\text{-Cr}(\text{CO})_3$	15
21	$\eta^6\text{-}(\text{C}_6\text{H}_5\text{-E})\text{-Cr}(\text{CO})_3$	16
22	$\eta^5\text{-}(\text{C}_6\text{H}_5\text{-R})\text{-Cr}^-(\text{R})(\text{CO})_3$	18
23	$\eta^5\text{-}(\text{C}_6\text{H}_5\text{-R})\text{-Cr}^-(\text{R})(\text{CO})_3$	18
24	$\eta^6\text{-}(\textit{o}\text{-anisaldehyde})\text{-Cr}(\text{CO})_3(\text{s})\text{-}(+)$	19
25	$\eta^6\text{-}(\text{S,S})\text{-}(\textit{-})(\textit{o}\text{-methoxy-1-phenyl-ethanol})\text{-Cr}(\text{CO})_3$	19

26'	$[\eta^5\text{-CpRh}(\text{NCMe})_2\text{-}\eta^1\text{-(C}_{10}\text{H}_9\text{N})]^2+$	24
27'	$[\eta^5\text{-CpRh}(\text{NCMe})_2\text{-}\eta^6\text{-(C}_{10}\text{H}_9\text{N})]^2+$	24
28'	$[(\eta^5\text{-(C}_5\text{H}_5)\text{Re}(\text{NO})(\text{PPh}_3)\text{-}(\text{NC}_9\text{H}_7))]^+$	24
29'	$[(\eta^5\text{-(C}_5\text{H}_5)\text{Re}(\text{NO})(\text{PPh}_3)\text{-}(\text{NC}_9\text{H}_6\text{R}))]^+$	24
29''	$[(\eta^5\text{-(C}_5\text{H}_5)\text{Re}(\text{NO})(\text{PPh}_3)\text{-}(\text{NC}_9\text{H}_6\text{R}))]^+$	24
30	$\text{Os}_3(\text{CO})_9(\mu\text{-H}_2)(\mu\text{-}\eta^2\text{-C=N(CH}_2)_3\text{)Br}$	26
31	$\text{Os}_3(\text{CO})_{10}(\mu\text{-}\eta^2\text{-C=N(CH}_2)_3)(\mu\text{-}\eta^1\text{-C}_6\text{H}_5)$	26
32	$\text{Os}_3(\text{CO})_8(\mu\text{-}\eta^2\text{-C=N(CH}_2)_3)(\mu\text{-}\eta^1\text{:}\eta^6\text{C}_6\text{H}_5)$	26
33	$\text{Os}(\text{CO})_{10}(\mu\text{-}\eta^2\text{-C}_9\text{H}_6\text{N})(\mu\text{-H})$	27
33'	$\text{Ru}(\text{CO})_{10}(\mu\text{-}\eta^2\text{-C}_9\text{H}_6\text{N})(\mu\text{-H})$	27
34	$\text{Os}(\text{CO})_{10}(\mu\text{-}\eta^2\text{-C}_9\text{H}_6\text{N})(\mu\text{-H})$	27
35a	$\text{Os}(\text{CO})_9(\mu_3\text{-}\eta^2\text{-C}_9\text{H}_6\text{N})(\mu\text{-H})$	27
35b	$\text{Os}(\text{CO})_9(\mu_3\text{-}\eta^2\text{-C}_9\text{H}_6\text{RN})(\mu\text{-H})$ (R=3-CO ₂ CH ₃)	27
35c	$\text{Os}(\text{CO})_9(\mu_3\text{-}\eta^2\text{-C}_9\text{H}_6\text{RN})(\mu\text{-H})$ (R=3-NH ₂)	27
35d	$\text{Os}(\text{CO})_9(\mu_3\text{-}\eta^2\text{-C}_9\text{H}_6\text{RN})(\mu\text{-H})$ (R=4-CH ₃)	27
35e	$\text{Os}(\text{CO})_9(\mu_3\text{-}\eta^2\text{-C}_9\text{H}_6\text{RN})(\mu\text{-H})$ (R=4-Cl)	27
35f	$\text{Os}(\text{CO})_9(\mu_3\text{-}\eta^2\text{-C}_9\text{H}_6\text{RN})(\mu\text{-H})$ (R=4-OCH ₃)	27
35g	$\text{Os}(\text{CO})_9(\mu_3\text{-}\eta^2\text{-C}_9\text{H}_6\text{RN})(\mu\text{-H})$ (R=4-NH ₂)	27
35h	$\text{Os}(\text{CO})_9(\mu_3\text{-}\eta^2\text{-C}_9\text{H}_6\text{RN})(\mu\text{-H})$ (R=4-CO ₂ CH ₃)	27
35i	$\text{Os}(\text{CO})_9(\mu_3\text{-}\eta^2\text{-C}_9\text{H}_6\text{RN})(\mu\text{-H})$ (R=5-F)	27
35j	$\text{Os}(\text{CO})_9(\mu_3\text{-}\eta^2\text{-C}_9\text{H}_6\text{RN})(\mu\text{-H})$ (R=5-Cl)	27
35k	$\text{Os}(\text{CO})_9(\mu_3\text{-}\eta^2\text{-C}_9\text{H}_6\text{RN})(\mu\text{-H})$ (R=5-Br)	27
35l	$\text{Os}(\text{CO})_9(\mu_3\text{-}\eta^2\text{-C}_9\text{H}_6\text{RN})(\mu\text{-H})$ (R=NH ₂)	27
35m	$\text{Os}(\text{CO})_9(\mu_3\text{-}\eta^2\text{-C}_9\text{H}_6\text{RN})(\mu\text{-H})$ (R=6-CH ₃)	27
35n	$\text{Os}(\text{CO})_9(\mu_3\text{-}\eta^2\text{-C}_9\text{H}_6\text{RN})(\mu\text{-H})$ (R=6-Cl)	27
35o	$\text{Os}(\text{CO})_9(\mu_3\text{-}\eta^2\text{-C}_9\text{H}_6\text{RN})(\mu\text{-H})$ (R=6-OCH ₃)	27
35p	$\text{Os}(\text{CO})_9(\mu_3\text{-}\eta^2\text{-C}_9\text{H}_6\text{RN})(\mu\text{-H})$ (R=6-CO ₂ CH ₃)	27

35q	$\text{Os}(\text{CO})_9(\mu_3-\eta^2-\text{C}_9\text{H}_6\text{RN})(\mu\text{-H})$ (R=6-NH ₂)	27
35r	$\text{Os}(\text{CO})_9(\mu_3-\eta^2-\text{C}_9\text{H}_6\text{RN})(\mu\text{-H})$ (R=6-OH)	27
35s	$\text{Os}(\text{CO})_9(\mu_3-\eta^2-\text{C}_9\text{H}_4(5\text{-CH}_2\text{CO}_2^t\text{Bu})(6\text{-OCH}_3)\text{N})(\mu\text{-H})$	75
35t	$\text{Os}(\text{CO})_9(\mu_3-\eta^2-\text{C}_9\text{H}_4(5\text{-CH}_2\text{CO}_2^t\text{Bu})(6\text{-OH})\text{N})(\mu\text{-H})$	75
36a	$\text{Os}(\text{CO})_9(\mu_3-\eta^2-\text{C}_9\text{H}_6(5\text{-CH}_3)\text{N})(\mu\text{-H})$	51
37b	$\text{Os}(\text{CO})_9(\mu_3-\eta^2-\text{C}_9\text{H}_6(5\text{-}^n\text{Bu})\text{N})(\mu\text{-H})$	51
37c	$\text{Os}(\text{CO})_9(\mu_3-\eta^2-\text{C}_9\text{H}_6(5\text{-}^t\text{Bu})\text{N})(\mu\text{-H})$	51
37d	$\text{Os}(\text{CO})_9(\mu_3-\eta^2-\text{C}_9\text{H}_6(5\text{-CH}_2\text{C}_6\text{H}_5)\text{N})(\mu\text{-H})$	51
37e	$\text{Os}(\text{CO})_9(\mu_3-\eta^2-\text{C}_9\text{H}_6(5\text{-C}_6\text{H}_5)\text{N})(\mu\text{-H})$	51
37f	$\text{Os}(\text{CO})_9(\mu_3-\eta^2-\text{C}_9\text{H}_6(5\text{-CH}=\text{CH}_2)\text{N})(\mu\text{-H})$	51
37g	$\text{Os}(\text{CO})_9(\mu_3-\eta^2-\text{C}_9\text{H}_6(5\text{-C}_2(\text{CH}_3)_3\text{CH}_3)\text{N})(\mu\text{-H})$	51
37h	$\text{Os}(\text{CO})_9(\mu_3-\eta^2-\text{C}_9\text{H}_6(5\text{-CH}_2\text{CN})\text{N})(\mu\text{-H})$	51
37i	$\text{Os}(\text{CO})_9(\mu_3-\eta^2-\text{C}_9\text{H}_6(5\text{-C}(\text{CH}_3)_2\text{CN})\text{N})(\mu\text{-H})$	51
37k	$\text{Os}(\text{CO})_9(\mu_3-\eta^2-\text{C}_9\text{H}_6(5\text{-CH}_2\text{CO}_2^t\text{Bu})\text{N})(\mu\text{-H})$	51
37l	$\text{Os}(\text{CO})_9(\mu_3-\eta^2-\text{C}_9\text{H}_6(5\text{-CH}_2\text{-CH}=\text{CH}_2)\text{N})(\mu\text{-H})$	51
37a	$\text{Os}(\text{CO})_9(\mu_3-\eta^3-\text{C}_9\text{H}_7(5\text{-CH}_3)\text{N})(\mu\text{-H})$	52
37b	$\text{Os}(\text{CO})_9(\mu_3-\eta^3-\text{C}_9\text{H}_7(5\text{-}^n\text{Bu})\text{N})(\mu\text{-H})$	52
37c	$\text{Os}(\text{CO})_9(\mu_3-\eta^3-\text{C}_9\text{H}_7(5\text{-}^t\text{Bu})\text{N})(\mu\text{-H})$	52
37d	$\text{Os}(\text{CO})_9(\mu_3-\eta^3-\text{C}_9\text{H}_7(5\text{-CH}_2\text{C}_6\text{H}_5)\text{N})(\mu\text{-H})$	52
37e	$\text{Os}(\text{CO})_9(\mu_3-\eta^3-\text{C}_9\text{H}_7(5\text{-C}_6\text{H}_5)\text{N})(\mu\text{-H})$	52
37f	$\text{Os}(\text{CO})_9(\mu_3-\eta^3-\text{C}_9\text{H}_7(5\text{-CH}=\text{CH}_2)\text{N})(\mu\text{-H})$	52
37g	$\text{Os}(\text{CO})_9(\mu_3-\eta^3-\text{C}_9\text{H}_7(5\text{-C}_2(\text{CH}_3)_3\text{CH}_3)\text{N})(\mu\text{-H})$	52
37h	$\text{Os}(\text{CO})_9(\mu_3-\eta^3-\text{C}_9\text{H}_7(5\text{-CH}_2\text{CN})\text{N})(\mu\text{-H})$	52
37i	$\text{Os}(\text{CO})_9(\mu_3-\eta^3-\text{C}_9\text{H}_7(5\text{-C}(\text{CH}_3)_2\text{CN})\text{N})(\mu\text{-H})$	52
37k	$\text{Os}(\text{CO})_9(\mu_3-\eta^3-\text{C}_9\text{H}_7(5\text{-CH}_2\text{CO}_2^t\text{Bu})\text{N})(\mu\text{-H})$	52
37l	$\text{Os}(\text{CO})_9(\mu_3-\eta^3-\text{C}_9\text{H}_7(5\text{-CH}_2\text{-CH}=\text{CH}_2)\text{N})(\mu\text{-H})$	52
38b	$\text{Os}(\text{CO})_9(\mu_3-\eta^3-\text{C}_9\text{H}_6(3\text{-CO}_2\text{CH}_3)(5\text{-C}(\text{CH}_3)_2\text{CN})\text{N})(\mu\text{-H})$	56

38c	$\text{Os}(\text{CO})_9(\mu_3-\eta^3\text{-C}_9\text{H}_6(3\text{-NH}_2)(5\text{-C}(\text{CH}_3)_2\text{CN})\text{N})(\mu\text{-H})$	56
38d	$\text{Os}(\text{CO})_9(\mu_3-\eta^3\text{-C}_9\text{H}_6(4\text{-CH}_3)(5\text{-C}(\text{CH}_3)_2\text{CN})\text{N})(\mu\text{-H})$	56
38e	$\text{Os}(\text{CO})_9(\mu_3-\eta^3\text{-C}_9\text{H}_6(4\text{-Cl})(5\text{-C}(\text{CH}_3)_2\text{CN})\text{N})(\mu\text{-H})$	56
38e'	$\text{Os}(\text{CO})_9(\mu_3-\eta^3\text{-C}_9\text{H}_6(4\text{-Cl})(5\text{-CH}_2\text{CO}_2^t\text{Bu})\text{N})(\mu\text{-H})$	56
38f	$\text{Os}(\text{CO})_9(\mu_3-\eta^3\text{-C}_9\text{H}_6(4\text{-OCH}_3)(5\text{-C}(\text{CH}_3)_2\text{CN})\text{N})(\mu\text{-H})$	56
38f'	$\text{Os}(\text{CO})_9(\mu_3-\eta^3\text{-C}_9\text{H}_6(4\text{-COCH}_3)(5\text{-CH}_2\text{CO}_2^t\text{Bu})\text{N})(\mu\text{-H})$	56
38g	$\text{Os}(\text{CO})_9(\mu_3-\eta^3\text{-C}_9\text{H}_6(4\text{-NH}_2)(5\text{-C}(\text{CH}_3)_2\text{CN})\text{N})(\mu\text{-H})$	56
38h	$\text{Os}(\text{CO})_9(\mu_3-\eta^3\text{-C}_9\text{H}_6(4\text{-CO}_2\text{CH}_3)(5\text{-CHCH}_2=\text{CH}_2)\text{N})(\mu\text{-H})$	57
38i	$\text{Os}(\text{CO})_9(\mu_3-\eta^3\text{-C}_9\text{H}_6(4\text{-CO}_2\text{CH}_3)(5\text{-C}(\text{CH}_3)_2\text{CN})\text{N})(\mu\text{-H})$	57
cis-38m	$\text{Os}(\text{CO})_9(\mu_3-\eta^3\text{-C}_9\text{H}_6(5\text{-C}(\text{CH}_3)_2\text{CN})(6\text{-CH}_3)\text{N})(\mu\text{-H})$	63
cis-38m'	$\text{Os}(\text{CO})_9(\mu_3-\eta^3\text{-C}_9\text{H}_6(5\text{-CH}_3)(6\text{-CH}_3)\text{N})(\mu\text{-H})$	64
cis-38n	$\text{Os}(\text{CO})_9(\mu_3-\eta^3\text{-C}_9\text{H}_6(5\text{-C}(\text{CH}_3)_2\text{CN})(6\text{-Cl})\text{N})(\mu\text{-H})$	58
cis-38p	$\text{Os}(\text{CO})_9(\mu_3-\eta^3\text{-C}_9\text{H}_6(5\text{-CHCH}_2=\text{CH}_2)(6\text{-CO}_2\text{CH}_3)\text{N})(\mu\text{-H})$	64
trans-38m	$\text{Os}(\text{CO})_9(\mu_3-\eta^3\text{-C}_9\text{H}_6(5\text{-C}(\text{CH}_3)_2\text{CN})(6\text{-CH}_3)\text{N})(\mu\text{-H})$	67
trans-38m'	$\text{Os}(\text{CO})_9(\mu_3-\eta^3\text{-C}_9\text{H}_6(5\text{-CH}_3)(6\text{-CH}_3)\text{N})(\mu\text{-H})$	68
trans-38z	$\text{Os}(\text{CO})_9(\mu_3-\eta^3\text{-C}_9\text{H}_6(5\text{-CH}_3)(6\text{-COCH}_3)\text{N})(\mu\text{-H})$	68
39i	$\text{Os}(\text{CO})_9(\mu_3-\eta^2\text{-C}_9\text{H}_6(4\text{-C}(\text{CH}_3)_2\text{CN})(5\text{-F})\text{N})(\mu\text{-H})$	72
39i'	$\text{Os}(\text{CO})_9(\mu_3-\eta^2\text{-C}_9\text{H}_6(4\text{-}^n\text{Bu})(5\text{-F})\text{N})(\mu\text{-H})$	72
39j	$\text{Os}(\text{CO})_9(\mu_3-\eta^2\text{-C}_9\text{H}_6(4\text{-C}(\text{CH}_3)_2\text{CN})(5\text{-Cl})\text{N})(\mu\text{-H})$	72
39j'	$\text{Os}(\text{CO})_9(\mu_3-\eta^2\text{-C}_9\text{H}_6(4\text{-}^n\text{Bu})(5\text{-Cl})\text{N})(\mu\text{-H})$	72
39k	$\text{Os}(\text{CO})_9(\mu_3-\eta^2\text{-C}_9\text{H}_6(4\text{-C}(\text{CH}_3)_2\text{CN})(5\text{-Br})\text{N})(\mu\text{-H})$	72
39k'	$\text{Os}(\text{CO})_9(\mu_3-\eta^2\text{-C}_9\text{H}_6(4\text{-}^n\text{Bu})(5\text{-Br})\text{N})(\mu\text{-H})$	72
39l	$\text{Os}(\text{CO})_9(\mu_3-\eta^2\text{-C}_9\text{H}_6(4\text{-C}(\text{CH}_3)_2\text{CN})(5\text{-NH}_2)\text{N})(\mu\text{-H})$	72
39l'	$\text{Os}(\text{CO})_9(\mu_3-\eta^2\text{-C}_9\text{H}_6(4\text{-}^n\text{Bu})(5\text{-NH}_2)\text{N})(\mu\text{-H})$	72
39n	$\text{Os}(\text{CO})_9(\mu_3-\eta^2\text{-C}_9\text{H}_5(5\text{-C}(\text{CH}_3)_2\text{CN})(6\text{-Cl})\text{N})(\mu\text{-H}_2)$	58
40	$\text{Os}_3(\text{CO})_8(\text{PPh}_3)-(\mu_3-\eta^2\text{-C}_9\text{H}_6\text{N})(\mu\text{-H})$	105
41	$\text{Os}_3(\text{CO})_9-(\mu_3-\eta^2\text{-C}=\text{N}(\text{-CH}_2\text{-})_3)(\mu\text{-H})$	105

42	$\text{Os}_3(\text{CO})_9-(\mu_3-\eta^2-\text{C}=\text{N}(-\text{CH}_2)_3)(\mu-\text{H})\text{L}$	105
42'	$\text{Os}_3(\text{CO})_9-(\mu_3-\eta^2-\text{C}=\text{N}(-\text{CH}_2)_3)(\mu-\text{H})\text{L}$	105
43	$\text{Os}_3(\text{CO})_9-(\mu_3-\eta^2-\text{C}=\text{N}(-\text{CH}_2)_3)(\mu-\text{H})_2(\text{CF}_3\text{CO}_2)$	106
44	$\text{Os}_3(\text{CO})_9(\mu_3-\eta^3-\text{C}_6\text{H}_{12}\text{N})$	110
45	$\text{Os}_3(\text{CO})_9(\mu_3-\eta^2-\text{C}_6\text{H}_{12}\text{N})(\mu-\text{H})$	110
46	$[\text{Os}_3(\text{CO})_9(\mu_3-\eta^2-\text{C}_9\text{H}_6\text{N})(\mu-\text{H}_2)]^+$	116
47	$[\text{Os}_3(\text{CO})_9(\mu_3-\eta^3-\text{C}_9\text{H}_5(4-\text{Cl})(5-\text{CH}_2\text{CO}_2^t\text{Bu})\text{N})(\mu-\text{H})]^-$	123
48	$[\text{Os}_3(\text{CO})_9(\mu_3-\eta^3-\text{C}_9\text{H}_5(4-\text{Cl})(5-\text{C}_8\text{H}_{13}\text{O}_3)\text{N})(\mu-\text{H})]^-$	123
49	$[\text{Os}_3(\text{CO})_9(\mu_3-\eta^3-\text{C}_9\text{H}_5(4-\text{Cl})(5-\text{C}_8\text{H}_{13}\text{O}_3)\text{N})(\mu-\text{H})]^-$	123
50	$[\text{Os}_3(\text{CO})_9(\mu_3-\eta^3-\text{C}_9\text{H}_5(4-\text{Cl})(5-\text{C}_8\text{H}_{13}\text{O}_3)\text{N})(\mu-\text{H})]^-$	123
51	$[\text{Os}_3(\text{CO})_9(\mu_3-\eta^3-\text{C}_9\text{H}_5(4-\text{Cl})(5-\text{CH}_2\text{COCH}_2\text{CO}_2\text{H})\text{N})(\mu-\text{H})]$	123
52	$[\text{Os}_3(\text{CO})_9(\mu_3-\eta^3-\text{C}_9\text{H}_5(4-\text{Cl})(5-\text{CH}_2\text{COCH}_2)\text{N})(\mu-\text{H})]^-$	123
53	$[\text{Os}_3(\text{CO})_9(\mu_3-\eta^3-\text{C}_9\text{H}_5(4-\text{Cl})(5-\text{CH}_2\text{COCH}_3)\text{N})(\mu-\text{H})]$	123
54	$\text{Os}_3(\text{CO})_9-(\mu_3-\eta^2-\text{C}_9\text{H}_5(5-\text{O}^n\text{Bu})\text{N})(\mu-\text{H})$	129
55	$\text{Os}_3(\text{CO})_9(\mu_3-\eta^3-\text{C}_9\text{H}_5(5-^t\text{Bu})(6-\text{CH}_3)(6-\text{OH})\text{N})(\mu-\text{H})$	133
<i>Cis-56</i>	$\text{Os}_3(\text{CO})_9(\mu_3-\eta^3-\text{C}_9\text{H}_5(5-\text{CH}_2\text{CO}_2^t\text{Bu})(6-\text{Cl})\text{N})(\mu-\text{H})$	138
57h	$\text{Os}_3(\text{CO})_9(\mu_3-\eta^3-\text{C}_9\text{H}_5(4-\text{CO}-\text{CH}_2\text{CH}=\text{CH}_2)(5-\text{CH}_2\text{CH}=\text{CH}_2)\text{N})(\mu-\text{H})$	143
57i	$\text{Os}_3(\text{CO})_9(\mu_3-\eta^3-\text{C}_9\text{H}_5(4-\text{CO}-\text{C}(\text{CH}_3)_2\text{CN})(5-\text{C}(\text{CH}_3)_2\text{CN})\text{N})(\mu-\text{H})$	143

* Denotes compounds synthesized by others, previously reported.

List of Figures

		Page
Figure 1.1	Effects of Metal Coordination on η^6 - π Arenes.	3
Figure 1.2	Common Metal p-Arene Complexes.	7
Figure 2.1	Solid State Structure for $\text{Os}_3(\text{CO})_9(\mu_3\text{-}\eta^2\text{-C}_9\text{H}_5(6\text{-Cl})\text{N})(\mu\text{-H})$ 35n Showing the Calculated Position of the Hydride.	33
Figure 3.1	Solid State Structure for $\text{Os}_3(\text{CO})_9(\mu_3\text{-}\eta^3\text{-C}_9\text{H}_7(5\text{-C}_6\text{H}_5)\text{N})(\mu\text{-H})$ 37e Showing the Calculated Position of the Hydride.	55
Figure 3.2	Solid State Structure for $\text{Os}_3(\text{CO})_9(\mu_3\text{-}\eta^2\text{-C}_9\text{H}_7(5\text{-C}(\text{CH}_3)_2\text{CN})(6\text{-Cl})\text{N})(\mu\text{-H}_2)$ 39n Showing the Calculated Positions of the Hydrides.	63
Figure 3.3	Solid State Structure for $\text{Os}_3(\text{CO})_9(\mu_3\text{-}\eta^3\text{-C}_9\text{H}_6(5\text{-C}_6\text{H}_5)(6\text{-CH}_3)\text{N})(\mu\text{-H})$ <i>cis</i> - 38m Showing the Calculated Position of the Hydride.	67
Figure 3.4	Solid State Structure for $\text{Os}_3(\text{CO})_9(\mu_3\text{-}\eta^3\text{-C}_9\text{H}_6(5\text{-C}_6\text{H}_5)(6\text{-CH}_3)\text{N})(\mu\text{-H})$ <i>trans</i> - 38m Showing the Calculated Position of the Hydride.	71
Figure 3.5	Solid State Structure for $\text{Os}_3(\text{CO})_9(\mu_3\text{-}\eta^2\text{-C}_9\text{H}_6(5\text{-Cl})(4\text{-C}(\text{CH}_3)\text{CN})\text{N})(\mu\text{-H})$ 39j Showing the Calculated Position of the Hydride.....	75
Figure 4.1	Hammett s-r Plot of the Protonation for Compound 35a , 35c , 35k , 35q , and 35x Reacting with $\text{CF}_3\text{CO}_2\text{H}$	121
Figure 5.1	Solid State Structure for $\text{Os}_3(\text{CO})_9(\mu_3\text{-}\eta^3\text{-C}_9\text{H}_6(5\text{-Cl})(5\text{-CH}_2\text{COCH}_3)\text{N})(\mu\text{-H})$ 53 Showing the Calculated Position of the Hydride.....	128
Figure 5.2	Solid State Structure for $\text{Os}_3(\text{CO})_9(\mu_3\text{-}\eta^2\text{-C}_9\text{H}_5(5\text{-O}^n\text{Bu})\text{N})(\mu\text{-H})$ 54 Showing the Calculated Position of the Hydride.	133
Figure 5.3	Solid State Structure for $\text{Os}_3(\text{CO})_9(\mu_3\text{-}\eta^3\text{-C}_9\text{H}_5(5\text{-}^t\text{Bu})(6\text{-CH}_3)(6\text{-OH})\text{N})(\mu\text{-H})$ 55 Showing the Calculated Position of the Hydride.	138
Figure 5.4	Variable Temperature ^1H NMR Spectra for Proton H(7) in <i>cis</i> - 56	142

List of Tables

		Page
Table 1.1	Reactivity of Carbanions (RLi) Towards η^6 -(benzene-Cr(CO) ₃).....	11
Table 1.2	Regioselective Addition of (indole)-Cr(CO) ₃	14
Table 2.1	Yields of Monosubstituted Electron Deficient Triosmium Clusters.....	31
Table 2.2	Selected Bond Distances (Å) and Angles (°) for 35n	34
Table 3.1	Isolated Nucleophilic Addition Yields for the Reaction of Os ₃ (CO) ₉ -(μ^3 - η^2 -C ₉ H ₆ N)(μ -H) 35a with Carbanions.	54
Table 3.2	Selected Bond Distances (Å) and Angles (°) for 37e	56
Table 3.3	Selected Bond Distances (Å) and Angles (°) for 39n	64
Table 3.4	Selected Bond Distances (Å) and Angles (°) for <i>cis</i> - 38m	68
Table 3.5	Selected Bond Distances (Å) and Angles (°) for <i>trans</i> - 38m	72
Table 3.6	Selected Bond Distances (Å) and Angles (°) for 39j	76
Table 4.1	Chemical Shifts (ppm) and Isomer Ratios for Amine Adducts of Os ₃ (CO) ₉ (μ_3 - η^2 -C ₉ H ₆ N)(μ -H) 35a	109
Table 4.2	ΔH° (KJ/mol) ΔS° (J/mol) for Amine Adducts of Os ₃ (CO) ₉ (μ_3 - η^2 -C ₉ H ₆ N)(μ -H) 35a	115
Table 4.3	Equilibrium Constants and Isomer Ratios for n-BuNH ₂ Complexes of Electron Deficient Quinoline Complexes.	117
Table 4.4	Protonation Equilibria for Electron Deficient Triosmium Clusters.	120
Table 5.1	Selected Bond Distances (Å) and Angles (°) for 53	129
Table 5.2	Selected Bond Distances (Å) and Angles (°) for 54	134
Table 5.3	Selected Bond Distances (Å) and Angles (°) for 55	139

Chapter 1

Introduction

1.1 General Background for Transition Metal Arene Complexes

Transition metals are of increasing importance in chemistry as a means of activating organic molecules towards specific reagents. Transition metals have outer d-orbitals that are only partially filled, acting as donors or acceptors of electron density and enabling them to influence the electron distributions in the coordinated organic molecules. A related and equally important area of chemistry is the study of transition metals being coordinately attached to a ligand for use in asymmetric synthesis.^{1,2}

The organic chemistry of benzene is dominated by electrophilic aromatic substitution reactions, but as a coordinated ligand benzene undergoes nucleophilic addition / substitution. This stark contrast in chemical behavior is a good example of the powerful influence coordination to a metal can have on the chemistry of an organic

molecule. To better learn how these systems work, it is important to understand how the coordination mode of the ligand influences its reactivity.¹⁻³

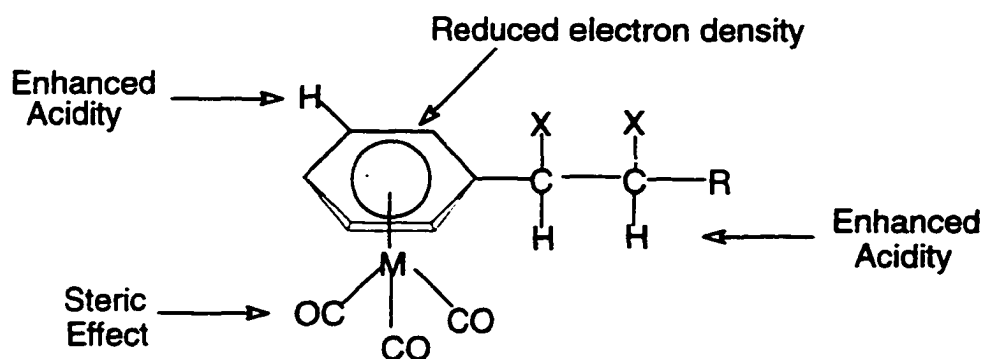
Interest in exploring the scope and selectivity of nucleophilic attack on aromatic systems to yield asymmetric stereoselective products became increasingly important with the development of pharmaceuticals and agrochemicals which require better methods for producing homochiral materials. This has in turn led the synthetic chemist to explore and invent new types of methodology using transition metals suitable for homochiral synthesis.

The first arene-metal complexes were prepared in the 1950's, and it was immediately recognized that the polarization (electron withdrawal) of aromatic π -electron density would promote addition of nucleophiles to the arene-ligand.^{4,5} In the early 1980's many groups built upon this knowledge and began to examine the potential role of arene-metal complexes as substrates for nucleophiles.¹

The reactivity of η^6 -arene ligands is summarized in Figure 1.1 which shows the general changes in arene reactivity that are observed when a metal ($M=Cr, Mn, \text{ or } Fe$) is coordinated with the π -system. The most dramatic effect of metal coordination to an arene is the powerful withdrawal of electron density from the aromatic ring, much like a nitro substituent which is sigma bound to the ring. This factor is responsible for the significant enhancement of acidity of the benzylic hydrogens in π -bound η^6 -(alkylarene)-metal complex (Figure 1.1).^{6,7} Coordination of metals has been known for many years to reverse the normal reactivity of carbon π bonds, from being reactive towards electrophiles to being reactive towards nucleophiles.^{1,8} Arene ligands show a

dramatic effect of this reversed reactivity and this opened up new reaction Pathways for aromatic addition and substitution.

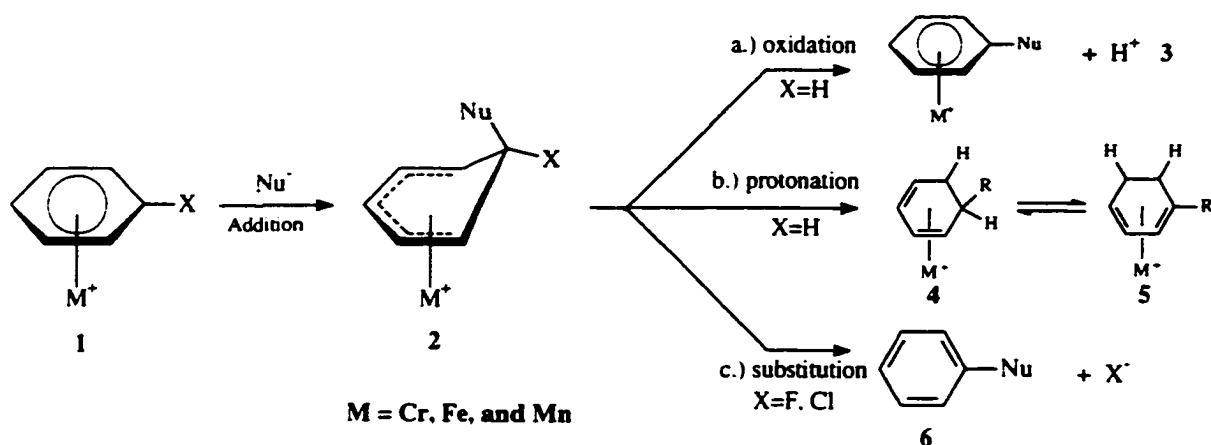
Figure 1.1 Effects of Metal Coordination on η^6 -bound π -Arene Complexes.



1.2 Arene-Metal Complexes as Substrates for Nucleophiles

The nucleophilic attack (electrophilic reactivity) of an arene π -coordinated to a transition metal has been developed by three distinct methods for coupling nucleophiles with aromatic rings: 1.) addition/oxidation (Path a, Scheme 1.1), 2.) addition/protonation (Path b, Scheme 1.1), 3.) substitution (Path c, Scheme 1.1).^{1-3,9-14} Each method will be discussed in the following sections.

Scheme 1.1



1.2.1 Nucleophilic Substitution on Metal Arene Complexes

Addition of reactive carbon nucleophiles to arene-metal complexes **1** produces a stable intermediate η^5 -cyclohexadienyl (complex **2**) shown in Scheme 1.1.^{1,2} In **2** a new carbon-carbon bond has been formed which can be converted to a variety of products. One such product **3** (shown Scheme 1, Path a) can be formed by oxidation of **2** with a variety of oxidizing agents (I_2 , Ce^{IV} , Cr^{VI}) to induce the loss of the *endo* hydrogen and cleavage from the metal, resulting in nucleophilic substitution for the hydrogen.^{1,2,10-12} The resulting formal replacement of a hydride by a carbanion, is referred to as addition/oxidation.^{1,10} This makes for a general substitution process which does not depend on the leaving group on the arene. Oxidation of the nucleophilic addition product is usually associated with cleavage from the metal for the chromium complexes.^{1,2}

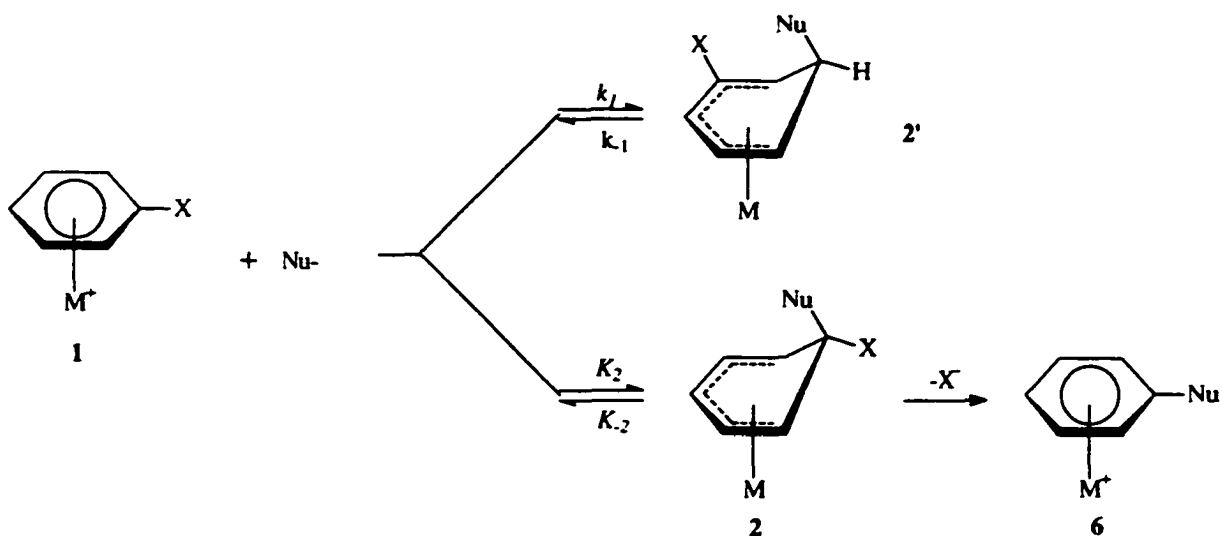
1.2.2 Nucleophilic Addition / Protonation on Metal Arene Complexes

Alternatively, after addition of the nucleophile, the η^5 -cyclohexadienyl anionic complex **2** (Scheme 1.1) is highly electron rich and is susceptible to reactions with protons (and electrophiles discussed later in sections 1.7 and 1.8).^{1,2,15-17} Thus complex **2** can be protonated with a strong acid to produce a labile η^4 -2,4 cyclohexadiene complex **4** which undergoes H migration (sigmatropic rearrangement) to give the more stable η^4 -1,3- cyclohexadiene isomer **5** affecting nucleophilic addition with reduction of one double bond (Path b, Scheme 1.1).^{1,2} The overall conversion amounts to the addition of R-H across the π -bond of the arene and is referred to as addition/protonation.^{1,2,14}

1.2.3 Nucleophilic Substitution on Metal Arene Complexes

If an electronegative atom is present in the *ipso*-position, elimination of the heteroatom (X) leads to nucleophilic substitution (Path c, Scheme 1.1).² Nucleophilic substitution is not commonly used in organic synthesis because of the necessity of introducing and then removing an activating group.^{1,2,4,10,11} With these organometallic arene complexes, the activating group (metal moiety) can be easily detached resulting in nucleophilic substitution. The smooth replacement of a heteroatom (halide) from arene ligands requires reversible addition of the nucleophiles, since the kinetic site of the addition is usually at a position bearing a hydrogen substituent for steric reasons (Scheme 1.2, Path k_f).^{1,2}

Scheme 1.2



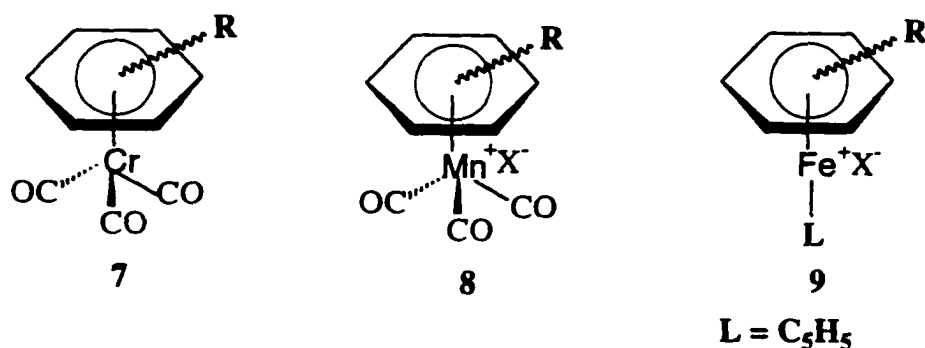
The nucleophilic substitution for halogen is a somewhat limited process where the relative rates of each step depend on the nature of the metal and the nucleophile.² More reactive nucleophiles and more reactive complexes disfavor equilibration ($k_1 \gg k_{-1}$) and the reaction can stop with the formation of the cyclohexadienyl intermediate.² Very reactive nucleophiles add to the substituted position, and then slowly isomerize to the *ipso*-position from which loss of halide can occur.^{1,2} Equilibration leads through to the substitution product, as the nucleophile migrates about the arene ligand, then loss of the halide occurs consistent with classical nucleophilic aromatic substitution for halogens in electron-deficient haloarenes.^{1,2}

1.3 Effects of Metal Complexation on Arenes

There are three (π -bound) metal-arene complexes that have played significant

roles in organic synthetic methodology (Figure 1.2): neutral η^6 -arene- $\text{Cr}(\text{CO})_3$ **7**^{1,2,4,36-38}, the isoelectronic cationic η^6 -arene- $\text{Mn}^+(\text{CO})_3$ **8**^{1-4,9,39}, and the cationic (η^6 -arene)(η^6 -cyclopentadienyl) $\text{Fe}(\text{II})$ **9** complexes and their ruthenium analogs.^{1-4,9,12} The overall order of reactivity for electron-deficient arenes is $(\text{arene})(\text{CO})_3\text{Mn}^+ > 2,4\text{-(NO}_2\text{)}_2\text{C}_6\text{H}_3\text{Cl} > (\text{arene})\text{CpFe}^+ > (\text{NO}_2\text{)}_2\text{C}_6\text{H}_4\text{Cl} > (\text{arene})(\text{CO})_3\text{Cr}$.^{2,4,18}

Figure 1.2 Common Metal Arene Complexes



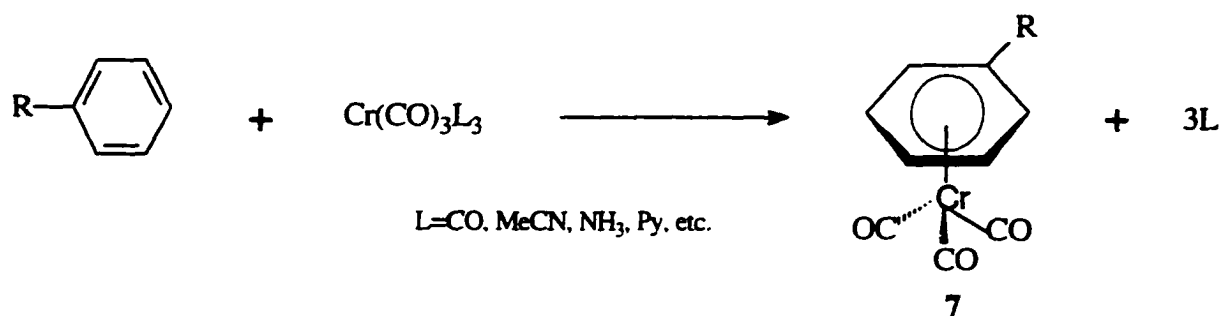
There are two general methods for formation of these arene-metal complexes: 1.) direct thermal displacement of ligands; 2.) Lewis acid-promoted attachment of the arene to the metal.^{1,2} The simplest is direct thermal replacement of other ligands on the metal, and is a process that is carried out very efficiently with chromium complexes **7** under mild, low temperature conditions.^{1,2} The Lewis acid-promoted attachment of arene rings to metals is the general preparation for cationic arene metal complexes (**8** and **9**).

1.3.1 Preparation of Arene- $\text{Cr}(\text{CO})_3$ Metal Complexes

The arene $\text{Cr}(\text{CO})_3$ complexes are formed by simple displacement of neutral ligands ($\text{L} = \text{CO}, \text{MeCN}, \text{NH}_3, \text{Py}, \text{etc.}$) from $\text{Cr}(\text{CO})_3\text{L}_3$ by the arene (Equation 1.1).^{1,2} This process has been very useful for preparation of many η^6 -arene $\text{Cr}(\text{CO})_3$ complexes

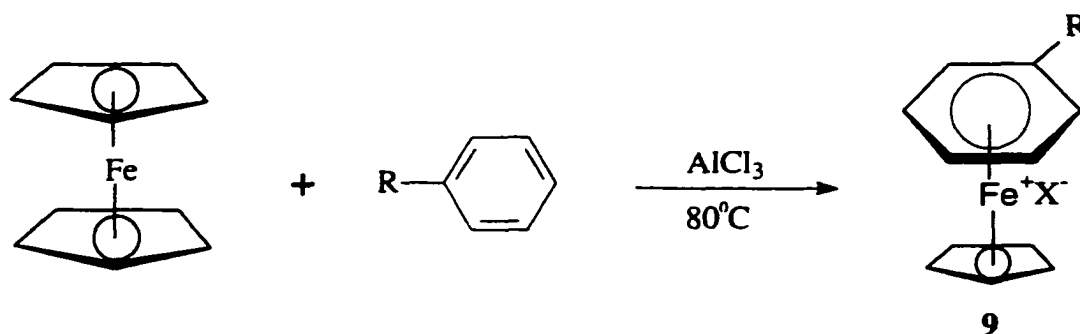
with a variety of substituents on the ring.^{1,2,5} The complexes are somewhat sensitive to air while in solution, but crystalline solids can be stored without special precautions. However, even mild oxidation will detach the arene by oxidizing the metal.²

Equation 1.1

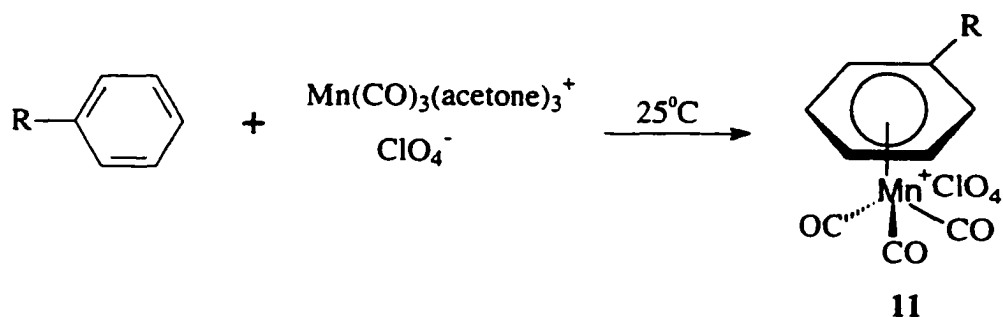


1.3.2 Preparation of (Arene)-FeCp⁺ Complexes

Mild and general syntheses of cationic iron and manganese complexes have only recently been possible, explaining why the development of complexes **9** as synthetic intermediates has progressed less far.² The most common reactions for preparation for the arene-FeCp cationic complex **9** involves the AlCl₃-catalyzed exchange of one of the Cp groups on the ferrocene for the arene ligand (Equation 1.2).^{2,9,19-22} This variation of the Fischer-Hafner method employs a Lewis acid such as AlCl₃ with a reducing agent such as aluminum metal, and involves the reduction of the transition metal during the process.^{1,2} A difficulty with this method is that certain functional groups on the arene ring will undergo serious side reactions.² These complexes are very air and heat stable, but there are few methods of removing the arene from iron, besides the pyrolysis at > 200°C. or the use of powerful oxidizing agents.² This is also the case for their ruthenium analogs.

Equation 1.2**1.3.3 Preparation of (Arene)-Mn(CO)₃⁺ Complexes**

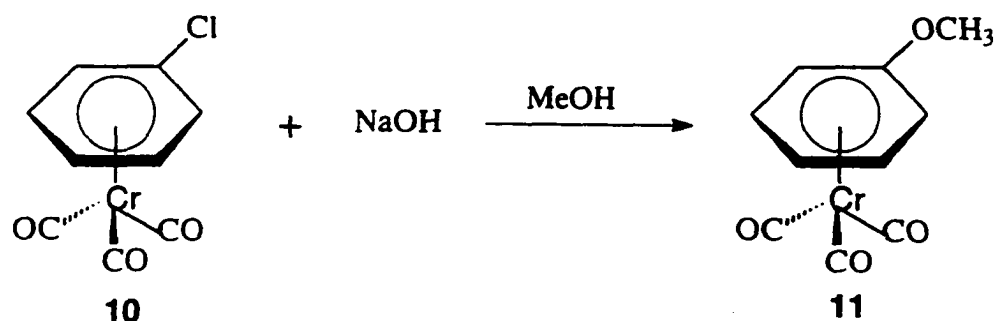
A recent mild procedure has made the [(arene)Mn(CO)₃]⁺ **8** complexes available with a variety of substitutions on the arenes.^{2,7,9} Direct displacement of CO from the perchlorate salts of [Mn⁺(CO)₃(acetone)₃] or Mn(CO)₆ with the arene in dichloromethane at reflux leads to the precipitation of **8** [(arene)-Mn⁺(CO)₃] as the perchlorate salt (Equation 1.3).² These conditions are milder than the previous AlCl₃-promoted procedure mentioned earlier (Section 1.3.2). These complexes are air stable and very reactive towards nucleophiles, but again like the iron complexes removing the arene from the manganese requires powerful oxidizing agents such as the Jones Reagent [Cr^{VI}].^{2,23}

Equation 1.3

1.4 Nucleophilic Reactivity of η^6 -(Benzene)-Cr(CO)₃ Complexes

While aromatic rings are known to form stable complexes with almost every transition metal,¹ the η^6 -arene-chromium tricarbonyl species have been studied in detail for development of practical applications in organic synthesis especially in the area of substituted arenes where the regioselectivity becomes important and is obtainable in high yields.¹

Equation 1.4



Isolation of the first halo-benzene complex **10** (η^6 -chlorobenzene) chromium tricarbonyl (0), allowed a test for a direct analogue of classical S_NAr reactivity.^{1,2,11,24} The activating effect of the Cr(CO)₃ unit is comparable with a *p*-nitro-substituent, and it was shown that complex **10** undergoes nucleophilic substitution by methoxide ion at roughly the same rate as *p*-nitrochlorobenzene (Equation 1.4).^{1,24}

For benzene-Cr(CO)₃ **7**, an extensive series of carbanions have been tested and generally fall into one of three groups: A.) unreactive, B.) successful, and C.) metalation (Table 1.1, and Scheme 1.1).^{1,2} The unreactive carbanions (group A) consisting of

Grignards, organocuprates, and ketone enolates fail to give conversion to **2** (the anionic cyclohexadienyl-Cr(CO)₃ complex). Also included in this group A are heteroatom anions such as alkoxide and amines. The successful (group B) anions are formed from carbon acids with $pK_a > 20$.^{1,2} Proton abstraction (or metalation) is the primary reaction with carbanions of group C (discussed later in Section 1.7).^{1,2,11}

Scheme 1.3

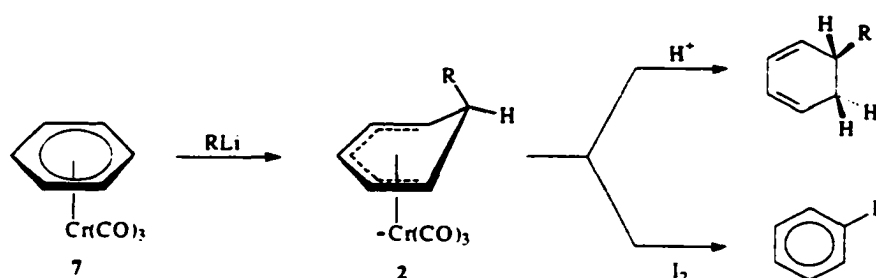


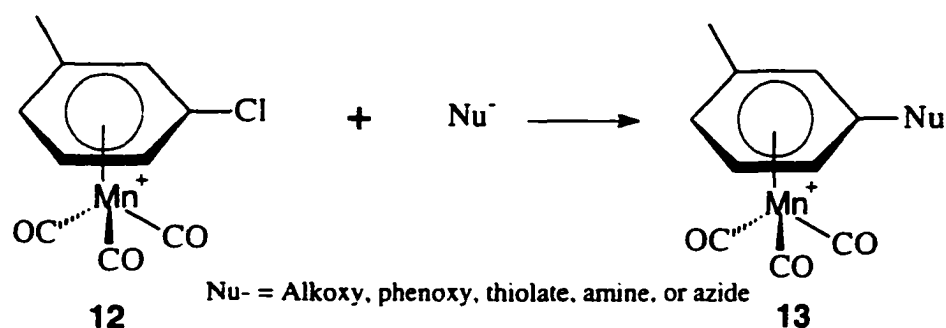
Table 1.1 Reactivity of carbanions with (RLi) towards η^6 -(benzene) Cr(CO)₃.

A.) Unreactive	B.) Successful	C.) Metalation
1. LiCH(CO ₂ Me) ₂	7. LiCH ₂ CO ₂ ^t Bu	18. Bu ⁿ Li
2. LiCH ₂ COBu ^t	8. LiCH ₂ CN	19. MeLi
3. MeMgBr	9. KCH ₂ COBu ^t	20. Bu ^s Li
4. Bu ^t MgBr	10. LiCH(CN)(OR)	
5. Me ₂ CuLi	11. LiCH ₂ SPh	
6. LiC(CN)(Ph)(OR)	12. 2-Li-1,3-dithiane	
	13. LiCH=CH ₂	
	14. LiPh	
	15. LiC=CR	
	16. LiCH ₂ CH=CH ₂	
	17. LiC(Me) ₃	

1.5 Nucleophilic Substitution with Heteroatom Nucleophiles

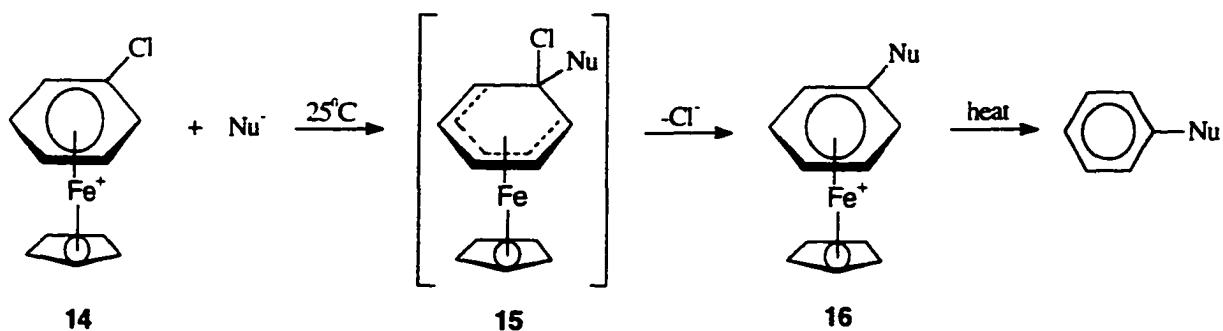
The cationic arene-Mn(CO)₃ complexes are the most reactive of the three common arene-metal complexes, and easily undergo nucleophilic substitution for halide with alkoxy, phenoxy, thiolate, amine or azide (Equation 1.5), unlike the chromium complexes.^{1-3,7,9}

Equation 1.5



The potential for the (halobenzene)Fe-Cp cationic complex **14** to undergo nucleophilic substitution is demonstrated in the two-stage addition/substitution process (Equation 1.6). In the first stage (addition) the nucleophile is added to give the neutral intermediate **15** (spectroscopically characterized), followed by the second stage (elimination of the chloride) resulting in **16**. This process is successful with a variety of nitrogen, oxygen, and sulfur nucleophiles.^{1-3,25}

Equation 1.6



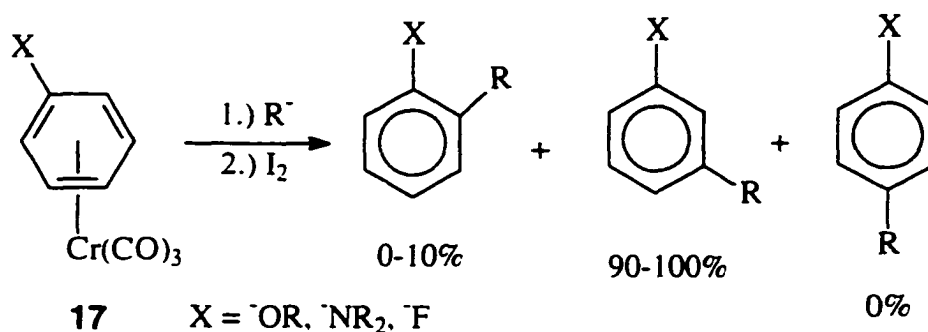
1.6 Regioselective Nucleophilic Addition on Metal-Arene Complexes

Substituted arenes generally bear more than one hydrogen substituent which can be the kinetic site of attack by the nucleophile.² This leads to an important question. Can regioselectivity be obtained and what factors influence the site of the attack? This question will be briefly addressed in the following sections 1.6.1 and 1.6.2 for substituted benzene- $\text{Cr}(\text{CO})_3$ **17** complexes and indole- $\text{Cr}(\text{CO})_3$ complexes **18**.^{1,2,26}

1.6.1 Regioselectivity on η^6 -(Benzene)- $\text{Cr}(\text{CO})_3$ Complexes

Regioselective nucleophilic addition to substituted arene systems has been the subject of numerous studies.² Substituents attached by σ -bonds to the arene ligand are the primary influence on site selectivity.^{1,2} Correlations can be made to predict regioselectivity with a modest degree of accuracy.² For example, with arenes bearing a single resonance donor substituent (NR_2 , OMe , and F) the addition is strongly preferred at the *meta* position with small amounts of *ortho* substitution (0-10%) (Equation 1.7).^{1,2,27,28}

Equation 1.7



However, the selectivity is more complicated with a methyl or chloro-substituent. In this case the *meta* accounts for a significant percentage, but *ortho* substitution can also account for 50-70% of the mixture in some cases.^{1,2,27,28}

1.6.2 Regioselectivity of (Indole)-Cr(CO)₃ Complexes 18

The (indole)-Cr(CO)₃ complex **18** is particularly interesting because the Cr(CO)₃ unit selectively activates the six-membered carbocyclic ring, while in free indole the five-membered heterocyclic ring dominates the reactivity towards nucleophiles.^{2,26,29,30} The selectivity in the addition to the indole-Cr(CO)₃ complexes shows a preference for addition at C-4 and C-7 (indole numbering Equation 1.8).^{2,26,30}

Equation 1.8

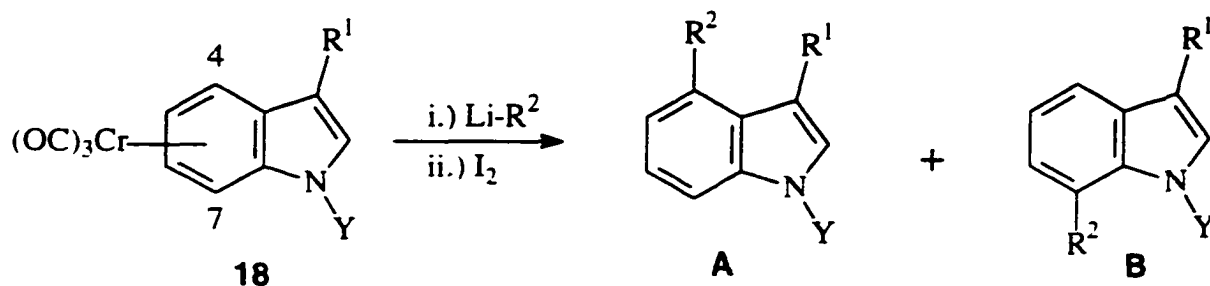


Table 1.2 Regioselective addition of (indole)-Cr(CO)₃, Ratio of Products

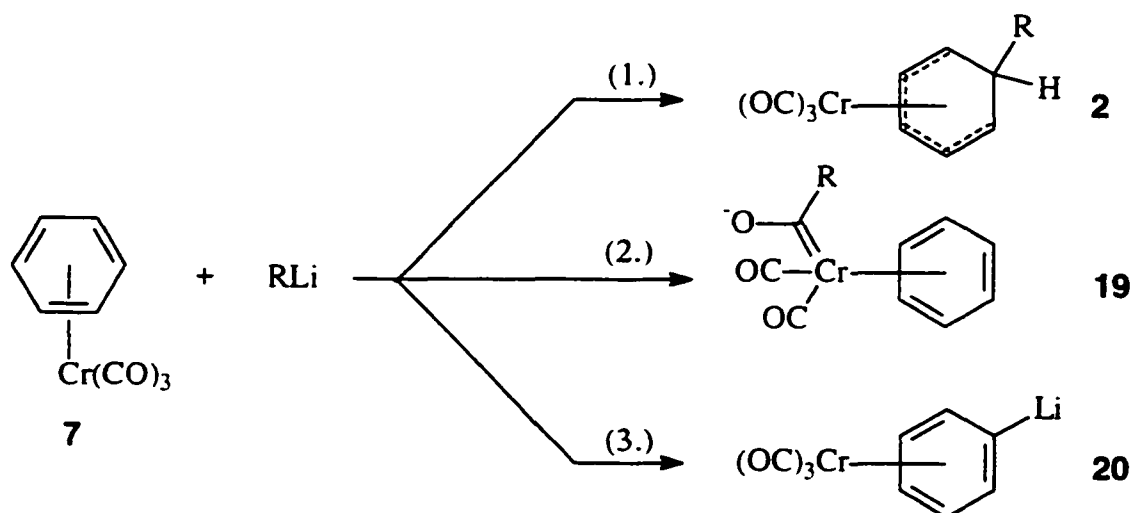
Substituents	Ratio of products A : B (%)
1.) R ² =C(Me) ₂ CN, R ¹ =H, Y=Me	99:1
2.) R ² =C(Me) ₂ CN, R ¹ =CH ₂ TMS	17:83
3.) R ² =C(Me) ₂ CN, R ¹ =CH ₂ TMS, Y=SiBu ^t (Me) ₂	95:5

The selectivity can be somewhat controlled by steric bulkiness of the substituents at C-3 and N-1, and the anion.^{2,26,30} In Equation 1.8, (Example 1, Table 1.2), with a hydrogen substituent at C-3 and attack with a tertiary carbanion, leads to selective C-4 substitution. With a trimethylsilylmethyl substituent at C-3 (Example 2, Table 1.2), the addition is preferred at C-7. However, even with a trimethylsilylmethyl substituent at C-3, a sufficiently large N-protecting group can disfavor addition at C-7 (Example 3, Table 1.2).^{2,26}

1.7 Ring Lithiation on Arene-Cr(CO)₃ complexes

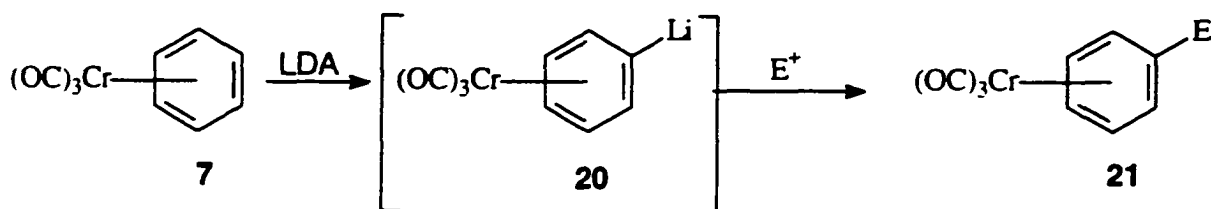
One strong effect of transition metal coordination as mentioned earlier is the enhanced acidity of the ring protons, which allows direct proton abstraction from an arene ligand, or lithium-halogen exchange to give an aryllithium derivative coordinated to the metal. The first examples of metalation of arene ligands were reported in 1968, and the first examples with Cr(CO)₃ appeared shortly thereafter.^{2,31,32}

Scheme 1.4



There are three electrophilic sites in $[\text{Cr}(\text{CO})_3(\text{C}_6\text{H}_6)]$ **7** as shown in (Scheme 1.3): 1.) the aromatic ring, 2.) attack at carbonyl on the chromium, and finally 3.) metalation by attacking the ring protons.² Most common nucleophiles or bases will add to the ring (via nucleophilic addition) as shown in Path 1, although a few organolithium reagents are known to react with the CO ligand (Path 2).^{2,17,33,34} Selective proton abstraction requires high kinetic basicity and low nucleophilic reactivity, this can be accomplished in $[\text{Cr}(\text{CO})_3(\text{C}_6\text{H}_6)]$ **7** with lithium diisopropylamide.^{2,35} This lithiated intermediate complex **20** can be trapped with an electrophile to provide a new substituted arene complex **21** (Equation 1.9). There are only a few examples where this process has been shown to be synthetically useful.²

Equation 1.9



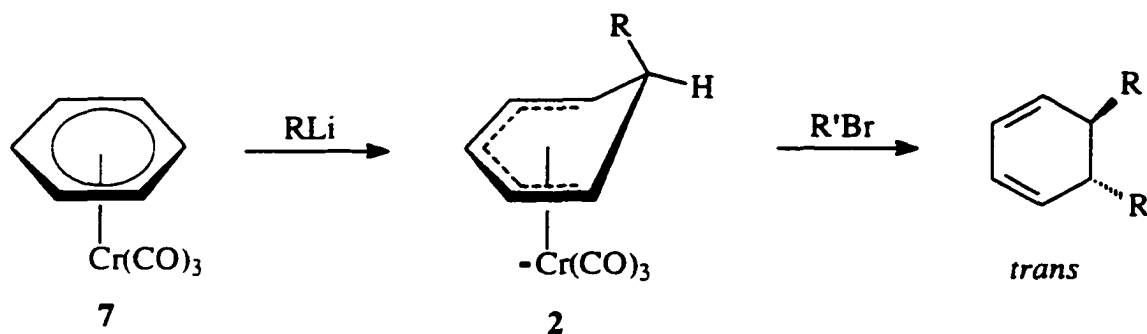
In general for η^6 -arene-metal complexes quenching with electrophiles other than protons leads primarily to electrophilic alkylation of the carbanion owing to the reversibility of the nucleophilic addition.²

1.8 Stereoselective Carbon-Carbon Bond Formation to $\eta^6\text{-C}_6\text{H}_6\text{-Cr}(\text{CO})_3$

Reactions that transform benzene and substituted benzenes into functionalized

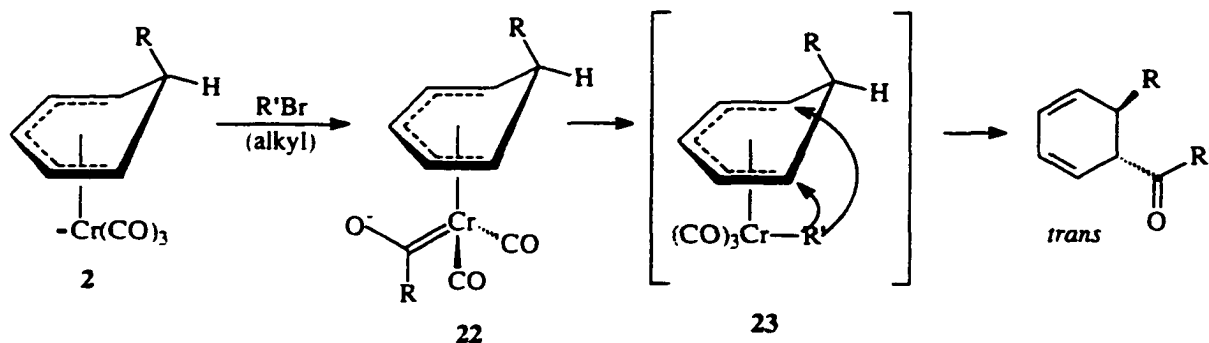
dihydrobenzenes with complete regio- and stereoselective C-C bond formation are scarce.¹⁵ However, when the arene is complexed to the electrophilic $\text{Cr}(\text{CO})_3$ group, the arenes can be transformed stereospecifically into *trans*-disubstituted cyclohexadienes (Equation 1.10).^{2,15,16} This straightforward procedure is carried out by addition of a carbanion followed by reaction with carbon based electrophiles (Equation 1.10) yielding *trans*-disubstituted cyclohexadienes. Addition of carbon substituents stereoselectively across an arene double bond is of great interest to organic chemists'.¹⁵⁻¹⁶

Equation 1.10



In Equation 1.10, alkyl, vinyl, and aryllithium reagents react with η^6 -arene-chromium tricarbonyl complex (7), the *exo*-nucleophilic addition results in the anionic cyclohexadienyl complex 2 previously discussed.^{15,16} Next, addition of an electrophile such as primary alkyl, allyl, and benzyl bromides at the carbonyl on the metal from the *endo*-direction resulted in direct reductive elimination yielding the *trans*-disubstituted cyclohexadiene.^{15,16} Incorporation of CO in this sequence depends on the nature of the arene and the migratory aptitude of R'.^{15,16}

Equation 1.11

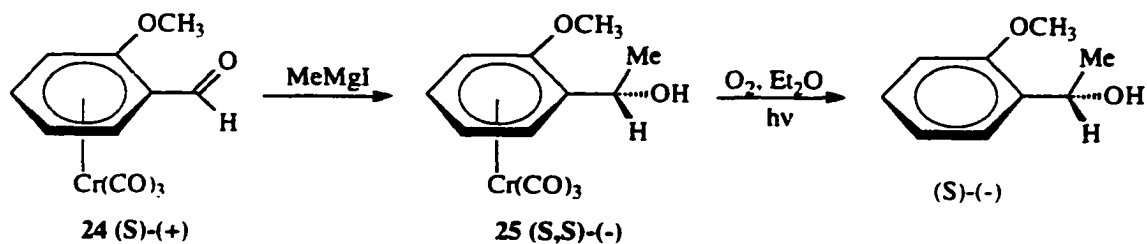


In some cases with alkyl halides the electrophile adds to a CO ligand (CO insertion) resulting in a acyl complex **22**, which upon warming the acyl complex to 25°C brings about a *trans*-disubstituted acylcyclohexadiene (Equation 1.11).^{2,15,16}

1.9 Asymmetric Synthesis Using Homochiral *o*-Anisaldehyde- $\text{Cr}(\text{CO})_3$ as a Chiral Auxiliary

ortho-Anisaldehyde chromium tricarbonyl complexes are chiral, and nucleophilic addition to the aldehyde carbonyl *via* Grignard reagents occurs completely stereoselectively to give, following decomplexation, homo α -substituted *o*-methoxybenzyl alcohol's result.⁴⁰⁻⁴⁵ As shown in Equation 1.12, addition of methyl magnesium iodide to (S)-(+)-*o*-anisaldehyde chromium tricarbonyl **24** at -78°C gives quantitatively (S,S)-(-)-*o*-methoxy-1-phenethanol chromium tricarbonyl **25**.⁴³ Decomplexation gave (S)-(-)-*o*-methoxy-1-phenyl-ethanol whose absolute configuration

Equation 1.12



was established via ^1H NMR, relative to the other known (S)-(+)-isomer. This methodology has been extended to include cyclization reactions producing *o*-aryl-tetrahydropyrans. In this application the metal acts as a steric blocking group rather than as an activator.

References for Chapter 1

1. Semmelhack, M.F.; Clark, G.R.; Garcia, D.C.; Harrison, J.J.; Thebtamongth, Y.; Wuff, W.A.; Yamashita, A., *Tetrahedron*, **1981**, *37*, 3957.
2. Semmelhack, M.F. in, "*Comprehensive Organometallic Chemistry II*", eds. Stone, F.G.A.; Abel, E.; Wilkinson, G.; Elsevier Science, Oxford, **1995**, *Vol. 12*, Chap. 9.1, p. 979.
3. KanMaguire, L.A.P.; Honig, E.D.; Sweigart, D.A., *Chem. Review*, **1994**, *84*, 525.
4. Zeiss, H.; Wheatley, P.J.; Winkler, H.J.S., "*Benzoid-Metal Complexes*", The Ronald Press Company, New York, **1966**.
5. Silverton, W.E., *Adv. Organomet. Chem.*, **1975**, *13*, 47.

6. Semmelhack, M.F.; Hall, H.T.; Yoshifuji, M.; Clark, G.; Bargar, T.; Hirotsu, C., *J. Amer. Chem. Soc.*, **1979**, *101*, 3535.
7. Bhasim, K.K.; Balkeen, W.G.; Pauson, P.L., *J. Organomet. Chem.*, **1981**, *204*, C25.
8. Collman, P.; Hegedus, L., "Principles and Applications of Transition Metal Chemistry" University Science Books, Mill Valley, California, **1980**, p.303-306, 604-625, 629, 653-668.
9. Schounheng, S.; Yeung, L.K.; Sweigart, D.A.; Lee, S.S.; Chung, Y.K.; Switzer, S.R.; Pike, R.D.: *Organometallics*, **1995**, *14*, 2613
10. Semmelhack, M.F.; Hall, H.T., *J. Amer. Chem. Soc.*, **1974**, *96*, 7091.
11. Evans, J.; Johnson, B.F.G.; Lewis, J.; Matheson, T., *J. Chem. Soc.*, **1975**, *97*, 1247.
12. Semmelhack, M.F.; Hall, H.T. Farina, R.; Yoshifuji, M.; Clark, G., *J. Amer. Chem. Soc.*, **1979**, *101*, 3536.
13. Astruc, D.*et. al.*, *Tetrahedron*, **1983**, *39*, 4027.
14. Sutherland, M, Iqbal, M.; Piorko, A., *J.Organomet. Chem.*, **1986**, *302*, 307.
15. Quattropiani, A.; Anderson, G.; Bernardinelli, G.; Kundig, P., *J. Amer. Chem. Soc.*, **1997**, *119*, 4773.
16. Kungig, E.P.; Ripa, A.; Liu, R.; Bernardinelli, G., *J. Org. Chem.*, **1994**, *59*, 4773.
17. Grutzner, J.B., *J. Amer. Chem. Soc.*, **1976**, *98*, 6387.
18. Knipes, A.C.; McGuinness, J.; Watts, W.E., *J. Chem. Soc. Chem. Commun.*, **1979**, 842.
19. Khand, I.V. Pauson, P.L.; Watts, W.E.: *J. Chem. Soc. (C)*, **1968**, 2257.
20. Nesmeyanov, A.N.; Vol' Kenau, N.A.; Bolesova, I.N., *Tetrahedron Lett.*, **1963**, 1725.

21. Lee, C.C.; Iqbal, M.; Gill, U.S.; Sutherland, R.G., *J. Organomet. Chem.*, **1985**, *288*, 89.
22. Helling, J.F.; Hedrickson, W.A., *J. Organomet. Chem.*, **1977**, *141*, 99.
23. Chung, Y.K.; Williard, P.G.; Sweigart, D.A.; *Organometallics*, **1982**, *1*, 1053.
24. Nicholls, B.; Whiting, M.C., *J. Chem. Soc.*, **1959**, *81*, 551.
25. Moriarty, R.M.; Gill, U.S., *Organometallics*, **1986**, *5*, 253.
26. Gill, U.S.; Moriarty, R.M.; Ku, Y.Y.; Butler, I.R., *J. Organomet. Chem.*, **1991**, *417*, 313.
27. Semmelhack, M.F.; Clark, G.; *J. Amer. Chem. Soc.*, **1977**, *99*, 1675.
28. Semmelhack, M.F.; Clark, G.R.; Farina, R.; Saeman, M., *J. Amer. Chem. Soc.*, **1979**, *101*, 217.
29. Kozikowski, A.P.; Isobe, K., *J. Chem. Soc., Chem. Commun.*, **1978**, 1076.
30. a.) Semmelhack, M.F.; Wulff, W.; Garcia, J.L., *J. Organomet. Chem.*, **1983**, *105*, 6962. b.) Semmelhack, M.F.; Garcia, J.L.; Cortes, D.; Farina, R.; Hong, R.; Carpenter, B.K., *Organometallics*, **1983**, *2*, 467.
31. Elsenbroich, C., *J. Organomet. Chem.*, **1968**, *14*, 157.
32. Rausch, M.D., *Pure Appl. Chem.*, **1972**, *30*, 523.
33. Beck, H.-J.; Fischer, E.O.; Kreiter, G.C., *J. Organomet. Chem.*, **1971**, *26*, C41.
34. Fischer, E.O.; Stucker, P.; Beck, H.-J.; Kreisel, F.R., *Chem. Ber.*, **1976**, *109*, 3089.
35. Fraser, R.R.; Mansour, T.S.; *J. Organomet. Chem.*, **1986**, *310*, C60.
36. Ceccon, A.; Catelani, G.; *J. Organomet. Chem.*, **1974**, *72*, 179.
37. Helling, J.F.; Cash, G.C.; *J. Organomet. Chem.*, **1974**, *73*, C10.
38. Semmelhack, M.F.; Harrison, J.J.; Thebtaranonth, Y., *J. Org. Chem.*, **1979**, *44*, 3275.

39. Walker, P.C.; Mawby, R.J., *Inorg. Chim. Acta.*, **1973**, 7, 621.
40. Blagg, J.; Davies, S.G.; Holman, N.J.; Laughton, C.A., Mobbs, B.E., *J. Chem. Soc. Perkins Trans.*, **1986**, 1581.
41. Davies, S.G.; Goodfellow, C.L.; *J. Chem. Soc. Perkins Trans.*, **1989**, 192.
42. Solladie-Covallo, A.; Solladie, G.; Tsamo, E.; *J. Org. Chem.*, **1979**, 44, 4189.
43. Bromely, L.A.; Davies, S.G.; Goodfellow, C.L., *Tet. Asymmetry*, **1991**, 2, 139.
44. Davies, S.G.; Donohoe, T.J.; Lister, M.A., *Tet. Asymmetry*, **1991**, 2, 1085.
45. Davies, S.G.; Donohoe, T.J.; Lister, M.A., *Tet. Asymmetry*, **1991**, 2, 1089.

Chapter 2

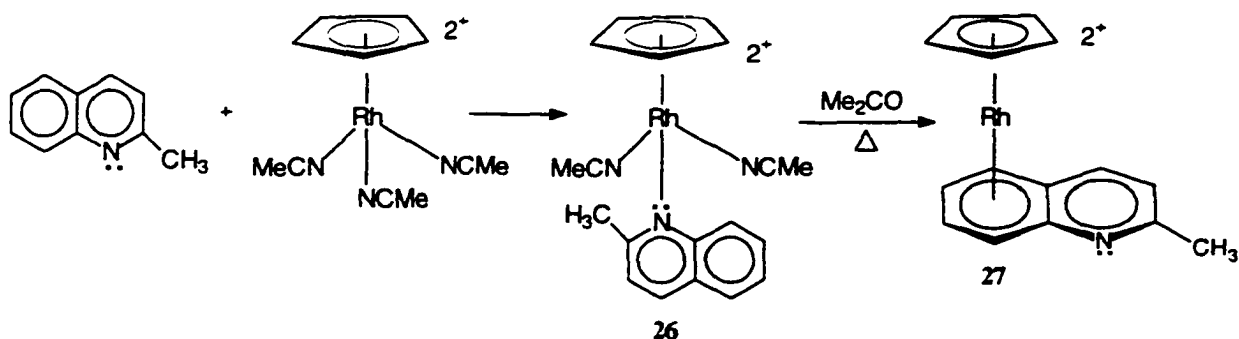
The Synthesis of Electron Deficient Quinoline

Triosmium Clusters

2.1 Introduction and Background of Quinolines Complexed to Transition Metals

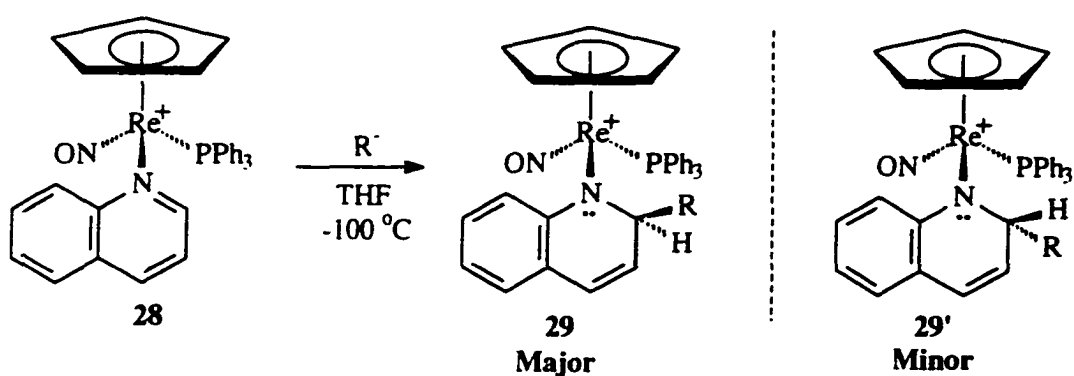
As previously discussed (Chapter 1) one can see that transition metal activated nucleophilic addition and substitution reactions of π -bound arenes have proven to be an extremely useful addition to the organic chemists' arsenal for functionalizing arenes, cyclizations, and asymmetric synthesis.¹⁻³ Recently, this methodology has been extended to include bicyclic arenes, heterocycles,⁴ and indoles,^{3,5} with nucleophilic addition to the coordinated ring. However, one notable substrate missing from this group for nucleophilic activation by transition metals is the quinoline family. One explanation for this is that the quinoline prefers η^1 -N coordination over η^6 coordination to the carbocyclic ring, due to the greater basicity of quinolines (from having the lone electron pair on the nitrogen exocyclic to the ring).⁶ There are only a few reported π - η^6 arene complexes of quinoline, one such example **27** is shown in Equation 2.1.

Equation 2.1



In this example 2-methylquinoline is coordinated to $[\eta^5\text{-CpRh}(\text{NCMe})_3]^{2+}$ to form a new η^1 -nitrogen bound complex **26** $[\eta^5\text{-CpRh}-\eta^1\text{-(C}_{10}\text{H}_9\text{N})]^{2+}$, which undergoes a thermal rearrangement when heated in acetone resulting in complex **27** with the rhodium η^6 coordinated to the carbocyclic ring. The overall yield is too low to study its reactivity towards nucleophiles. However, transition metal activation of quinoline towards nucleophilic addition and substitution has been studied for the η^1 -N complexes (as demonstrated in **28** Equation 2.2), showing selective nucleophilic addition to the heterocyclic ring of the quinoline as is the case for free quinolines.⁷

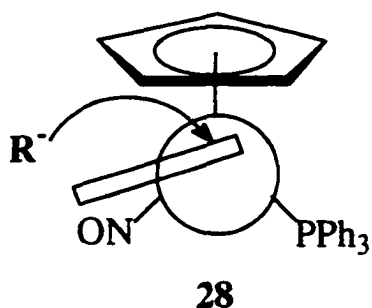
Equation 2.2



The chiral rhenium Lewis acid $[(\eta^5\text{-C}_5\text{H}_5)\text{Re}(\text{NO})(\text{PPh}_3)^+(\text{THF})]$ activates quinoline forming complex **28** $[(\eta^5\text{-C}_5\text{H}_5)\text{Re}(\text{NO})(\text{PPh}_3)\text{-(NC}_9\text{H}_7)]^+$ towards diastereoselective

nucleophilic addition at C-2 (Equation 2.2). The major product **29** is obtained with >92% diastereoselectivity, resulting from steric crowding of the bulky triphenylphosphines as shown in the stereoview of complex **28** (Scheme 2.1).

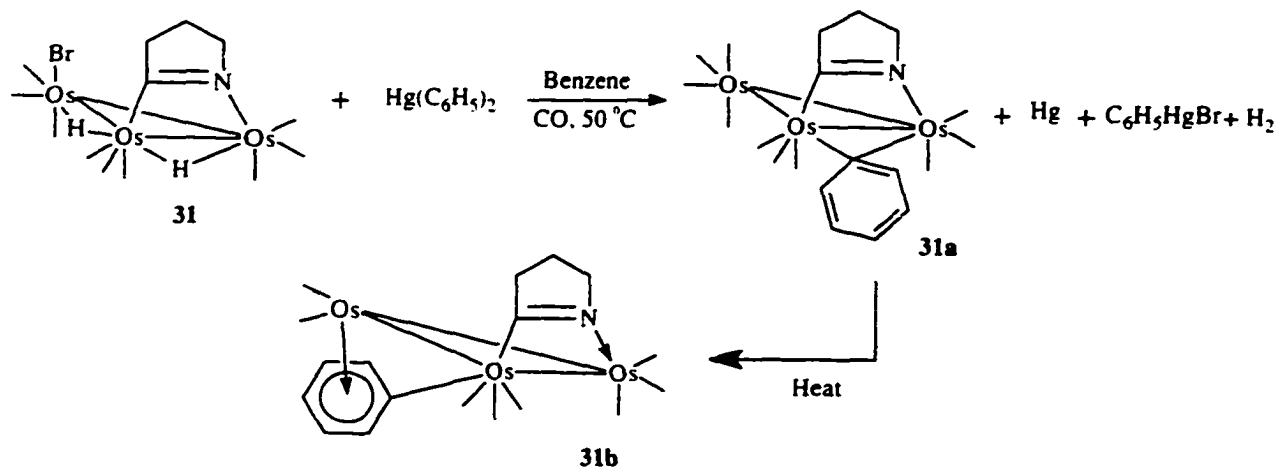
Scheme 2.1



The use of polymetallic complexes containing organic ligands in unusual bonding modes has shed considerable light on how a given organic ligand can interact with a polymetallic site on a metal surface.¹⁴ The use of polymetallic complexes leads to the possibility of multi-site coordination to the ligand. In some cases one metal can coordinate or protect one site, while the others can activate the complex by forming an electron deficient bond. An earlier example showing this involves the reaction of an unusual example of a trimetallic cluster containing a terminal halide (Equation 2.3) $\text{Os}_3(\text{CO})_9(\mu\text{-H})_2(\mu\text{-}\eta^2\text{-C=N(CH}_2)_3\text{)Br}$ **30** with diphenylmercury under a CO atmosphere, which yielded $\text{Os}_3(\text{CO})_{10}(\mu\text{-}\eta^2\text{-C=N(CH}_2)_3(\mu\text{-}\eta^1\text{-C}_6\text{H}_5)$ **31**. Thermolysis of **31** at 100°C leads to rapid decarbonylation and formation of one major product $\text{Os}_3(\text{CO})_8(\mu\text{-}\eta^2\text{-C=N(CH}_2)_3)(\mu\text{-}\eta^1\text{:}\eta^6\text{-C}_6\text{H}_5)$ **32**, making a unique example of a new μ -bonding mode for the phenyl ligand. Several other examples of trimetallic clusters containing a $\mu_1\text{-}\eta^1\text{-}$

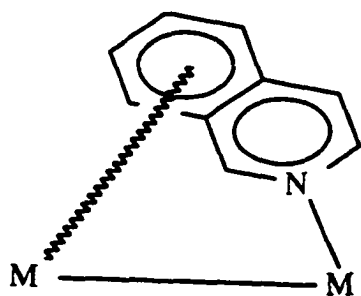
benzene interactions where the benzene ring is part of a more complex ligand system have been reported.¹⁴

Equation 2.3



This multi-metal coordination could be extended to include the quinoline ligand. In this case, the use of polymetallic binding holds out the possibility of multisite interactions which can alter the molecules reactivity (Scheme 2.2).

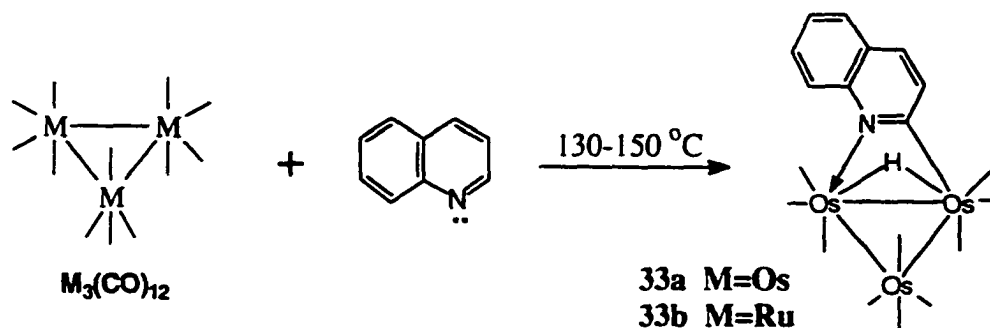
Scheme 2.2



The reaction of quinoline with $\text{M}_3(\text{CO})_{12}$ ($\text{M}=\text{Ru}, \text{Os}$) at elevated temperatures ($130\text{-}150^\circ\text{C}$) has been previously examined and yields complexes of the type $\text{M}_3(\text{CO})_{10}(\mu\text{-}\eta^2\text{-C}_9\text{H}_6\text{N})(\mu\text{-H})$ in which the C(2) C-H bond has oxidatively added to the

cluster, coordinating exclusively at the heterocyclic ring via coordination of C(2) and the nitrogen lone pair (Scheme 2.3).^{15,16} The mechanism by which this reaction is thought to occur involves a dissociation of a single CO from the metal at elevated temperatures, to open a single coordination site, followed by coordination of the nitrogen lone pair, and

Scheme 2.3



rearrangement to an $\eta^2-C=N$ complex, dissociation of a second CO and finally C(2)-H bond cleavage.^{15,16} These complexes are formed in very low yields and were found to be unreactive towards hydride donors.¹⁵

We have recently studied the reactions of quinoline (and substituted quinolines) with the lightly stabilized cluster $Os_3(CO)_{10}(CH_3CN)_2$ at ambient temperatures resulting in the major product $Os_3(CO)_{10}(\mu-\eta^2-C_9H_6N)(\mu-H)$ **34** where the nitrogen lone pair and the C(8) carbon hydrogen bond has been oxidatively added to the cluster. Minor amounts of the previously reported isomeric compound $Os_3(CO)_{10}(\mu-\eta^2-C_9H_6N)(\mu-H)$ **33a** were also formed. Decarbonylation of **34** thermally or photochemically gives the novel electron deficient (46 e⁻ system) deep green complexes $Os_3(CO)_9(\mu_3-\eta^2-C_9H_6N)(\mu-H)$ **35a-r**. The quinoline ring is bound to the cluster by coordination of the nitrogen lone pair and a three center two electron bond with C(8). Studies with ¹H NMR showed that

the proton on C(5) of these structures **35a-h**, **35m-r** all show significant downfield shifts (0.8 to 1.2 ppm) relative to structures **34**.

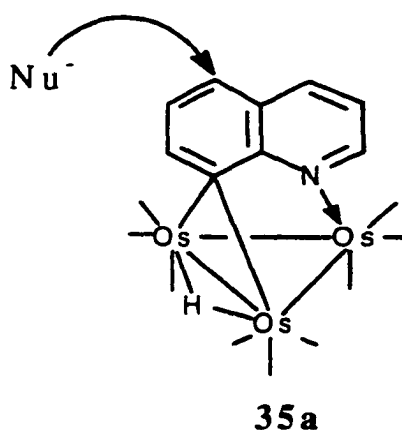
These electron deficient quinoline complexes are shown to undergo phosphine, CO, and H₂ addition to the metal which proceeds reversibly (for CO) under moderate conditions, analogous to other 46e- trimetallic complexes (discussed later in Chapter 4).⁸⁻

11

We recently studied the reactivity of this family of electron deficient $\sigma\text{-}\mu_3\text{-}\eta^2$ complexes of quinoline **35a** which undergo regioselective nucleophilic addition of hydride and a wide range of carbanions at the 5-position (Scheme 2.4).⁸⁻¹¹

Scheme 2.4

Regioselective Nucleophilic attack



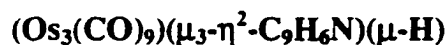
The nucleophilic attack we observed at the 5-position of the carbocyclic ring is unprecedented. In quinolines (or $\eta^1\text{-N}$ coordinated) the normal site of electrophilic attack is the 5- and 8- positions, while nucleophilic attack is usually at the 2- or the 4- position if the former is blocked (quinoline numbering).^{7,11} There has previously been reported

nucleophilic attack on " σ . π vinyl" complexes of triosmium clusters;⁷ however, the regioselective nucleophilic attack at the 5- position that we have observed is unprecedented in complexes of aromatic nitrogen heterocycles which are not π -complexed to the metal center and is completely unique for the quinoline system.⁷

A discussion of the results of a new methodology for the addition of carbon based nucleophiles to the carbocyclic ring will follow, which is based on the electron deficient bonding of C(8) carbon and the protective coordination of the nitrogen atom to the metal core. In light of the importance of the quinoline ring system in drug design and development,¹² as agonists for neurotransmitters molecules,¹² and as intermediates in natural product syntheses¹³ these results represent a potentially useful synthetic methodology not available via complexation by mono-metallic species. The structural features of the compounds reported and the mechanistic implications of the reported transformations are discussed and compared with the previously reported activation of aromatic systems (Chapter 1). First however, we will discuss the scope of the synthesis of these electron deficient triosmium clusters.

2.2 Results and Discussion

2.2.1 The Synthesis of Electron Deficient Monosubstituted Analogs of 35a



The synthesis of mono-substituted quinoline analogs of 35 opens the possibility for stereochemically controlled functionalization of the quinoline systems, after addition of the appropriate nucleophile. In cases with attractive functional groups on C(6) or C(4) adjacent to the nucleophilic site, it is possible to construct tricyclic systems.

The synthesis of these electron deficient complexes can be extended to a wide range of quinolines substituted in the 3, 4, 5, and 6 - positions (Scheme 2.5) in moderate to good yields (Table 2.1). Substitution in the 2 or 7- positions, however, does not result in formation of the decacarbonyl precursors to complexes of structural type **35a**, presumably due to steric crowding of the incipient coordination sites at the 2 and 8 - positions. Complexes **35a-r** are prepared by the reaction of quinoline (and substituted quinolines) with the lightly stabilized cluster **32** $[(Os_3(CO)_9(CH_3CN)_2)]$ at ambient temperatures resulting in the major product **34** $[(Os_3(CO)_9)(\mu-\eta^2-C_9H_6N)(\mu-H)]$ yellow in color, where the nitrogen lone pair and C(8) carbon-hydrogen bond has been oxidatively added to the cluster.

Scheme 2.5

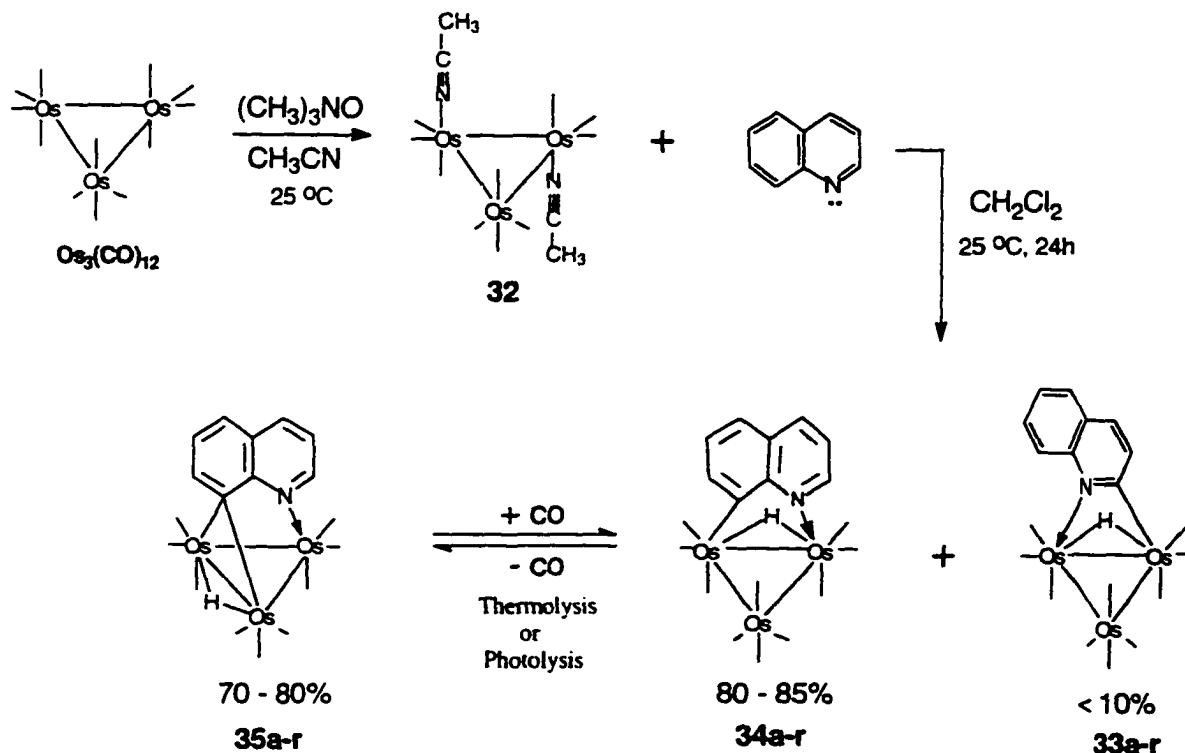


Table 2.1 Yields of Monosubstituted Electron Deficient Quinoline Triosmium Clusters

Compound	Substituent	Yield (%)
35a	H	68
35b	3-CO ₂ CH ₃	59
35c	3-NH ₂	50-60
35d	4-CH ₃	72
35e	4-Cl	76
35f	4-OCH ₃	69
35g	4-NH ₂	72
35h	4-CO ₂ CH ₃	40
35i	5-F	70
35j	5-Cl	70
35k	5-Br	83
35l	5-NH ₂	82
35m	6-CH ₃	84
35n	6-Cl	74
35o	6-OCH ₃	56
35p	6-CO ₂ CH ₃	61
35q	6-NH ₂	50-60
35r	6-OH	43

Minor amounts of the previously reported isomeric compound $[(Os_3(CO)_{10})(\mu-\eta^2-C_9H_6N)(\mu-H)]$ **33a** were also formed.¹⁷ Decarbonylation of **34** (by photochemical or thermal dissociation) gives the novel 46-electron deep green complexes $[(Os_3(CO)_{10})(\mu_3-\eta^2-C_9H_6N)(\mu-H)]$ **35a-r**.

The quinoline rings in **35a-r** are bound to the cluster by coordination of the nitrogen lone pair and a three center - two electron bond with carbon C(8). A solid state structure of **35n** $[(Os_3(CO)_{10})(\mu_3-\eta^2-C_9H_5(6-Cl)N)(\mu-H)]$ (the 6-chloro analogue of **35a**) is shown in Figure 2.1 with the selected bond lengths and angles in Table 2.2. The bond lengths given in Table 2.2 indicate that the aromatic nature of the carbocyclic ring remains unperturbed making **35n** and its analogues unique examples of an electron deficient species containing a μ_3 -heterocyclic aromatic ligand.

The structure of **35n** consists of a Os_3 triangle with three approximately equal Os-Os bonds (Table 2.2). The quinoline ligand sits perpendicular to the metal triangle, and Os(1)-C(8) and Os(3)-C(8) bonds are almost symmetrical suggesting a three center-two electron bond with carbon C(8).

In order to assess the impact of an electron donating group on the coordination chemistry observed for **35a**, we undertook the synthesis of the 3-,5- and 6- amino analogs of **35a**. The synthesis of these complexes proceeded in a straightforward manner as shown in Scheme 2.5. Significantly, the 5-amino derivative, $Os_3(CO)_9(\mu_3-\eta^2-5-NH_2C_9H_5)(\mu-H)$ (**35l**) formed directly, at ambient temperatures, without requiring thermal or photochemical decarbonylation (Equation 2.4).¹⁻³

Figure 2.1 Solid State Structure for 35n $[(Os_3(CO)_9)(\mu_3-\eta^2-C_9H_5(6-Cl)N)(\mu-H)]$
Showing the Position for the Hydride.

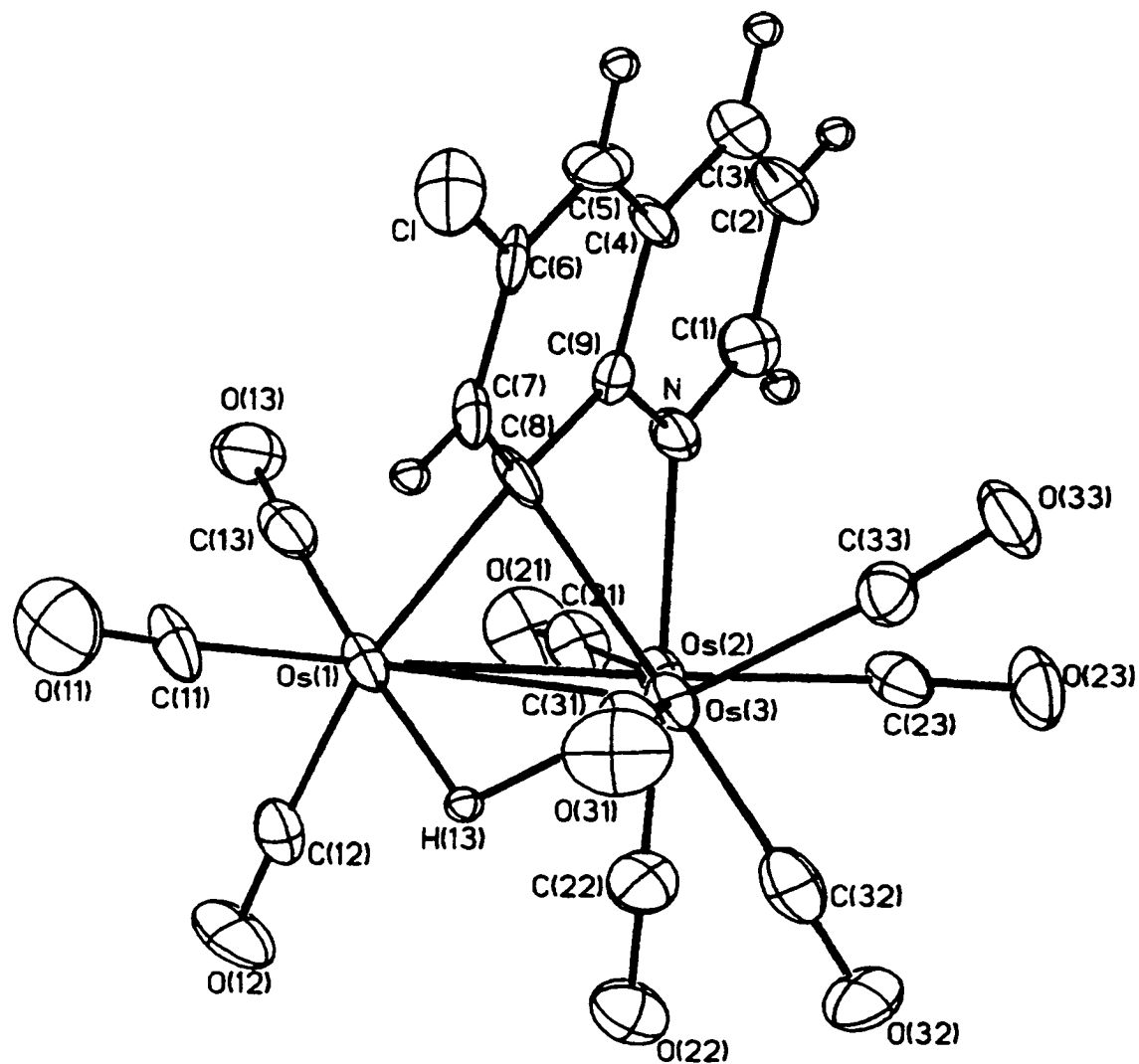


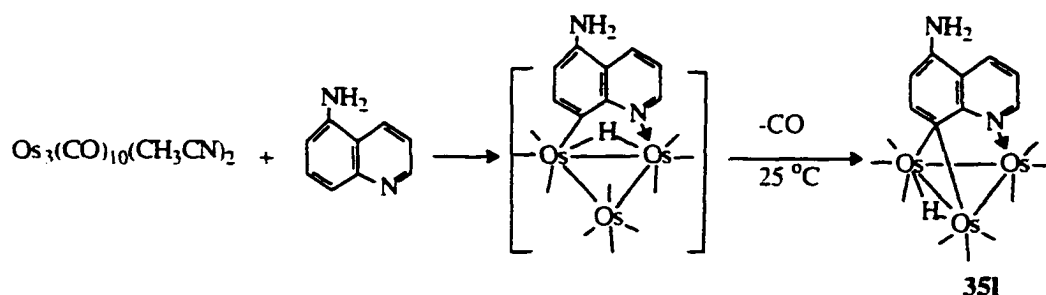
Table 2.2 Selected Bond Distances (Å) and Angles (°) for (35n) [(Os₃(CO)₉)(μ₃-η²-C₉H₅(6-Cl)N)(μ-H)]

Distances			
Os(1)-Os(2)	2.75(10)	C(1)-N	1.30(1)
Os(2)-Os(3)	2.78(10)	C(2)-C(1)	1.41(2)
Os(3)-Os(1)	2.77(10)	C(3)-C(2)	1.36(2)
Os(1)-C(8)	2.24(2)	C(4)-C(3)	1.41(2)
Os(2)-N	2.18(12)	C(5)-C(4)	1.39(2)
Os(3)-C(8)	2.32(2)	C(6)-C(5)	1.34(2)
C(7)-C(6)	1.39(2)	C(8)-C(7)	1.36(2)
C(4)-C(9)	1.42(2)	N-C(9)	1.35(2)
C(8)-C(9)	1.44(2)	C-O ^b	1.15(2)
Os-CO ^b	1.88(2)		
Angles			
Os(1)-Os(2)-Os(3)	60.04(3)	C(7)-C(8)-C(9)	115.7(3)
Os(1)-Os(3)-Os(2)	59.41(3)	C(8)-Os(1)-Os(3)	53.8(5)
Os(2)-Os(1)-Os(3)	60.55(3)	C(8)-Os(3)-Os(2)	77.1(3)
Os(1)-C(8)-Os(3)	74.90(3)	C(8)-Os(3)-Os(1)	51.3(3)
N(1)-Os(2)Os(3)	83.70(2)	Os-C-O ^b	177(3)

^a Numbers in parentheses are average standard deviations.

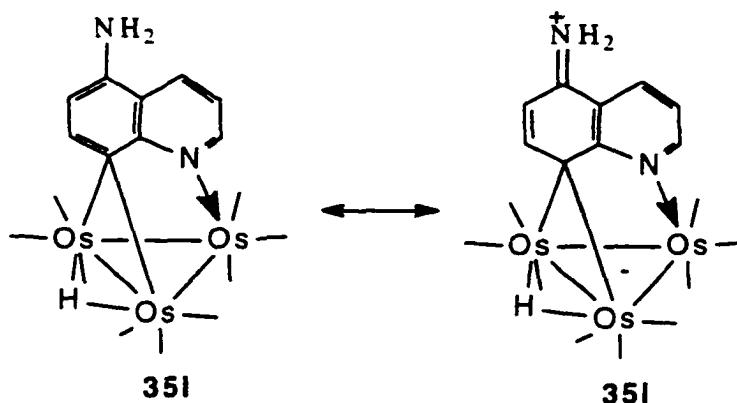
^b Average values.

Equation 2.4



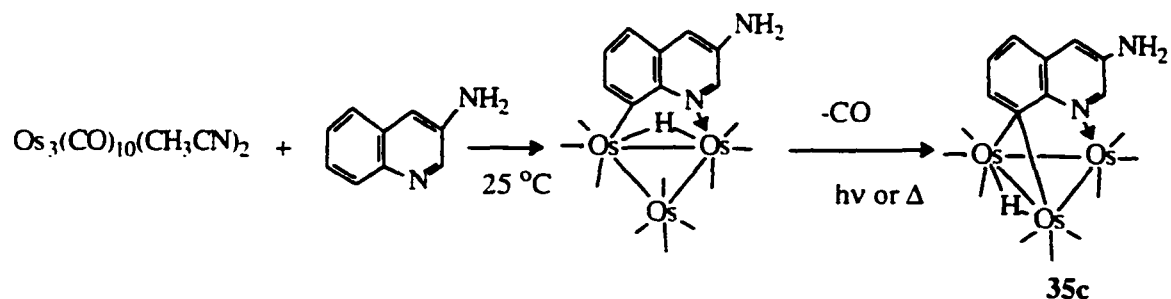
This undoubtedly reflects the impact of the strong π -electron donor in a position *para*- to the incipient three center-two electron band (Scheme 2.6). The 3- and 6- amino

Scheme 2.6

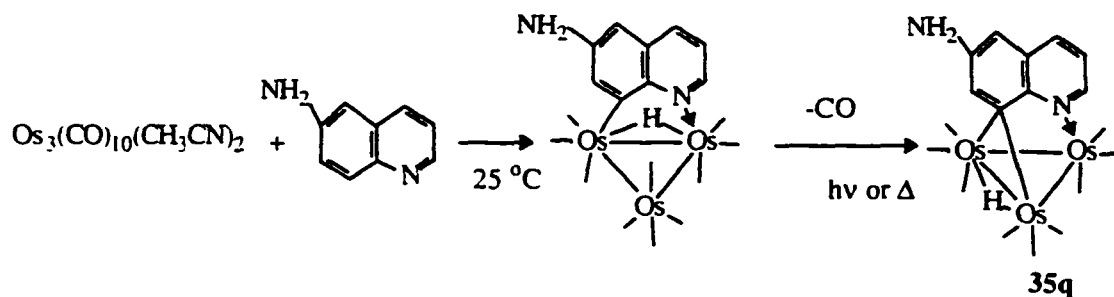


derivatives 35c and 35q did require the usual decarbonylation procedure (Equation 2.5 and 2.6). In all of these reactions (Equations 2.4-2.6) no detectable competition for coordination of the quinoline nitrogen by the aniline amino groups is seen but the yields of 35c and 35q were significantly lower than for 35I and 35a (Table 2.1). This is nicely explained by the two resonance structures that are formed as shown in Scheme 2.6.

Equation 2.5



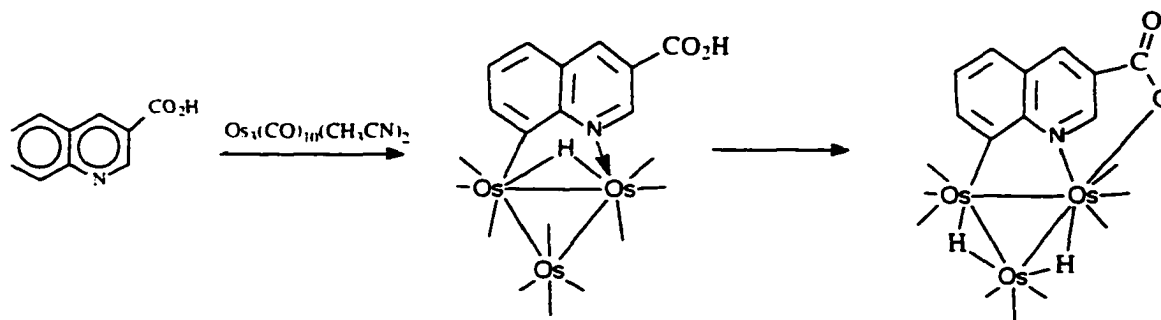
Equation 2.6



In the case of 3-carboxy quinoline, $\eta^2\text{-N-C}(8)$ is realized but further reaction with the free carboxyl group occurs to give a complex whose ^1H NMR suggests $[\text{Os}_3(\text{CO})_9(\mu_3\text{-}\mu^3\text{-C}_9\text{H}_5(3\text{-CO}_2)\text{N})(\mu\text{-H})_2]$ where the carboxylic acid hydrogen has oxidatively added to the cluster (Equation 2.7).

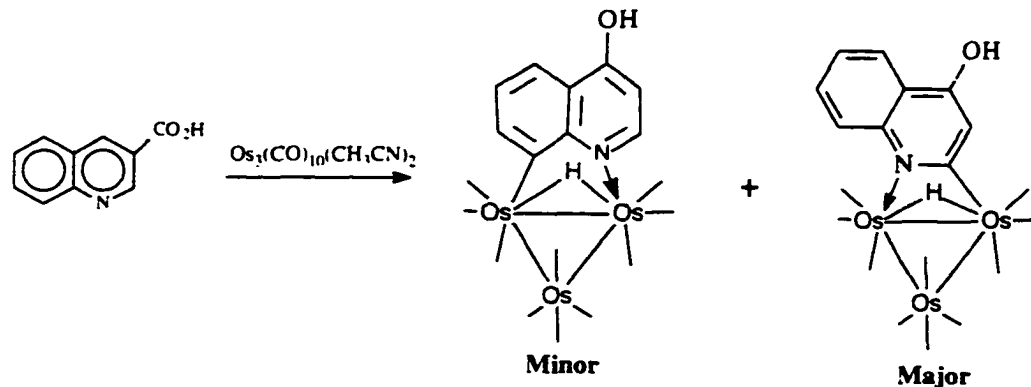
Methylation of the carboxyl group obviously blocks this secondary reaction and good yields of the desired analog, **35b**, are obtained after photolysis (Table 2.1). Similar results are realized for 4-carboxy quinoline and 6-carboxy quinoline methyl esters both of which give the desired products, **35h** and **35p**, in reasonable yields (Table 2.1).

Equation 2.7



The oxidative addition of the phenolic OH does not compete with CH oxidative addition or N coordination but does reverse the relative yields of the η^2 -N-C(8) and η^2 -N-C(2) products (Equation 2.8) with the desired decarbonyl product being obtained in insufficient amounts to warrant further reaction to the 4-hydroxy analog of **35a**.

Equation 2.8



This suggests that making the heterocyclic ring electron rich favors CH oxidative addition at C(2). This is a fairly subtle effect since the normal ratio of products is obtained with 4-methoxy quinoline and good yields are obtained of the 4-methoxy analog, **35f**, upon photolysis (Table 2.1). The 6-hydroxy derivative, **35r**, is obtained in reasonable yield as is the 6-methoxy derivative, **35o**.¹¹

2.4 Experimental Section

2.4.1 Material and General Considerations

All reactions were carried out under an atmosphere of nitrogen but were worked up in air. Tetrahydrofuran was distilled from benzophenone ketyl, additionally methylene chloride and acetonitrile from calcium hydride. Acetone- d_6 , methylene chloride- d_2 , and methanol- d_4 were purchased from Aldrich Chemical Co. in single ampules and used as received. Chloroform- d_1 was dried over molecular sieves before use.

Infrared spectra were recorded on a Perkin-Elmer 1600 FT-IR spectrometer and ^1H and ^{13}C NMR were recorded on a Varian Unity Plus 400. Elemental analyses were done by Schwarzkopf Microanalytical Labs, Woodside, New York. Chemical shifts are reported downfield relative to tetramethylsilane. Coupling constants are reported only for those resonances relevant to the stereochemistry and while only the multiplicities of resonances with standard couplings are reported.

Osmium carbonyl was purchased from Strem Chemical, used as received and converted to $\text{Os}_3(\text{CO})_{10}(\text{CH}_3\text{CN})_2$ by published procedures.²¹ Quinoline was purchased from Aldrich Chemical and distilled from calcium hydride before use. The 3-amino, 4-chloro, 5-amino, 6-methoxy, 6-methyl, 6-amino, 6-hydroxy, and 6-chloro quinolines were purchased from Aldrich Chemical and used as received. The 5-chloro²², 5-Br²², 5-F²³, and 4-methoxy²⁴ were prepared according to literature procedures. The 3- CO_2CH_3 , 4- CO_2CH_3 , and 6- CO_2CH_3 quinolines were prepared from the corresponding carboxylic acids (purchased from Aldrich) via an esterification reaction by refluxing for 3h in a 10% ($\text{H}_2\text{SO}_4:\text{MeOH}$) solution.²⁵ The 4-amino quinoline was prepared by the Raney Nickel

catalyzed reduction (6hrs. at 70°C. 350 p.s.i. H₂) of 4-nitro-quinoline-N-oxide.²⁶
 Compounds **35a**, **35d**, and **35m** were previously reported.⁸⁻¹⁰

2.4.2 The Preparation of Electron Deficient Mono-substituted Quinoline

Complexes: Os₃(CO)₉(μ₃-η²-C₉H₅(R)N)(μ-H) (R=3-CO₂CH₃, **35b**; R=3-NH₂, **35c**; R=4-Cl, **35e**; R=4-OCH₃, **35f**; R=4-NH₂, **35g**; R=4-CO₂CH₃, **35h**; R=5-F, **35i**; R=5-Cl, **35j**; R=5-Br, **35k**; R=6-Cl, **35n**; R=6-OMe, **35o**; R=6-CO₂CH₃, **35p**; R=6-NH₂, **35q**; R=OH, **35r**).

The following procedure was used for synthesizing the substituted quinoline triosmium complexes in Section 2.4.2. Os₃(CO)₁₀(CH₃CN)₂ (0.250-0.500 g, 0.27-0.54 mmol) were dissolved in 150-300 mL CH₂Cl₂ and a two-fold molar excess of the appropriate quinoline was added. The reaction mixture was stirred for 12-20 h and then filtered through a short silica gel column to remove excess ligand. The yellow-green reaction solution was collected in a 500 mL quartz reaction vessel and irradiated in a Rayonet photo-reaction chamber for 2-4 h until no further conversion was detected by analytical thin layer chromatography (TLC). One exception to this procedure was **35l** (shown separately below). The dark green solution was then filtered through a short silica gel column concentrated to 50-150 mL and cooled at -20°C to yield 200-300 mg of Os₃(CO)₉(μ₃-η²-C₉H₅(R)N)(μ-H). The mother liquor was rotary evaporated and taken up in a minimum amount of CH₂Cl₂ and eluted on 0.1x20x40 cm silica gel TLC plates using (20-40%) CH₂Cl₂ / hexane as the eluent. Three bands were eluted. The two faster moving yellow bands contained minor amounts of the decacarbonyl quinoline triosmium

complexes and slower moving dark green band contained additional product which was crystallized from methylene chloride hexanes. The combined total yields (based on $\text{Os}_3(\text{CO})_{12}$) of the products are listed below with the analytical and spectroscopic data.

Preparation of $\text{Os}_3(\text{CO})_9(\mu_3\text{-}\eta^2\text{-(5-NH}_2\text{)C}_9\text{H}_5\text{N})(\mu\text{-H})$ **35l**

$\text{Os}_3(\text{CO})_{10}(\text{MeCN})_2$ (0.250 g, 0.268 mmol) was dissolved in CH_2Cl_2 (150 mL) and 5- amino quinoline (0.080 g, 0.5 mmol) was added. The reaction mixture was stirred for 16 h at room temperature. The resulting deep green solution was separated and filtered through a 14" column containing silica gel and eluted with hexane / CH_2Cl_2 (70:30), giving two bands. The first yellow band was a mixture of the isomers $\text{Os}_3(\text{CO})_{10}(\mu\text{-}\eta^2\text{-(5-NH}_2\text{)C}_9\text{H}_5\text{N})(\mu\text{-H})$ (less than 10%). The second fraction yielded (0.223 g, 0.219 mmol, 82.3% overall from $\text{Os}_3(\text{CO})_{10}(\text{CH}_3\text{CN})_2$) of the green major product **35l**, $\text{Os}_3(\text{CO})_9(\mu_3\text{-}\eta^2\text{-(5-NH}_2\text{)C}_9\text{H}_5\text{N})(\mu\text{-H})$ which gave green crystals from hexane / CH_2Cl_2 at -20°C .

2.4.3 Analytical and Spectroscopic Data for **35b**, **35c**, **35e-35l**, and **35n-35r**.

Compound **35b**: Yield for **35b**: 59.1%. Anal. Calcd. for $\text{C}_{20}\text{H}_9\text{NO}_{11}\text{Os}_3$: C, 23.76; H, 0.99; N, 1.38 %. Found: C, 23.52; H, 0.82; N, 1.40 %. IR (ν CO) in CH_2Cl_2 : 2078 s, 2050 s, 2022 s, 1994 br, 1954 w cm^{-1} . ^1H NMR of **35b** at 400 MHz in CDCl_3 : δ 9.74 (s, H(2)), 8.69 (s, H(4)), 8.66 (dd, H(5)), 8.48 (dd, H(7)), 7.28 (t, H(6)), 4.04 (s, CH_3), -12.063 (s, hydride).

Compound **35c**: Yield for **35c**: 50-60%. Anal. Calcd for $C_{18}H_8N_2O_9Os_3$: C, 22.38; H, 0.78; N, 2.76. Found: C, 22.12; H, 1.02; N, 2.84. IR(ν (CO) in CH_2Cl_2): 2076w, 2050s, 2017s, 1989m, br. 1H NMR at 400 MHz in Acetone- d_6 : δ 9.31(d, 1H), 8.68(dd, 1H), 8.61(dd, 1H), 7.41(d, 1H), 7.30(dd, 1H), 4.14(s, br, 2H), -12.23(s, 1H).

Compound **35e**: Yield for **35e**: 75.9%. Anal. Calcd for $C_{18}H_6ClNO_9Os_3$: C, 21.90; H, 0.61; N, 1.41%. Found: C, 22.50; H, 0.70; N, 1.38%. IR (ν CO) in hexane: 2077 m, 2050 s, 2021 m, 1991 br, 1969 w. 1H NMR of **35e** at 400 MHz in $CDCl_3$: * 9.16 (dd, H(2)), 8.83 (dd, H(5)), 8.67 (d, H(7)), 7.29 (dd, H(6)) 7.18 (dd, H(3)), -12.06 (s, hydride).

Compound **35f**: Yield for **35f**: 69.0%. Anal. Calcd for $C_{19}H_9NO_{10}Os_3$: C, 23.24; H, 0.91; N, 1.43%. Found: C, 23.44; H, 0.93; N, 1.46%. IR (ν CO) in hexane: 2075 m, 2046 s, 2018 m, 1988 br. 1H NMR of **35f** at 400 MHz in $CDCl_3$: δ 9.03 (d, H(2)), 8.88 (dd, H(5)), 8.65 (dd, H(7)), 7.14 (dd, H(6)), 6.42 (d, H(3)), 4.08 (s, OCH_3) -12.01 (s, hydride).

Compound **35g**: Yield for **35g**: 72.2%. Anal. Calcd. $C_{18}H_8N_2O_9Os_3$: C, 22.34; H, 0.83; N, 2.89 %. Found: C, 21.07; H, 0.79; N, 2.58 %. IR (ν CO) in CH_2Cl_2 : 2078 s, 2050 s, 2022 s, 1994 br, 1954 w cm^{-1} . 1H NMR of **35g** at 400 MHz in CD_3COCD_3 : δ 9.09 (s, H(2)), 8.81 (d, H(5)), 8.65 (dd, H(3)), 7.46 (S broad, NH_2), 7.23 (t, H(6)), 6.48 (d, H(7)), -12.072 (s, hydride).

Compound **35h**: Yield for **35h**: 40.3%. Anal. Calcd. $C_{20}H_9NO_{11}Os_3$: C, 23.76; H, 0.99; N, 1.38 %. Found: C, 23.14; H, 0.88; N, 1.35 %. IR (ν CO) in CH_2Cl_2 : 2078 s, 2050 s, 2022 s, 1994 br, 1954 w cm^{-1} . 1H NMR of **35h** at 400 MHz in $CDCl_3$: δ 9.45 (d, H(2)), 9.41 (d, H(5)), 8.62 (d, H(7)), 7.56 (t, H(3)), 7.28 (t, H(6)), 4.02 (s, CH_3), -12.242 (s, hydride).

Compound **35i**: Yield for **35i**: 70.1%. Anal. Calcd. $C_{18}H_6NO_9FOs_3$: C, 22.27; H, 0.99; N, 1.38 %. Found: C, 22.84; H, 1.12; N, 1.44 %. IR (ν CO) in CH_2Cl_2 : 2076 s, 2050 s, 2026 s, 1996 m, 1980 m, 1962 w, 1948 w cm^{-1} . 1H NMR of **35i** at 400 MHz in $CDCl_3$: δ 9.32 (dd, H(2)), 8.65 (d, H(6)), 8.32 (dd, H(4)), 7.16 (dd, H(7)), 6.95 (t, H(3)), -12.204 (s, hydride).

Compound **35j**: Yield for **35j**: 69.7%. Anal. Calcd for $C_{18}H_6ClNO_9Os_3$: C, 21.90; H, 0.61; N, 1.41%. Found: C, 22.66; H, 0.71; N, 1.37%. IR (ν CO) in hexane: 2078 m, 2049 s, 2023 s, 1990 br. 1H NMR of **35j** at 400 MHz in $CDCl_3$: δ 9.33 (dd, H(2)), 8.52 (d, H(6)), 8.48 (dd, H(4)), 7.27 (d, H(7)) 7.20 (t, H(3)), -12.09 (s, hydride).

Compound **35k**: Yield for **35k**: 83.1%. Anal Calcd. for $C_{18}H_6NO_9BrOs_3$: C, 20.97; H, 0.48, N, 1.36. Found: C, 20.84 ; H, 0.38; N, 1.37; IR(ν (CO) in CH_2Cl_2): 2077m, 2050s, 2020s, 1990s, 1977w, 1952w. 1H NMR of **35k** at 400 MHz in $CDCl_3$: δ 9.32(dd, 1H), 8.49(dd, 1H), 8.39(d, 1H), 7.46(d, 1H), 7.19(dd, 1H), -12.07(s, 1H).

Compound 35l: Yield for **35l**: 82.3%. Anal. calcd for $C_{18}H_8N_2O_9Os_3$: C, 22.38, H, 0.78; N, 2.76. Found: C, 22.37; H, 0.75; N, 2.83. IR (ν (CO) in hexane): 2080w, 2069m, 2040s, 2013s, 1981s, 1967w. 1H -NMR of **35l** at 400 MHz in $CDCl_3$: δ 9.25 (dd, H(2)), 7.07 (t, H(3)), 8.00 (dd, H(4)), 8.16 (dd, H(6)), 6.43 (d, H(7)), 5.60 (broad singlet, NH_2), -13.01 (s, hydride).

Compound 35n: Yield for **35n**: 73.6%. Anal. Calcd for $C_{18}H_6ClNO_9Os_3$: C, 21.90; H, 0.61; N, 1.41%. Found: C, 22.90; H, 1.01; N, 1.16 %. IR (ν CO) in hexane: 2060 m, 2031 s, 2027s, 1992 w, 1983 br. 1H NMR of **35n** at 400 MHz in $CDCl_3$: δ 9.24 (dd, H(2)), 8.35 (dd overlap, H(5) & H(7)), 7.97 (dd, H(4)), 7.13 (dd, H(3)), -12.12 (s, hydride).

Compound 35o: Yield for **35o**: 56.1%. Anal. Calcd for $C_{19}H_9NO_{10}Os_3$: C, 23.21; H, 0.91; N, 1.43%. Found: C, 22.58; H, 0.87; N, 1.15%. IR (ν CO) in hexane: 2102 m, 2077 s, 2047 s, 2019 s, 1989 br. 1H NMR of **35o** at 400 MHz in $CDCl_3$: δ 9.04 (d, H(2)), 8.06 (d, H(7)), 7.92 (dd, H(4)), 7.53 (d, H(5)), 7.04 (dd, H(3)), 3.89 (s, OCH_3) -12.27 (s, hydride).

Compound 35p: Yield for **35p**: 61.4%. Anal. Calcd. $C_{20}H_9NO_{11}Os_3$: C, 23.76; H, 0.99; N, 1.38 %. Found: C, 23.70; H, 1.04; N, 1.57 %. IR (ν CO) in CH_2Cl_2 : 2079 s, 205 s, 2023 s, 1994 br, 1954 w cm^{-1} . 1H NMR of **35p** at 400 MHz in $CDCl_3$: δ 9.32 (dd, H(2)), 9.02

(s. H(5)), 8.93 (s, H(7)), 8.12 (dd, H(4)), 7.17 (t, H(3)), 4.01 (s, CH₃), -12.063 (s, hydride).

Compound **35q**: Yield for **35q**: 50-60%. Anal. Calcd. for C₁₈H₈N₂O₉Os₃: C, 22.38; H, 0.78; N, 2.76. Found: C, 22.49, H, 0.86; N, 2.71. IR (ν(CO) in CH₂Cl₂): 2076w, 2041s, 2018s, 1988m, br. 1973w, br. ¹H NMR of **35q** at 400 MHz in CDCl₃: δ 8.92(dd, 1H), 7.83(d, 1H), 7.79(dd, 1H), 7.36(d, 1H), 6.97(dd, 1H), 4.79(s, br 2H), -12.23(s, 1H).

Compound **35r**: Yield for **35r**: 43%. Anal. calcd. for C₁₈H₇NO₁₀Os₃: C, 22.34; H, 0.72; N, 1.45%. Found: C, 21.99; H, 0.75; N, 1.41 %. IR (ν CO) in CH₂Cl₂: 2076 m, 2058 s, 2047 s, 2018 s, 1990s, br. 1941 w, br cm⁻¹. ¹H NMR of **35r** at 400 MHz in CDCl₃: δ 9.08 (d, H(2)), 8.15 (d, H(7)), 7.91 (d, H(4)), 7.71 (d, H(5)), 7.05 (dd, H(3)), 6.01 (br, OH), -12.07 (s, hydride).

2.5 X-ray Structure Determination of **35n**.

Crystals of **35n** for X-ray examination were obtained from saturated solutions of each in hexane / CH₂Cl₂ solvent systems at -20°C. Suitable crystals were mounted on glass fibers, placed in a goniometer head on the Enraf-Nonius CAD4 diffractometer, and centered optically. Unit cell parameters and an orientation matrix for data collection were obtained by using the centering program in the CAD4 system. For each crystal, the actual scan range was calculated by scan width = scan range + 0.35 tanθ and backgrounds were measured by using the moving-crystal moving-counter technique at the beginning and end of each scan. Two representative reflections were monitored every

2 h as a check on instrument and crystal stability. Lorentz, polarization, and decay corrections were applied, as was an empirical absorption correction based on a series of Ψ scans, for each crystal. The weighting Scheme used during refinement was $1/\sigma^2$, based on counting statistics.

Each of the structures was solved by the Patterson method using SHELXS-86,²⁷ which revealed the positions of the metal atoms. All other non-hydrogen atoms were found by successive difference Fourier syntheses. The expected hydride positions in each were calculated by using the program HYDEX,¹⁵ hydrogen atoms were included in each structure and were placed in their expected chemical positions using the HFIX command in SHELXL-93.²⁸ The hydrides were given fixed positions and U's; other hydrogen atoms were included as riding atoms in the final least squares refinements with U's which were related to the atoms ridden upon. All other non-hydrogen atoms were refined anisotropically in **35n**.

Scattering factors and anomalous dispersion coefficients were taken from International Tables for X-ray Crystallography.²⁹ All data processing was carried out on a DEC 3000 AXP computer using the Open MolEN system of programs.³⁰ Structure solution, refinement and preparation of Figures and Tables for publication were carried out on PC's using SHELXS-86,²⁷ SHELXL-93²⁸ and SHELXTL/PC³¹ programs.

2.6 References for Chapter 2

1. Kane.-Maguire, L.A.P.; Honig, E.D.; Sweigart, D.A. *Chem. Rev.*, **1994** *84*, 525.
2. a) Bromley, L.A.; Davies, S.G.; Goodfellow, C.L. *Tet. Asymmetry*, **1991**, *2*, 139.
b) Davies, S.G.; Donohoe, T.J.; Lister, M.A. *Tet. Asymmetry*, **1991**, *2*, 1089.
3. Semmelhack, M.F.; Clark, G.R.; Garcia, D.C.; Harrison, J.J.; Thebtarmonth, Y.; Wuff, W.A.; Yamashita, A. *Tetrahedron*. **1981** *37*, 3957.
4. Shouheng, S.; Yeung, L.K.; Sweigart, D.A.; Lee, T.Y.; Lee, S.S.; Chung, Y.K.; Switzer, S.R.; Pike, R.D. *Organometallics*, **1995**, *14*, 2613.
5. Gill, U.S.; Moriarty, R.M.; Ku, Y.Y.; Butler, I.R. *J. Organometal. Chem.*, **1991**, *417*, 313.
6. Fish, R.H.; Baralt, E.; Kim, H.S.; *Organometallics*, **1991**, *10*, 1965.
7. Gladysz, J.A.; Stark, G.A.; Arif, A.M. *Organometallics*, **1994**, *13*, 4523.
8. Kabir, S.E.; Kolwaite, D.S.; Rosenberg, E.; Hardcastle, K.; Cresswell, W.; Grindstaff, J. *Organometallics*, **1995**, *14*, 3611.
9. Arcia, E.; Kolwaite, D.S.; Rosenberg, E.; Hardcastle, K.I.; Ciurash, J.; Duque, R.; Milone, L.; Gobetto, R.; Osella, D.; Botta, M.; Dastru`, W.; Viale, A.; Fiedler, J. *Organometallics*, **1998**, *17*, 415.
10. Bar Din, A.; Bergman, B.; Rosenberg, E.; Smith, R.; Dastru`, W.; Viale, A.; Milone, L.; Gobetto, R. *Polyhedron*, **1998**, in press.
11. Jones, G.; in "Quinolines," ed. Jones, G., Wiley Interscience, London, **1977**.
12. a.) Schaus, J.M.; Kornfield, E.C.; Titus, R.D.; Nichols, C.L.; Clemens, J.A.; Smatstig, E.B.; Fuller, R.W.; *Drug Des. And Disc.*, **1993**, *9*, 323. b.) Van Wijngaarden, I.; Tulp, M. Th. M., *Eur. J. Pharmacol.*, **1990**, *188*, 301.

13. a.) Micheal, J.P.; *Nat. Prod. Rep.*, **1995**, 12, 77. a.) Avarez, M.; Salas, M.; Joule, J.A., *Heterocycles*, **1991**, 32, 759.
14. Kabir, K.E.; Rosenberg, E.; Stetson, J., *Organometallics*, **1996**, 15, 4473.
15. Fish, R.H.; Kim, J.J.; Stewart, J.L.; Busweller, J.H.; Rosen, R.K.; Dupon, J.W.; *Organometallics*, **1986**, 5, 2193.
16. Eisenstadt, A.; Gianomencio, C.M.; Frederick, M.F.; Laine, R.M., *Organometallics*, **1985**, 4, 2033.
17. Nelson, A., *Journal Amer. Chem. Soc.*, **1979**, 485.
18. Coleman, J.P.; Hegedus, L.S.; Norton, J.R.; Fink, R.G. "Principles and Applications of Organotransition Metal Chemistry, University Science Books, Mill Valley, Ca. 1987, Chap 3, p96.
19. Semmelhack, M.F.; Sanfert, W.; Keller, L. *J. Amer. Chem. Soc.*, **1980**, 102, 6584.
20. Bergman, B.; Kabir, S.E.; Abedin, Md. J.; Rosenberg, E.; Hardcastle, K.I. Manuscript in preparation.
21. Lewis, J.; Dyson, P.J.; Alexander, B.J.; Johnson, B.F.G.; Martin, C.M.; Nairn, J.G.M.; Parsini, E. *J. Chem. Soc., Dalton Trans.*, **1993**, 981.
22. Bradford, L.; Elliot, T.J.; Rowe, F.M. *J. Chem. Soc.*, **1947**, 437.
23. Roe, A.; Hawkins, G.F.; *J. Amer. Chem. Soc.*, 71, **1949**, 1785.
24. Backeberg, B. *J. Chem. Soc.*, **1933**, 618.
25. Uhle; Jacobs; *J. Org. Chem.*, 10, **1945**, 76, 82.
26. a.) Hauser; Reynolds; *J. Org. Chem.*, 15, **1950**, 4612. b.) Hauser; Reynolds; *J. Org. Chem.*, 18, **1953**, 12386.
27. Sheldrick, G.M. *Acta Crystallogr.*, **1990**, A46, 467.

28. Sheldrick, G.M. Program for Structure Refinement. University of Goettingen, Germany. **1993.**
29. Wilson, A.J.C.(ed). *International Tables for X-ray Crystallography, Volume C.* Kluwer Academic Publishers, **1992.** Dordrecht: Tables 6.1.1.4 (pp 500-502) and 4.2.6.8 (pp 219-222).
30. Fair, C. Kay. "*MolEN*" *Structure Determination System*, Enraf-Nonius, Delft, The Netherlands , **1990.**
31. SHELXTL/PC, Siemens Analytical X-ray Instruments, Inc., Madison, WI, USA, **1993.**

Chapter 3

Reactivity of Carbanions with $(\text{Os}_3\text{CO})_9(\mu_3\text{-}\eta^2\text{-C}_9\text{H}_6\text{N})(\mu\text{-H})$ and its Monosubstituted Analogues

3.1 Introduction

We have previously discussed in Chapter 2 the reactions of quinoline (and substituted quinolines) with the lightly stabilized cluster $\text{Os}_3(\text{CO})_{10}(\text{CH}_3\text{CN})_2$ at ambient temperatures resulting in the novel electron deficient (46 e⁻ system) deep green complexes $\text{Os}_3(\text{CO})_9(\mu_3\text{-}\eta^2\text{-C}_9\text{H}_6\text{N})(\mu\text{-H})$ **35a-r**.¹⁻⁴ The quinoline ring in complexes **35a-r** is bound to the cluster by coordination of the nitrogen lone pair and a three center two electron bond with C(8).¹⁻⁴ Studies with ¹H NMR showed that the proton on C(5) of these structures **35a-h**, **35m-r** all show significant downfield shifts (0.8 to 1.2 ppm) relative to structures **34**.¹⁻⁴

These electron deficient quinoline complexes are shown to undergo phosphine, CO, and H₂ addition to the metal which proceeds reversibly (for CO) under moderate conditions, analogous to other 46e⁻ trimetallic complexes (discussed later in Chapter 4).¹⁻⁴

We recently studied the reactivity of this family of electron deficient σ - μ_3 - η^2 complexes of quinoline **35a** which undergo regioselective nucleophilic addition of hydride and a wide range of carbanions at the 5-position (Equation 3.1).¹⁻⁴

The nucleophilic attack we observed at the 5-position of the carbocyclic ring is unprecedented. In quinolines (or η^1 -N coordinated) the normal site of electrophilic attack is the 5- and 8- positions, while nucleophilic attack is usually at the 2- or the 4- position if the former is blocked (quinoline numbering).^{7,11} There has previously been reported nucleophilic attack on " σ , π vinyl" complexes of triosmium clusters;⁷ however, the regioselective nucleophilic attack at the 5- position that we have observed is unprecedented in complexes of aromatic nitrogen heterocycles which are not π -complexed to the metal center and is completely unique for the quinoline system.⁷

A discussion of the results of a new methodology for the addition of carbon based nucleophiles to the carbocyclic ring will follow, which is based on the electron deficient bonding of C(8) carbon and the protective coordination of the nitrogen atom to the metal core. These results represent a potentially useful synthetic methodology not available via complexation by mono-metallic species. The structural features of the compounds reported and the mechanistic implications of the reported transformations are discussed and compared with the previously reported activation of aromatic systems (Chapter 1).

3.2 Results and Discussion

3.2.1 Reactions of Carbanions with $(\mu\text{-H})(\text{Os}_3\text{CO})_9(\mu_3\text{-}\eta^2\text{-C}_9\text{H}_6\text{N})$ **35a**

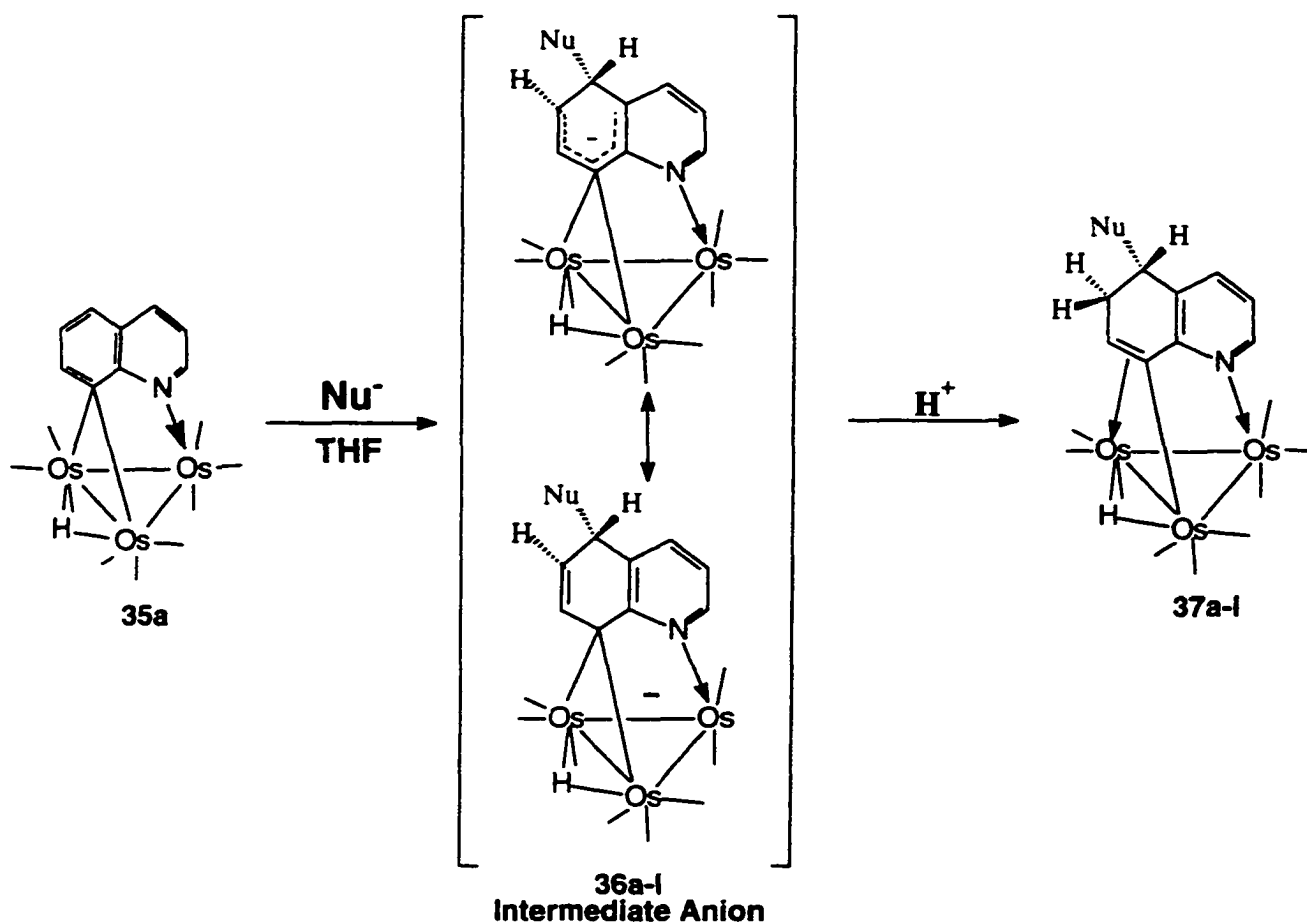
When compound **35a** is reacted with a two-to-three fold excess of the carbanions listed in Table 3.1 at -78°C , the dark green THF solution turns orange or amber. After stirring and warming to 0°C the solution is cooled to -78°C and quenched with a slight excess (relative to the total carbanion added) of trifluoroacetic acid to give a red orange solution (Equation 3.1). After chromatographic purification, the nucleophilic addition products $[\text{Os}_3(\text{CO})_9(\mu_3\text{-}\eta^3\text{-C}_9\text{H}_7(5\text{-R}')\text{N})(\mu\text{-H})]$ (**37a-37l**) are isolated in the moderate yields reported in Table 3.1.

One specific example that demonstrates this novel nucleophilic attack at the 5-position of the quinoline is shown when phenyllithium was reacted with **35a**, resulting in **37e** $[\text{Os}_3(\text{CO})_9(\mu_3\text{-}\eta^3\text{-C}_9\text{H}_7(5\text{-C}_6\text{H}_5)\text{N})(\mu\text{-H})]$ in a 66% yield (Equation 3.1). The solid state structure of this nucleophilic addition product **37e** was determined in order to compare it with the previously reported $\sigma\text{-}\pi$ -vinyl quinoline triosmium carbonyl complex **37m** $[\text{Os}_3(\text{CO})_9(\mu_3\text{-}\eta^3\text{-C}_9\text{H}_8\text{N})(\mu\text{-H})]$ formed by the H^-/H^+ addition to **35a**.¹

The structure of **37e** is given in Figure 3.1, selected bond angles and lengths in Table 3.2. The bond lengths and angles of **37m** and **37e** are almost identical, as shown below in the comparison of the two. The bond lengths of structure **37e** will be given first followed by the bond lengths for **37m** being underlined. The structure consists of an isosceles triangle of Os atoms with two approximately equal metal-metal bonds (Os(1)-Os(3) (2.85(3) Å)– (2.84(2) Å), and Os(2)-Os(3) at (2.89(3) Å)–(2.88(2) Å), and the shorter bond Os(1)-Os(2) at (2.77(2) Å)–(2.77(2) Å). The hydride was located using the

program HYDEX.⁵ The hydride is tucked below the plane of the metal triangle. This calculated position for the hydride is confirmed by the positions of the carbonyl groups CO(13) and CO(33). The most interesting aspects of the structure of **37e** are the carbon-carbon and carbon-nitrogen bond lengths. The N(1)-C(2) (1.34(2) Å) -- (1.35(2) Å), and N(1)-C(9) (1.35(2) Å) -- (1.35(2) Å) bonds lengths and those between the rest of the heterocyclic atoms range from 1.32-1.41 Å which indicate that the ring has retained its aromaticity. However, the saturated bonds on the carbocyclic ring results in a distortion away from planarity forming a puckered-boat configuration. The C(5)-C(6), C(6)-C(7), and C(7)-C(8) bonds can be considered as single, single, and double bonds respectively based on the observed distances (1.54(2)--1.54(2), 1.57(2)--1.54(2), and 1.39(2)--1.38(2) Å). The assignment of a σ interaction between Os(1)-C(8) (2.13(3)--2.14(2) Å) and a π interaction between Os(3)-C(8) (2.21(2)-- 2.23(2) Å) and Os(3)-C(7) (2.36 (3)--2.38(2) Å) is consistent with previous studies of σ - π interactions on triosmium clusters.⁶

Equation 3.1



The only carbanion tried which did not result in nucleophilic addition on the ring was sodium diethyl malonate which apparently complexes with **35a** at the metal core as evidenced by the reversible color change from green to yellow when this reagent is added to **35a** at $-78\text{ }^\circ\text{C}$ and then warmed to room temperature. This behavior, and the associated color change, is similar to that observed for the reaction of **35a** with neutral two electron donors as shown in Equation 3.2 (discussed later in chapter 3).¹⁻⁴ Methoxide also failed to react with **35a**. It can be seen from the yields listed in Table 3.1 that the harder, more

Table 3.1 Isolated Nucleophilic Addition Yields from the Reaction of $\text{Os}_3(\text{CO})_9(\mu_3\text{-}\eta^2\text{-C}_9\text{H}_6\text{N})(\mu\text{-H})$ (35a) with Carbanions

Compound	Carbanion	Yield (%)
37a	LiMe	65
37b	Li ⁿ Bu	45
37c	Li ⁱ Bu	52
37d	LiBz	48
37e	LiPh	66
37f	LiCH=CH ₂	51
37g	LiC ₂ (CH ₂) ₃ CH ₃	25
37h	LiCH ₂ CN	72
37i.	LiC(CH ₃) ₂ CN	69
37j	Li-CHS(CH ₂) ₂ S-	72
37k	LiCH ₂ CO ₂ ⁱ Bu	86
37a	MeMgBr	43
37l	CH ₂ =CHCH ₂ MgBr	53

Figure 3.1 Solid State Structure for $(\mu\text{-H})(\text{Os}_3(\text{CO})_9)(\mu_3\text{-}\eta^3\text{-C}_9\text{H}_7)(5\text{-C}_6\text{H}_5)$ (**37e**)
showing the calculated position of the hydride.

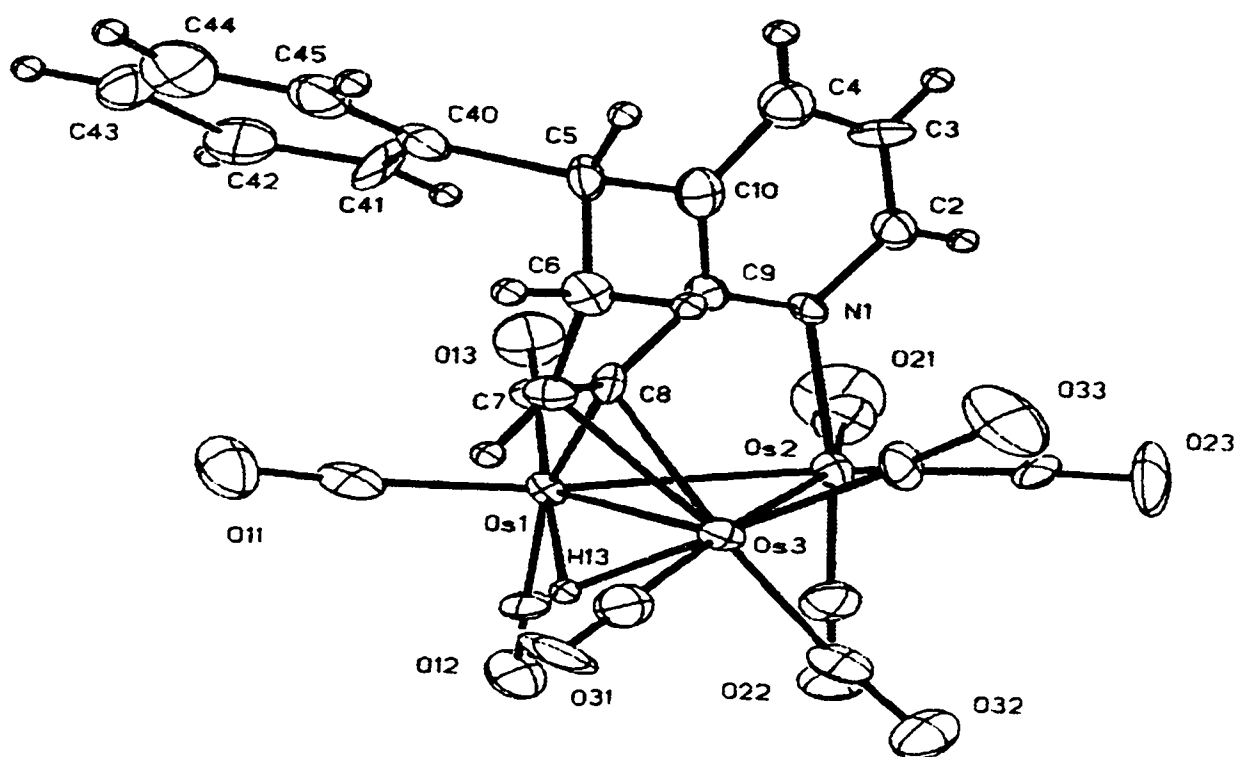


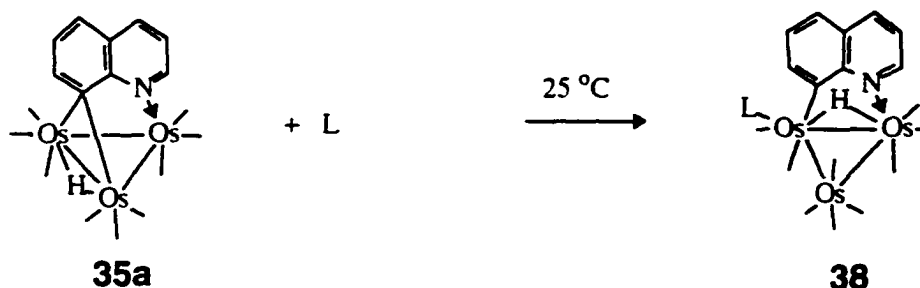
Table 3.2 Selected Bond Distances (Å) and Angles(°) for 37e

Distances			
Os(1)-Os(2)	2.77(2)	C(7)-C(8)	1.39(2)
Os(2)-Os(3)	2.89(3)	C(6)-C(7)	1.57(2)
Os(3)-Os(1)	2.85(3)	C(5)-C(6)	1.54(2)
Os(1)-C(8)	2.13(3)	C(5)-C(10)	1.55(2)
Os(3)-C(8)	2.21(2)	C(5)-C(40)	1.56(2)
Os(3)-C(7)	2.36(3)	C(10)-C(4)	1.38(2)
Os(2)-N(1)	2.18(3)	C(3)-C(4)	1.41(2)
C(9)-N(1)	1.35(2)	C(2)-C(3)	1.32(2)
Os-CO ^b	1.89(2)	N(1)-C(2)	1.34(2)
C-O ^b	1.14(2)		
Angles			
Os(1)-Os(2)-Os(3)	60.32(3)	C(6)-C(7)-C(8)	119.6(3)
Os(1)-Os(3)-Os(2)	57.90(3)	C(5)-C(6)-C(7)	108.9(3)
Os(2)-Os(1)-Os(3)	61.79(3)	C(6)-C(5)-C(10)	107.9(3)
Os(1)-C(8)-C(7)	119.9(4)	C(10)-C(5)-C(40)	115.3(3)
Os(3)-C(8)-C(7)	78.1(4)	C(2)-N(1)-C(9)	118.2(3)
Os(1)-Os(2)-N(1)	86.2(2)		
Os-C-O	176(4)		

^a Numbers in parentheses are average standard deviations

^b Average values.

Equation 3.2

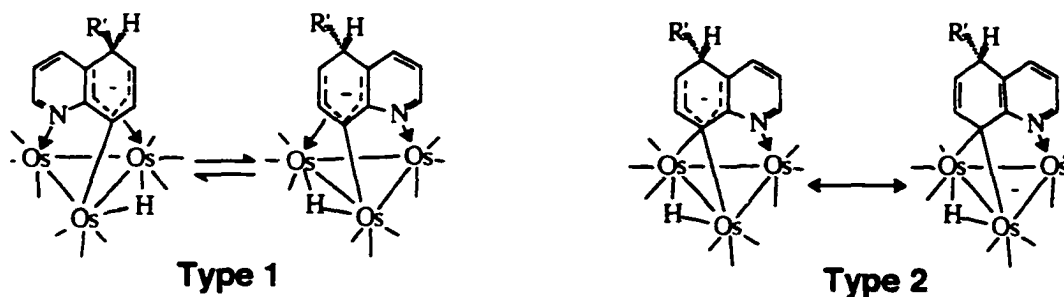


nucleophilic carbanions give somewhat lower yields than the softer nucleophiles. This is probably due to competing attack at the coordinated carbonyl groups, leading to decomposition. Overall, **35a** reacts with a broader range of nucleophiles relative to the neutral monometallic π -arene complexes.⁷ This is undoubtedly due to localization of the electron deficiency at the 5- position resulting from the electron deficient bonding to the cluster.^{1,4-6} Thus lithium t-butyl acetate reacts quite well with **35a** while in the case of $[(\pi-\eta^6\text{-arene})\text{Cr}(\text{CO})_3]$ yields were quite low except in the presence of very polar solvents such as HMPA.⁷ Methyl lithium and n-butyl lithium deprotonate $[(\pi-\eta^6\text{-arene})\text{Cr}(\text{CO})_3]$ while **35a** yields the usual nucleophilic addition products.⁷ Indeed, we have attempted deprotonation with lithium diisopropyl amide but observed no evidence for this mode of reaction with **35a**.

The structure of the intermediate anions **36a-l** produced after nucleophilic attack remained in question until examination of VT-NMR of a ^{13}C O enriched sample of the anion resulting from hydride attack on **35a**. Two possible structural types are possible based on room temperature ^1H NMR data: 1) a tilted $\mu_3-\eta^4$ -allyl which is undergoing rapid $\sigma-\pi$ -interchange; and 2) a $\mu-\eta^2$ alkylidene in which the quinoline remains

perpendicular to the metal and is stabilized by electron delocalization to the metal core (Scheme 3.1).

Scheme 3.1



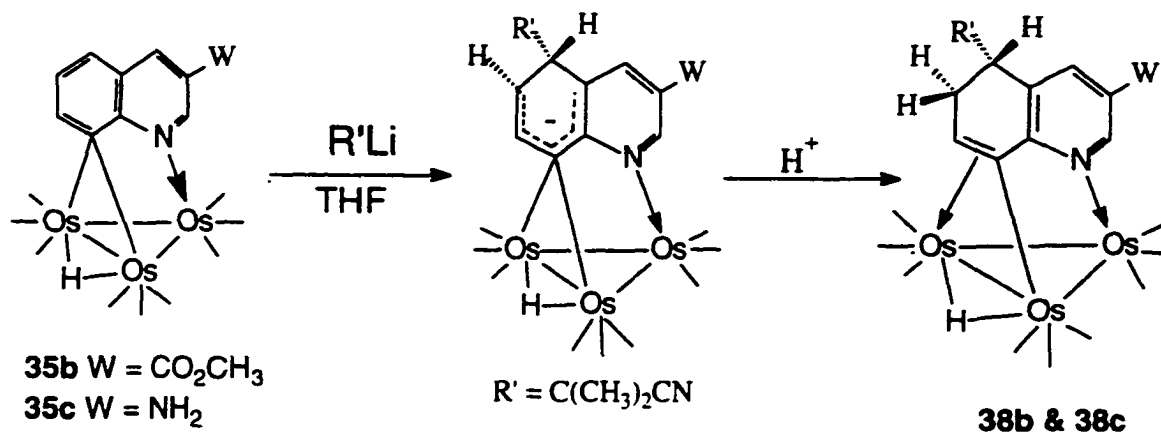
At both $+22^{\circ}\text{C}$ and -80°C , five carbonyl resonances are observed at 191.90, 186.76, 185.43, and 181.11 ppm in a relative intensity of 2:1:2:2:2. We feel this supports the perpendicular $\mu\text{-}\eta^2$ -structure since the $\sigma\text{-}\pi$ -interchange process usually has a barrier of 40-50 kJ/mole in related systems and should be at least partially frozen out on the NMR time scale at -80°C .¹

3.3 Reactions of the 3-, and 4- Monosubstituted ($\mu_3\text{-}\eta^2$)-Quinoline Triosmium Carbonyl Complexes with Carbanions

Substitution at both the carbocyclic and heterocyclic ring over a range of functional groups is well tolerated for the nucleophilic additions described above. Thus, the 3-substituted derivatives **35b** and **35c** (Equation 3.3) react with $\text{LiC}(\text{CH}_3)_2\text{CN}$ to give the expected nucleophilic addition products $[\text{Os}_3(\text{CO})_9(\mu_3\text{-}\eta^3\text{-C}_9\text{H}_6(3\text{-W})(5\text{-R}')\text{N})(\mu\text{-H})]$ ($\text{W}=\text{CO}_2\text{CH}_3$, $\text{R}'=\text{C}(\text{CH}_3)_2\text{CN}$ **38b**; $\text{W}=\text{NH}_2$, $\text{R}'=\text{C}(\text{CH}_3)_2\text{CN}$ **38c**; Equation 3.3) are obtained in reasonable yields. Similarly, the 4-substituted derivatives **35d-35g** react with

LiC(CH₃)₂CN and/or LiCH₂CO₂^tBu in an analogous manner to give [Os₃(CO)₉(μ₃-η³-C₉H₆(4-X)(5-R_r)N)(μ-H)] (X=CH₃, R_r'=C(CH₃)₂CN, **38d**; X=Cl, R_r'=C(CH₃)₂CN, **38e**; X=Cl, R_r'=CH₂CO₂^tBu, **38e'**; X=OCH₃, R_r'=C(CH₃)₂CN, **38f**; X=OCH₃, R_r'=CH₂CO₂^tBu, **38f'**; X=NH₂, R_r'=C(CH₃)₂CN, **38g**, Equation 3.4). The 4-carboxymethyl derivative, **35h**.

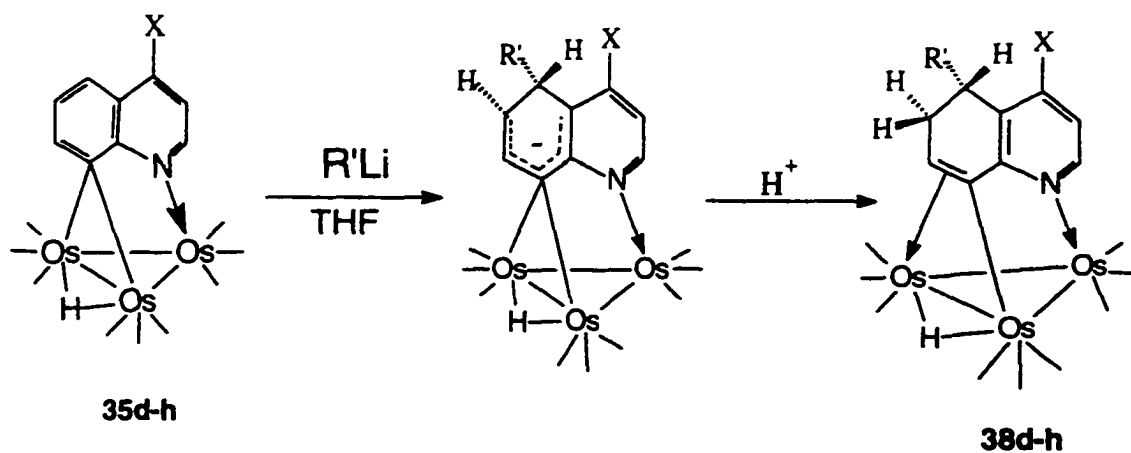
Equation 3.3



reacts cleanly with allyl magnesium bromide to give the expected nucleophilic addition product, [Os₃(CO)₉(μ₃-η³-C₉H₆(4-X)(5-R_r')N)(μ-H)] (X=CO₂CH₃, R_r'=C(CH₃)₂CN, **38h**,

Scheme 3.4).

Equation 3.4



It is significant that in the case of the 3- and 4-carboxymethyl derivatives, attack of the carbanion at the carbonyl group not does represent a competitive pathway since the expected nucleophilic addition products are obtained in good yield. Attack at the ester carbonyl group is only observed when an excess of carbanion is used, resulting in the normal addition product, and a second double alkylated product (Equation 5.8) as will be discussed later in section 5.5. Also if deprotonation of the methyl and amino groups in complexes **35c**, **35e** and **35g** is occurring it does not interfere with subsequent nucleophilic addition since reasonable yields of the expected products are obtained without the need to add an increased amount of carbanion relative to **35a**.

3.4 Stereospecific Nucleophilic Addition Across C(5)-C(6) of the Quinoline

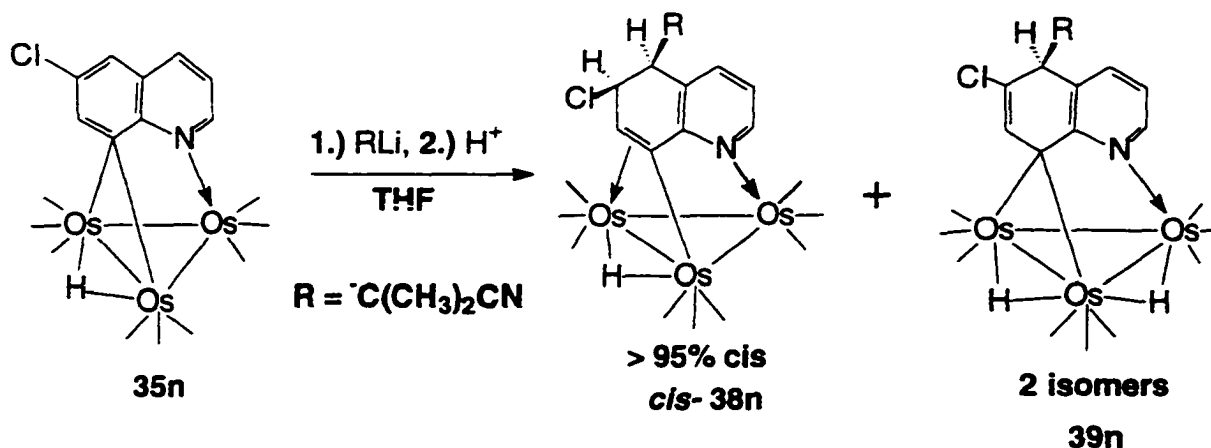
With a substituent on the 6-position of quinoline prior to nucleophilic addition it adds the element of stereochemistry across the C(5)-C(6) bond to be introduced. The stereochemistry can be controlled selectively to obtain either *trans* or *cis* isomers. The methodology for this stereochemically controlled addition will be discussed in this following section.

3.4.1 The Reaction of (**35n**) $[\text{Os}_3(\text{CO})_9(\mu_3\text{-}\eta^2\text{-C}_9\text{H}_5(6\text{-Cl})(\mu\text{-H}))]$ with $\text{LiC}(\text{CH}_3)_2\text{CN}$

The 6-substituted quinoline derivatives undergo nucleophilic addition with interesting differences. Complex **35n** reacts with $\text{LiC}(\text{CH}_3)_2\text{CN}$ to give two major products, the expected nucleophilic addition product, $[\text{Os}_3(\text{CO})_9(\mu_3\text{-}\eta^3\text{-C}_9\text{H}_6(6\text{-Cl})(5\text{-C}(\text{CH}_3)_2\text{CN})\text{N})(\mu\text{-H})]$ (**38n**) and a dihydrido complex $[\text{Os}_3(\text{CO})_9(\mu_3\text{-}\eta^2\text{-C}_9\text{H}_5(6\text{-Cl})(5\text{-C}(\text{CH}_3)_2\text{CN})\text{N})(\mu\text{-H})_2]$ (**39n**), apparently resulting from competitive protonation at the

metal core (Equation 3.5).^{5,6} From the NMR data alone, the bonding mode to the trimetallic core could not be assigned with certainty. A solid state structural investigation was therefore undertaken.

Equation 3.5



The solid state structure of **39n** is shown in Figure 3.2, selected distances and bond angles are shown in Table 3.3. The structure consists of an Os₃ triangle with two approximately equal metal-metal bonds (Os(1)-Os(3) and Os(2)-Os(3) at 2.814(1) and 2.786(1)Å) and one elongated metal-metal bond (Os(1)-Os(2), 2.962(1)Å). The two hydride ligands were located using the potential energy minimum program, Hydex.⁵ As expected, the elongated metal-metal bond has the hydride ligand located in-plane while the doubly bridged Os(1)-Os(3) edge has the hydride ligand tucked well below the Os₃ plane.¹ Compound **39n** is bound to the cluster by an electron precise sp³-μ-alkylidene linkage with C(8). The bonding is slightly asymmetric (Os(1)-C(8)=2.17(1) and Os(3)-C(8)=2.21(8)Å). These electron precise bonds are considerably shorter than the related electron deficient bonds in **35a** (2.28(1) and 2.32(1)Å). The Os(2)-N bond length in **39n** on the other hand is exactly the same as in **35a** (2.13(1)Å). The C(5)-C(6), C(6)-C(7) and

C(7)-C(8) bonds can be considered as single, double and single bonds respectively based on the observed distances (1.46(2), 1.36(2) and 1.48(2)Å). In the solid state, only one of two geometric isomers of **39n** is observed, with the hydride bridging the Os(1)-Os(2) edge *syn*- to the isobutyronitrile group. In solution, a minor isomer can be observed (about 10% of the major) by ¹H NMR. We have reported the solid state structure of **39n**.⁴

The formation of **39n** from **38n** can be rationalized by the electron withdrawing effect of the chloride, making protonation at the 6-position less favorable and resulting in competitive protonation at the metal core.^{3,4} To some extent, the relative amounts of **38n** and **39n** can be controlled. When a ten-fold excess of acid is used to quench the nucleophilic addition, **38n** and **39n** are formed in a 3:2 ratio. When one equivalent of acid is used, the ratio is 5:1. This reflects the greater statistical probability for protonation at the Os₃ core relative to the C(6) position of the ring. Attempts to convert **39n** to **38n** by heating at 80°C in C₆D₆ for several hours failed. In metal cluster chemistry it is not uncommon to observe the formation of two isomeric products which do not interconvert at temperatures below the decomposition temperature of the compounds.⁸ The formation of **39n** lends credence to our proposed structure for the intermediate anion as it is identical in structure to one of the resonance forms proposed (Equation 3.1).

The reaction of **35n** with LiC(CH₃)₂CN gave only one of two possible diastereomers of **38n** (Equation 3.5). The observed coupling constant between the C(5) and C(6) protons of 5.77 Hz gave no firm indication of the stereochemistry across the C(5)-C(6) bond since this value is right on the borderline between the values for *cis*- and *trans*- orientations around the C(3)-C(4) bonds in cyclohexenes.⁹ In addition, the metal ligand bonding framework for structural types **37** and **38** imparts an unusual puckered

geometry to the carbocyclic ring which makes inferring stereochemistry from coupling constants dangerous.¹ Unfortunately, we were unable to obtain X-ray quality crystals for 38n.

Figure 3.2 Solid State Structure for 39n $[\text{Os}_3(\text{CO})_9(\mu_3\text{-}\eta^2\text{-C}_9\text{H}_5(6\text{-Cl})(5\text{-C}(\text{CH}_3)_2\text{CN})\text{N})(\mu\text{-H})_2]$ Showing the Calculated Hydride Positions.

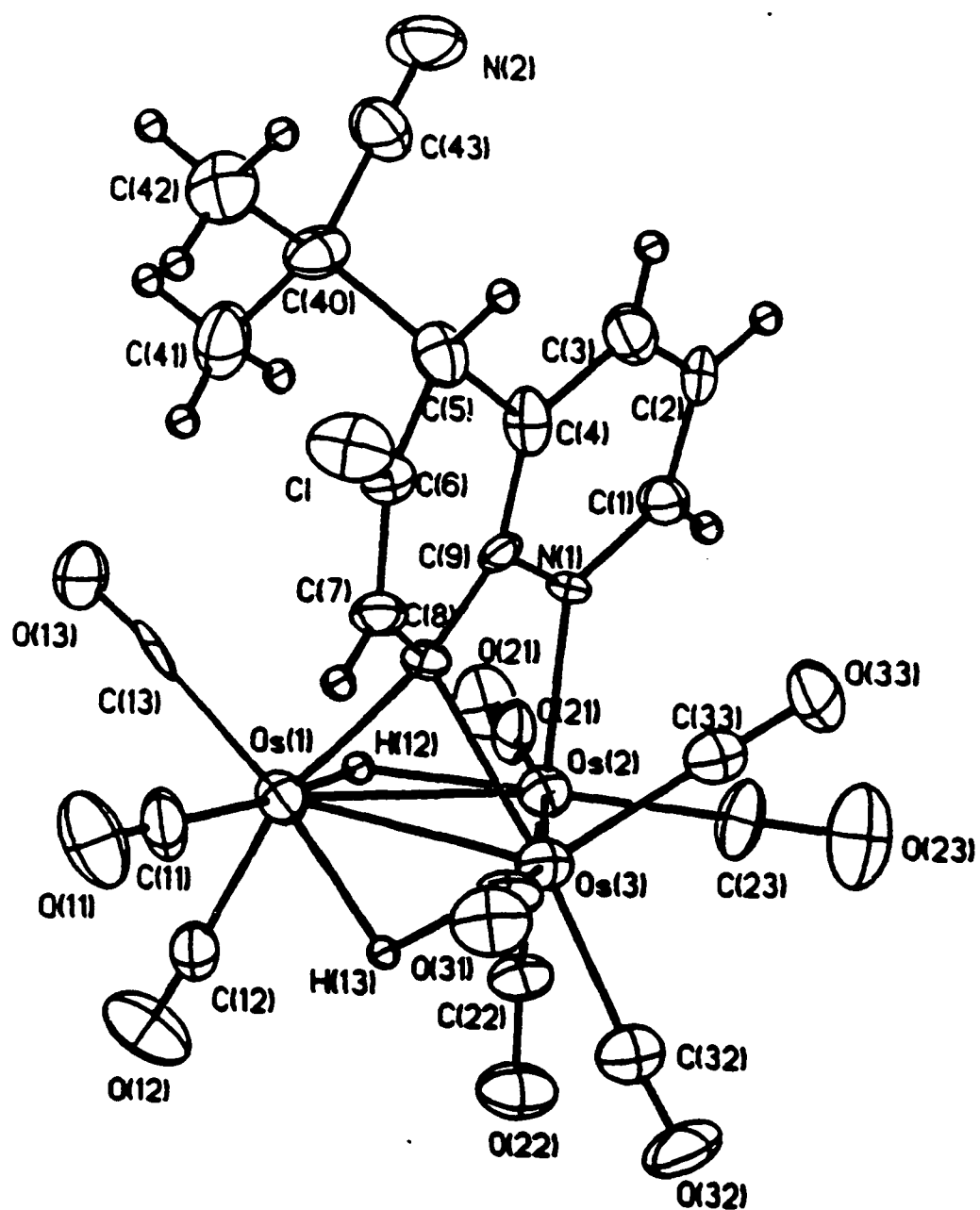


Table 3.3 Selected Distances (Å) and Angles(°) for 39n

Distances			
Os(1)-Os(2)	2.962(1)	C(8)-C(9)	1.46(2)
Os(1)-Os(3)	2.814(1)	C(7)-(8)	1.47(2)
Os(2)-Os(3)	2.786(1)	C(6)-C(7)	1.36(2)
Os(1)-C(8)	2.19(1)	C(6)-C(5)	1.46(2)
Os(3)-C(8)	2.21(1)	C(6)-C(1)	1.75(1)
Os(2)-N(1)	2.13(1)	C(5)-C(40)	1.59(2)
Os-CO ^b	1.89(2)	C-O ^b	1.13(2)
Angles			
Os(1)-Os(2)-Os(3)	58.53(2)	C(6)-C(7)-C(8)	125.(1)
Os(1)-Os(3)-Os(2)	63.86(2)	C(5)-C(6)-C(7)	124.(1)
Os(2)-Os(1)-Os(3)	57.61(2)	C(6)-C(5)-C(10)	109.(1)
Os(1)-C(8)-Os(3)	79.6(4)	C(10)-C(5)-C(40)	110.(1)
Os(3)-Os(2)-N(1)	81.9(3)	C(2)-N(1)-C(9)	117.(1)
Os-C-O ^b	177.(1)		

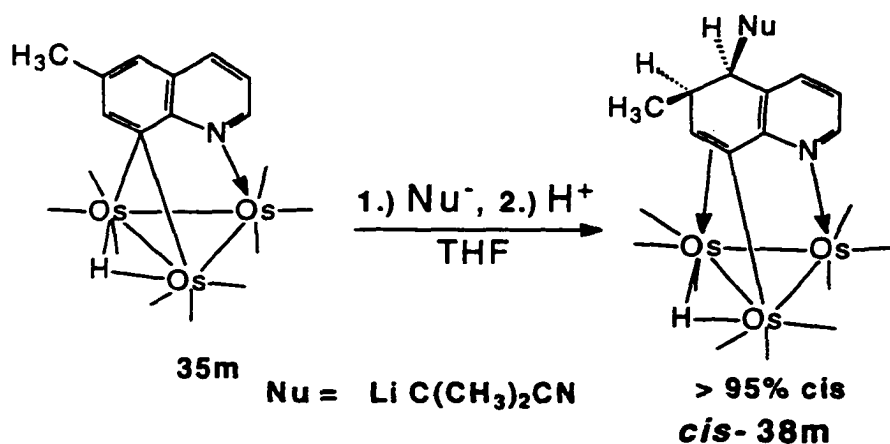
^a Numbers in parentheses are average standard deviations.

^b Average values.

3.4.2 The Reaction of $[\text{Os}_3(\text{CO})_9(\mu_3\text{-}\eta^2\text{-C}_9\text{H}_5(6\text{-CH}_3)(\mu\text{-H}))]$ (**35m**) with Carbanions LiR ($\text{R}=\text{C}(\text{CH}_3)_2\text{CN}$, CH_3)

The reaction of **35m** with $\text{Li C}(\text{CH}_3)_2\text{CN}$ gave one major product in 71% yield (Equation 3.6), *cis*- $\text{Os}_3(\text{CO})_9(\mu_3\text{-}\eta^3\text{-C}_9\text{H}_6(6\text{-CH}_3)(5\text{-C}(\text{CH}_3)_2\text{CN})\text{N})(\mu\text{-H})$ (**38m**). This compound was also isolated as one diastereomer and showed a vicinal coupling constant for the C(5)-C(6) protons of 5.95 Hz, very similar to **38n** (Equation 3.5).

Equation 3.6



Examination of the crude reaction mixture by ^1H NMR prior to chromatographic purification showed the presence of only one diastereomer of **38m** in addition to starting material. Thus, the single diastereomer appears to be the kinetic product and is not the result of equilibration on the silica gel used for purification. The solid state structure of **38m** revealed that it exists as the *cis*-diastereomer and therefore, based on the similar vicinal coupling constants, **38n** is as well. Suitable crystals of **38m** for X-ray analysis were obtained and allow us to firmly establish the stereochemistry across the C(5)-C(6) bond.

The solid state structure of **38m** is shown in Figure 3.3, selected distances and bond angles in Table 3.4. The *cis*- configuration around the C(5)-C(6) double bond is obvious from the solid state structure of *cis*-**38m** as is the anticipated puckered-boat configuration of the carbocyclic ring. The overall structure and bonding mode is very similar to the previously reported $\text{Os}_3(\text{CO})_9(\mu_3\text{-}\eta^3\text{-C}_9\text{H}_8\text{N})(\mu\text{-H})$ from the H^-/H^+ addition to **35a**, and complex **37e**.¹ The carbomethoxy derivative, **35p**, also exclusively gives the *cis*- isomer, **38p**, when reacted with allyl magnesium bromide in good yield (Scheme 1)

The $\sigma\text{-}\pi$ -vinyl bonding mode is most likely undergoing a $\sigma\text{-}\pi$ -interchange in solution as observed in related compounds but it is not possible to ascertain if this process is operative owing to the asymmetry in **38m**-**38p**.¹ The *cis*- stereochemistry can be rationalized by exclusive *trans*- protonation of an essentially planar anionic intermediate (Equation 3.1 and 3.6), where the bulky nucleophile blocks one face of the carbocyclic ring at C(6). This is not the case for deuteride as a nucleophile where both *cis*- and *trans*- isomers are observed in similar amounts when **35m** is treated with D^-/H^+ .¹ When **35m** is reacted with CH_3Li , one major stereoisomer is obtained in 67% yield, $\text{Os}_3(\text{CO})_9(\mu_3\text{-}\eta^3\text{-C}_9\text{H}_6(5.6\text{-CH}_3)_2\text{N})(\mu\text{-H})$ (**38m'**), which we can identify as the *cis*- diastereomer from ¹H NMR decoupling experiments which reveal a vicinal $^3J^{\text{H-H}}=4.5$ Hz across the C(5)-C(6) bond. A trace amount of a second diastereomer is observed as companion peaks in the ¹H NMR of **38m'**. Thus, even a relatively small alkyl group on C(5) is sufficient to induce almost exclusive *trans*- protonation.

Figure 3.3 Solid State Structure for *cis*-38m $[\text{Os}_3(\text{CO})_9(\mu_3\text{-}\eta^3\text{-C}_9\text{H}_6(6\text{-CH}_3)(5\text{-C}(\text{CH}_3)_2\text{CN})\text{N})(\mu\text{-H})]$ Showing the Calculated Hydride Position.

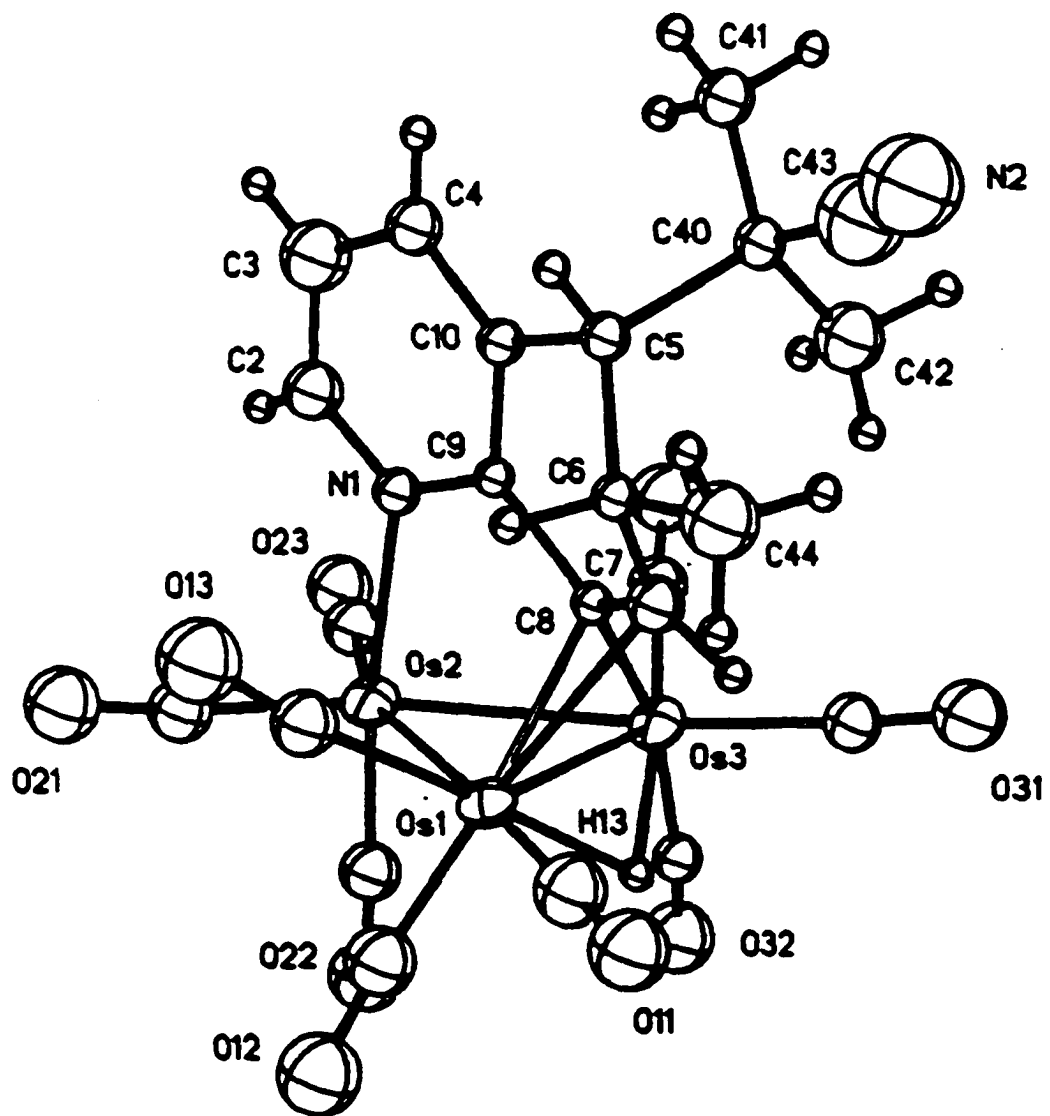


Table 3.4 Selected Distances(Å) and Angles(°) for *cis*-38m

Distances			
Os(1)-Os(2)	2.886(2)	C(7)-C(8)	1.35(3)
Os(1)-Os(3)	2.851(2)	C(5)-C(6)	1.52(3)
Os(2)-Os(3)	2.776(2)	C(6)-C(7)	1.54(3)
Os(1)-C(8)	2.16(3)	C(5)-C(10)	1.58(3)
Os(1)-C(7)	2.43(3)	C(5)-C(40)	1.65(4)
Os(3)-C(8)	2.09(2)	C(6)-C(44)	1.42(3)
Os(2)-N(1)	2.18(2)	C(9)-N(1)	1.33(3)
Os-CO ^b	1.86(3)	C(9)-C(10)	1.40(3)
		C-O ^b	1.16(2)
Angles			
Os(1)-Os(2)-Os(3)	60.44(5)	C(6)-C(7)-C(8)	127(2)
Os(1)-Os(3)-Os(2)	61.68(5)	C(5)-C(6)-C(7)	107(2)
Os(2)-Os(1)-Os(3)	57.88(5)	C(6)-C(5)-C(10)	110(2)
Os(1)-C(7)-C(8)	62(2)	C(10)-C(5)-C(40)	106(2)
Os(1)-C(8)-C(7)	84(2)	C(2)-N(1)-C(9)	126(2)
Os(3)-C(8)-C(7)	126(2)	Os(3)-Os(2)-N(1)	84.5(5)
Os-C-O ^b	173(3)		

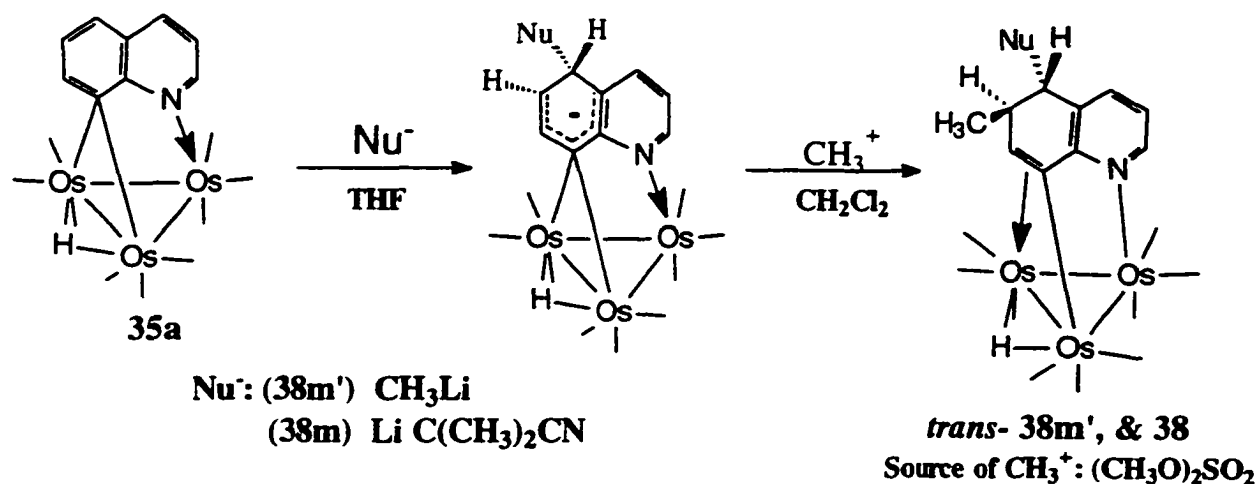
^a Numbers in parentheses are average standard deviations.

^b Average values.

3.4.3 Synthesis of the *trans*-**38m** $\text{Os}_3(\text{CO})_9(\mu_3\text{-}\eta^3\text{-C}_9\text{H}_6(5\text{-C}(\text{CH}_3)_2\text{CN})6\text{-CH}_3\text{N})(\mu\text{-H})$

If our hypothesis about *trans*-protonation is correct, then it should be possible to obtain *trans*-**38m** by treatment of **35a** with $\text{LiC}(\text{CH}_3)_2\text{CN}$ followed by reaction with an alkylating agent $(\text{CH}_3\text{O})_2\text{SO}_2$ (Equation 3.7).

Equation 3.7



This is indeed the case (Equation 3.7), although complete conversion to *trans*-**38m** is not realized, as significant amounts (~40%) of **37i** are formed. Presumably this occurs by incomplete alkylation of the anion intermediate, followed by protonation on workup with silica gel. It was not possible to separate *trans*-**38m** from **37i** by thin layer chromatography but analytically pure samples were obtained by reverse phase high pressure liquid chromatography. Although it was immediately obvious that *trans*-**38m** was a different stereoisomer than *cis*-**38m**, the vicinal coupling constant across the C(5)-

C(6) bond was observed to be <1 Hz. This seemed very unusual for a *trans*- isomer, but a solid state structure determination of this product revealed that it was indeed *trans-38m*.^{5,6}

The solid state structure of *trans-38m* is shown in Figure 3.4, selected distances and bond angles in Table 3.5. The geometry across the C(5)-C(6) bond is *trans*- and the conformation of the carbocyclic ring is such that the dihedral angle between the alkyl groups is 154° and between the calculated positions of the C(5) and C(6) hydrogen atoms is 80°. This explains the small coupling constant across this bond and suggests that the detailed conformation of the carbocyclic ring is controlled by steric interactions of the alkyl group across the C(5)-C(6) bond as well as the bonding mode to the metal core. The related dihedral angles in *cis-38m* are 52° and 51°, respectively. The remainder of the structure is virtually identical with *cis-38m*.

The same reaction sequence with **35a** using CH₃Li and (CH₃O)₂SO₂ yields *trans-38m'* (Equation 3.7). In this case, alkylation was also incomplete and **37a** was isolated as a coproduct. The vicinal coupling constant in the case of *trans-38m'* is 11.98 Hz indicating that with the smaller methyl group, the carbocyclic ring can adopt a conformation where the hydrogens are approximately *trans*- diaxial.⁹

The anion generated from the treatment of **35a** with CH₃Li can also be quenched with acetic anhydride to give *trans-38z* Os₃(CO)₉(μ₃-η³-C₉H₆(5-CH₃)(6-CH₃CO)N)(μ-H) (Equation 3.8). The vicinal coupling constant across the C(5)-C(6) bond is 12.12 Hz. As might be expected, the more sterically compact sp² carbon of the acetyl group allows the substituents on C(5) and C(6) to adopt a diequatorial conformation resulting in a *trans*-diaxial relationship for the hydrogens on these carbons as for *trans-38m'*.

Figure 3.4 Solid State Structure for *trans*-38m $[\text{Os}_3(\text{CO})_9(\mu_3-\eta^3\text{-C}_9\text{H}_6(6\text{-CH}_3)(5\text{-C}(\text{CH}_3)_2\text{CN})\text{N})(\mu\text{-H})]$ Showing the Calculated Hydride Position.

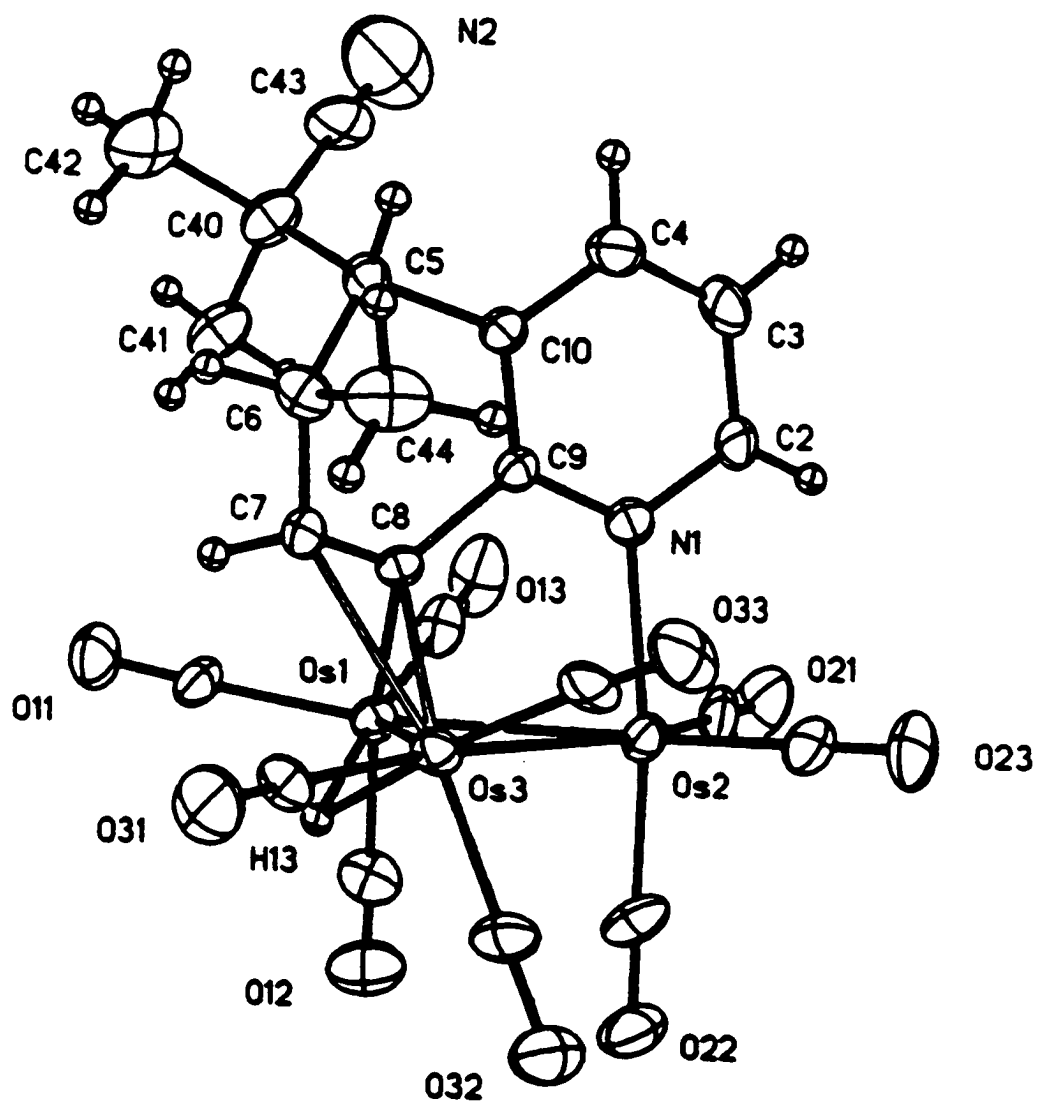


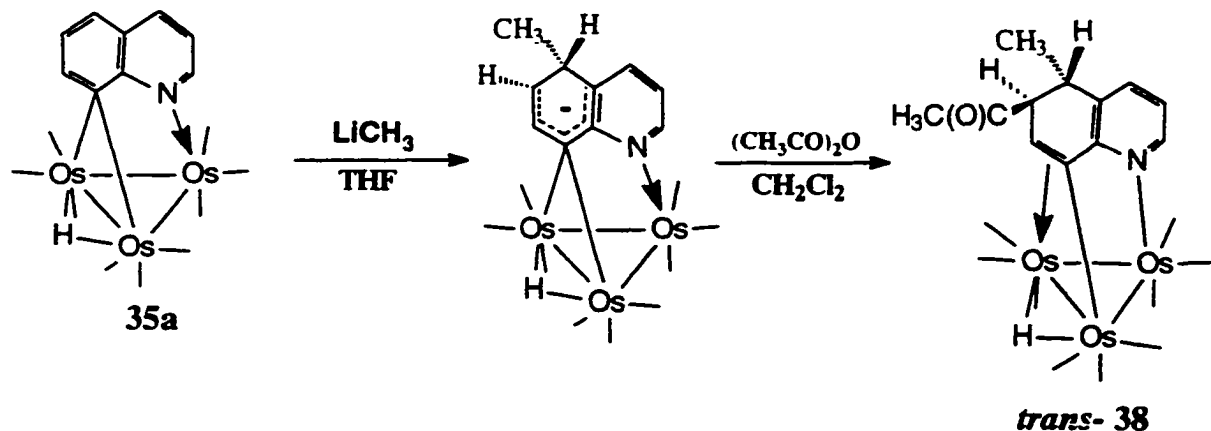
Table 3.5 Selected Distances(Å) and Bond Angles(°) for *Trans*-38m

Distances			
Os(1)-Os(2)	2.789(1)	C(7)-C(8)	1.37(2)
Os(1)-Os(3)	2.840(1)	C(6)-C(7)	1.55(2)
Os(2)-Os(3)	2.880(1)	C(5)-C(6)	1.55(2)
Os(1)-C(8)	2.11(1)	C(5)-C(10)	1.52(2)
Os(3)-C(8)	2.26(1)	C(5)-C(40)	1.56(3)
Os(3)-C(7)	2.45(2)	C(6)-C(44)	1.54(3)
Os(2)-N(1)	2.18(1)	C(9)-N(1)	1.30(3)
Os-CO ^b	1.91(2)	C-O ^b	1.14(2)
Angles			
Os(1)-Os(2)-Os(3)	60.09(3)	C(6)-C(7)-C(8)	124(1)
Os(1)-Os(3)-Os(2)	58.37(3)	C(5)-C(6)-C(7)	109(1)
Os(2)-Os(1)-Os(3)	61.54(3)	C(6)-C(5)-C(10)	109(1)
Os(1)-C(8)-C(7)	123(1)	C(10)-C(5)-C(40)	112(1)
Os(3)-C(8)-C(7)	80(1)	C(2)-N(1)-C(9)	120(1)
Os(3)-C(7)-C(8)	65(1)	Os(1)-Os(2)-N(1)	84.2(4)
Os-C-O ^b	177(1)		

^a Numbers in parentheses are average standard deviations

^b Average values.

Equation 3.8



3.5 Reactivity of 5-Substituted Complexes: Addition Across the C(3)-C(4) Bond

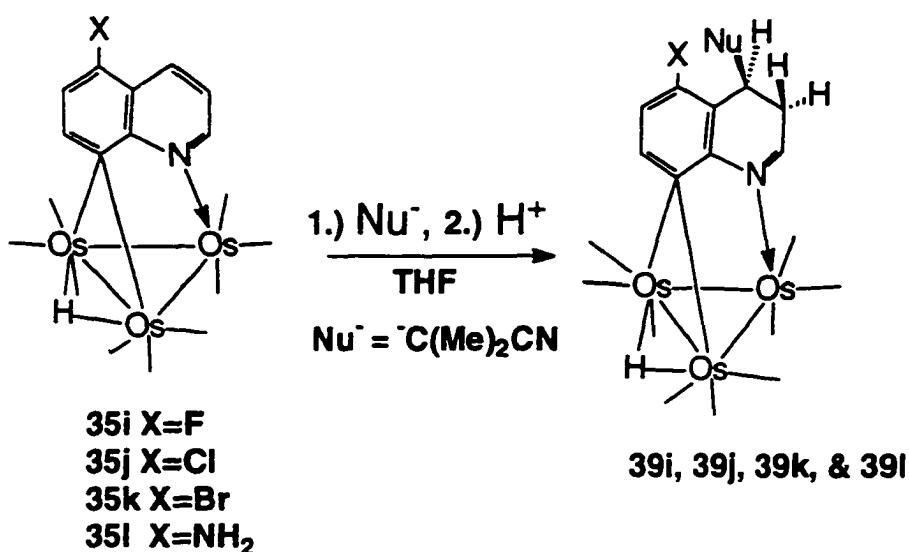
The highly regioselective nature of the nucleophilic additions observed for structural type **35** regardless of the nature or location of the substituents on the quinoline ring poses the question as to what would occur if the 5-position were substituted with a reasonable leaving group. In the case of halide substituted π - η^6 arene complexes, nucleophilic substitution competes with nucleophilic addition.⁷ The reaction of the 5-chloro derivative **35j** with $\text{LiC}(\text{CH}_3)_2\text{CN}$ results in nucleophilic addition across the 3,4-bond of the quinoline ring to yield $\text{Os}_3(\text{CO})_9(\mu_3\text{-}\eta^2\text{-C}_9\text{H}_6(5\text{-Cl})(4\text{-C}(\text{CH}_3)_2\text{-CN})\text{N})(\mu\text{-H})$ (**39j**, Equation 3.9).

In the 5-substituted complexes **35i-35l** addition with nucleophiles $\text{R}'\text{Li}$ ($\text{R}' = n\text{-BuLi}$, and $\text{C}(\text{CH}_3)_2\text{CN}$) is observed across the 3,4-bond of the quinoline, regardless of the size of the substituent, showing no evidence of nucleophilic substitution as with π -arene systems.⁷ The reaction of the 5-fluoro, **35i**; 5-bromo, **35k**; and 5-amino, **35l** derivatives with $\text{R}'\text{Li}$ ($\text{R}' = \text{C}(\text{CH}_3)_2\text{CN}$, $\text{R}' = n\text{-BuLi}$) yields the analogous nucleophilic addition

products $\text{Os}_3(\text{CO})_9(\mu_3\text{-}\eta^2\text{-C}_9\text{H}_6(5\text{-NH}_2)(4\text{-R}' \text{ or R})\text{N})(\mu\text{-H})$ **39i**, **39i'**, **39k**, **39k'**, **39l**, and **39l'** (Scheme 3.9).

The ^1H -COSY NMR of **39j** clearly shows the coupling of the most downfield aromatic resonance (i.e., the C(2)-H) resonance coupled to the most upfield aliphatic resonances and two separately coupled aromatic resonances. These data are consistent with the structure shown in Equation 3.9 and this has been verified by a solid state structure determination of this complex.^{3,4}

Equation 3.9



The solid state structure of **39j** is shown in Figure 3.5, selected distances and bond angles in Table 3.6. The solid state structure of **39j** is that proposed from the ^1H NMR data. The core consists of an essentially equilateral triangle with a hydride bridging the Os(1)-Os(3) edge. The electron deficient bonds between C(8), Os(1) and Os(3) are slightly asymmetric and the bond vectors are about the same as in **35a** (2.31(1) and 2.26(1)Å in **39j** and 2.32(1) and 2.28(1)Å in **35a**). The Os(2)-N(1) bond is slightly

Figure 3.5 Solid State Structure for $\text{Os}_3(\text{CO})_9(\mu_3\text{-}\eta^2\text{-C}_9\text{H}_6(5\text{-Cl})(4\text{-C}(\text{CH}_3)_2\text{-CN})\text{N})(\mu\text{-H})$ 39j Showing the Calculated Position of the Hydride.

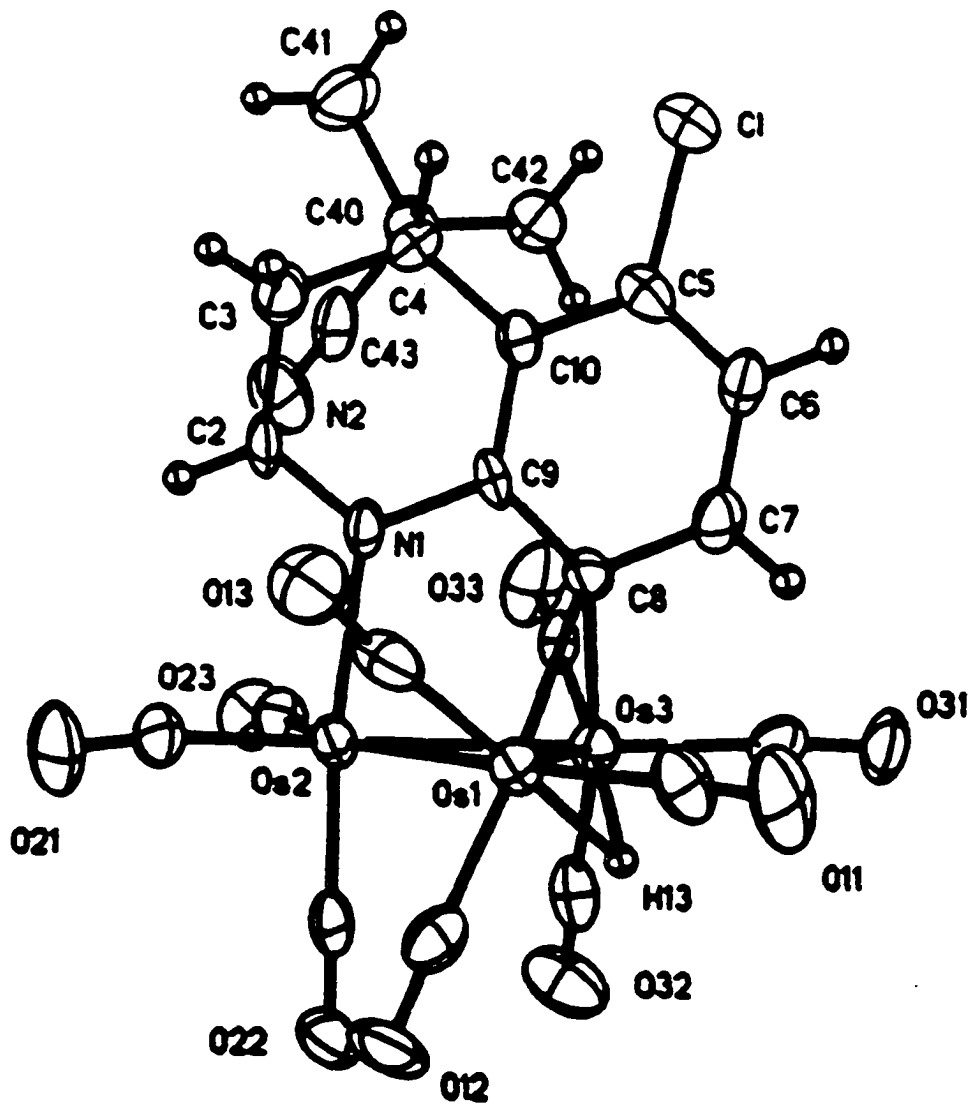


Table 3.6 Selected Distances(Å) and Bond Angles(Deg) for 39j

Distances			
Os(1)-Os(2)	2.772(1)	N(1)-C(2)	1.30(1)
Os(1)-Os(3)	2.756(1)	C(2)-C(3)	1.50(1)
Os(2)-Os(3)	2.770(1)	C(3)-C(4)	1.51(2)
Os(1)-C(8)	2.26(1)	C(4)-C(10)	1.51(1)
Os(3)-C(8)	2.31(1)	C(4)-C(40)	1.59(2)
Os(2)-N(1)	2.17(1)	C(5)-Cl	1.73(1)
Os-CO ^b	1.92(2)	C(5)-C(6)	1.36(2)
		C-O ^b	1.13(2)
Angles			
Os(1)-Os(2)-Os(3)	59.65(2)	N(1)-C(2)-C(3)	122(1)
Os(1)-Os(3)-Os(2)	60.22(2)	C(2)-C(3)-C(4)	112(1)
Os(2)-Os(1)-Os(3)	60.12(2)	C(3)-C(4)-C(10)	108(1)
Os(1)-C(8)-Os(3)	74.2(3)	C(3)-C(4)-C(40)	112(1)
Os(3)-Os(2)-N(1)	84.9(2)	C(10)-C(5)-Cl	120(1)
Os(1)-Os(2)-N(1)	82.4(2)	C(7)-C(8)-C(9)	116(1)
Os-C-O ^b	176(1)		

^a Numbers in parentheses are average standard deviations.

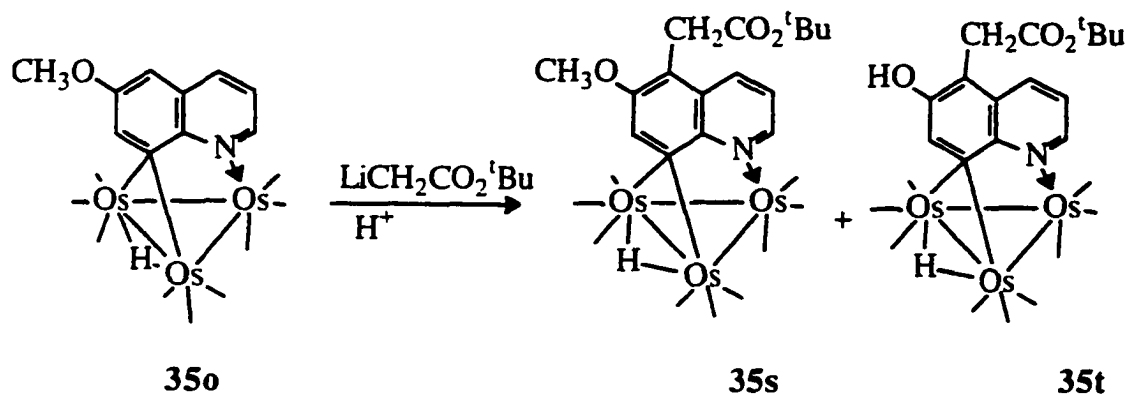
^b Average values.

elongated in **39j** with respect to **35a** (2.17(1) and 2.13(1)Å respectively) as observed in *cis*- and *trans*-**37m**. The N(1)-C(2) bond, at 1.30(1)Å is typical of a C-N double bond and the remaining bond lengths are unremarkable.

3.6 Rearomatization of the Nucleophilic Addition Products

The reaction of **35o** with $\text{LiCH}_2\text{CO}_2^t\text{Bu}$ gives the green aromatized complex $\text{Os}_3(\text{CO})_9(\mu_3\text{-}\eta^2\text{-C}_9\text{H}_4(6\text{-OCH}_3)(5\text{-CH}_2\text{CO}_2^t\text{Bu})\text{N})(\mu\text{-H})$ (**35s**, Equation 3.10) in 54% yield.

Equation 3.10

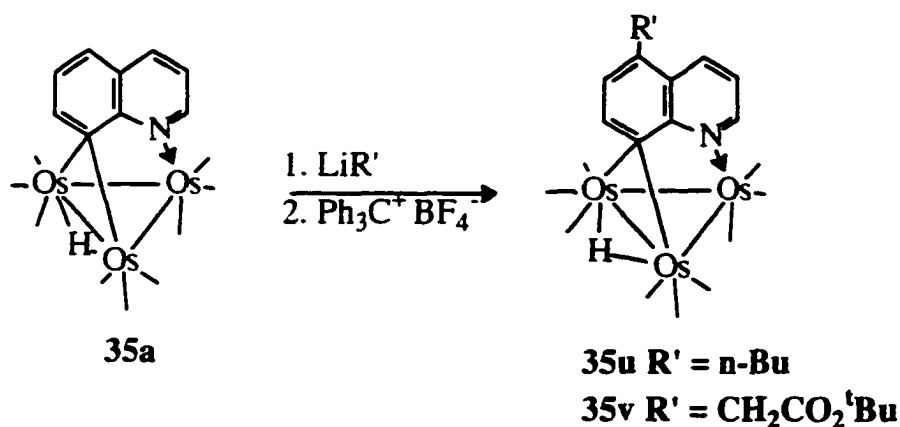


In addition, 35% of the corresponding phenol, $\text{Os}_3(\text{CO})_9(\mu_3\text{-}\eta^2\text{-C}_9\text{H}_4(6\text{-OH})(5\text{-CH}_2\text{CO}_2^t\text{Bu})\text{N})(\mu\text{-H})$ (**35t**) is also isolated, probably as a result of hydrolysis by trace moisture during the acid quench or on workup on silica gel. This probably takes place prior to rearomatization from the hydrolytically sensitive allyl ether intermediate. The facile oxidation (dehydrogenation) of the intermediate nucleophilic addition product is a result of the presence of the strongly π -electron donating 6-methoxy group and the alkyl substituent in the 5-position. Small amounts of rearomatized products were also noted in the reactions of **35m** with LiCH_3 and $\text{LiC}(\text{CH}_3)_2\text{CN}$. Consistent with this idea is the fact

that the 6-carboxymethyl derivative, **35p**, forms the expected nucleophilic addition product $\text{Os}_3(\text{CO})_9(\mu_3-\eta^3\text{-C}_9\text{H}_6(5\text{-CH}_2\text{CH}=\text{CH}_2)(6\text{-CO}_2\text{CH}_3)\text{N})(\mu\text{-H})$ (**38p**, Scheme 3.3) on reaction with allylmagnesium bromide in good yield.

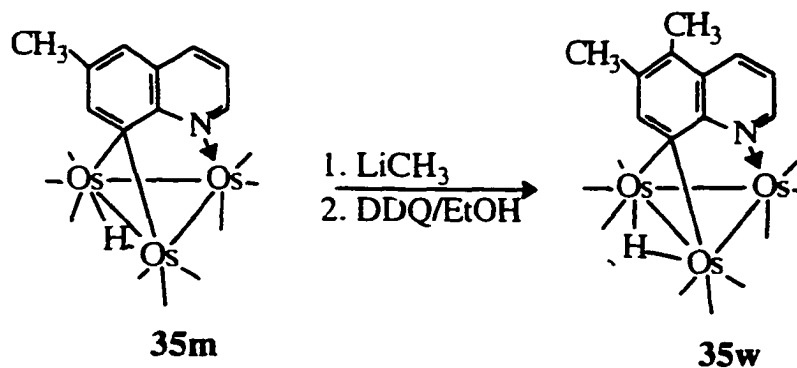
The facile rearomatization of the nucleophilic addition product derived from the addition of $\text{LiCH}_2\text{CO}_2^t\text{Bu}$ to **35o** (Equation 3.10) prompted us to attempt to reproduce this process in a deliberate manner. There are several methods which proved adequate. The addition of trityl cation to the anions (**36b** & **36k**, $\text{R}=\text{}^n\text{Bu}$, and $^t\text{BuOAc}$) resulting from the addition of alkylating agents $\text{R}'\text{Li}$ ($\text{R}'=\text{}^n\text{Bu}$, $\text{CH}_2\text{CO}_2^t\text{Bu}$) to **35a** gave the rearomatized products $\text{Os}_3(\text{CO})_9(\mu_3-\eta^2\text{-C}_9\text{H}_5(5\text{-R}')\text{N})(\mu\text{-H})$ (**35u**, $\text{R}'=\text{}^n\text{Bu}$; **35v**, $\text{CH}_2\text{CO}_2^t\text{Bu}$; Equation 3.11) in 53% and 83% yield respectively.

Equation 3.11



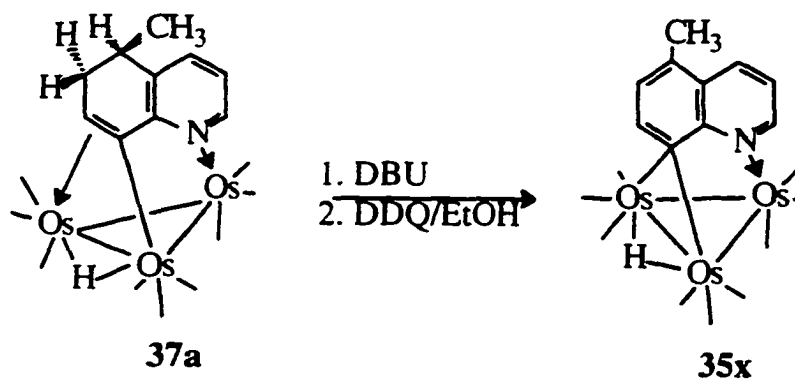
In some other cases, we found the coproduct, triphenyl methane difficult to separate from the products. An alternative route is the addition of dichlorodicyanoquinone (DDQ) followed by an ethanol quench of the resulting hydroquinone anion and excess carbanion. Thus, **35a** is treated with CH_3Li then DDQ/EtOH) to yield $\text{Os}_3(\text{CO})_9(\mu_3-\eta^2\text{-C}_9\text{H}_5(5,6\text{-CH}_3)_2\text{N})(\mu\text{-H})$ (**35w**, Equation 3.12).

Equation 3.13



Finally, one can add a deprotonating agent such as diazabicyclononane (DBU) to the isolated nucleophilic addition products of type 37 or 38 followed by DDQ/EtOH, as demonstrated with 37a, which yielded $[\text{Os}_3(\text{CO})_9(\mu_3\text{-}\eta^2\text{-C}_9\text{H}_5(5\text{-CH}_3)\text{N})(\mu\text{-H})]$ (35x) (Equation 3.13).

Equation 3.13



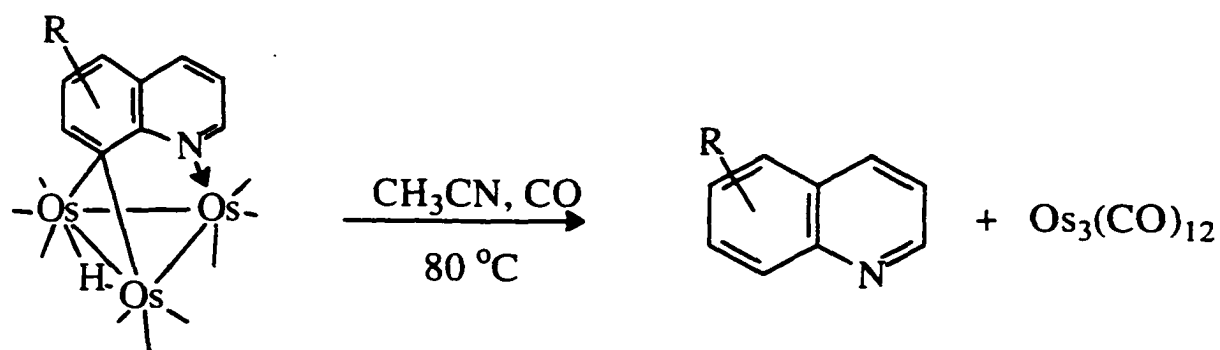
Attempts to react complexes 37 or 38 with DDQ directly failed. Choosing the best route from among these methods remains uncertain at present except that DDQ seems to tolerate functionality a bit better and its reaction products are easier to separate from the cluster reaction products. In cases where multiple products result, isolation of the

nucleophilic addition product followed by DBU/DDQ treatment would be the method of choice.

3.7 Cleavage of the Functionalized Quinoline from the Cluster

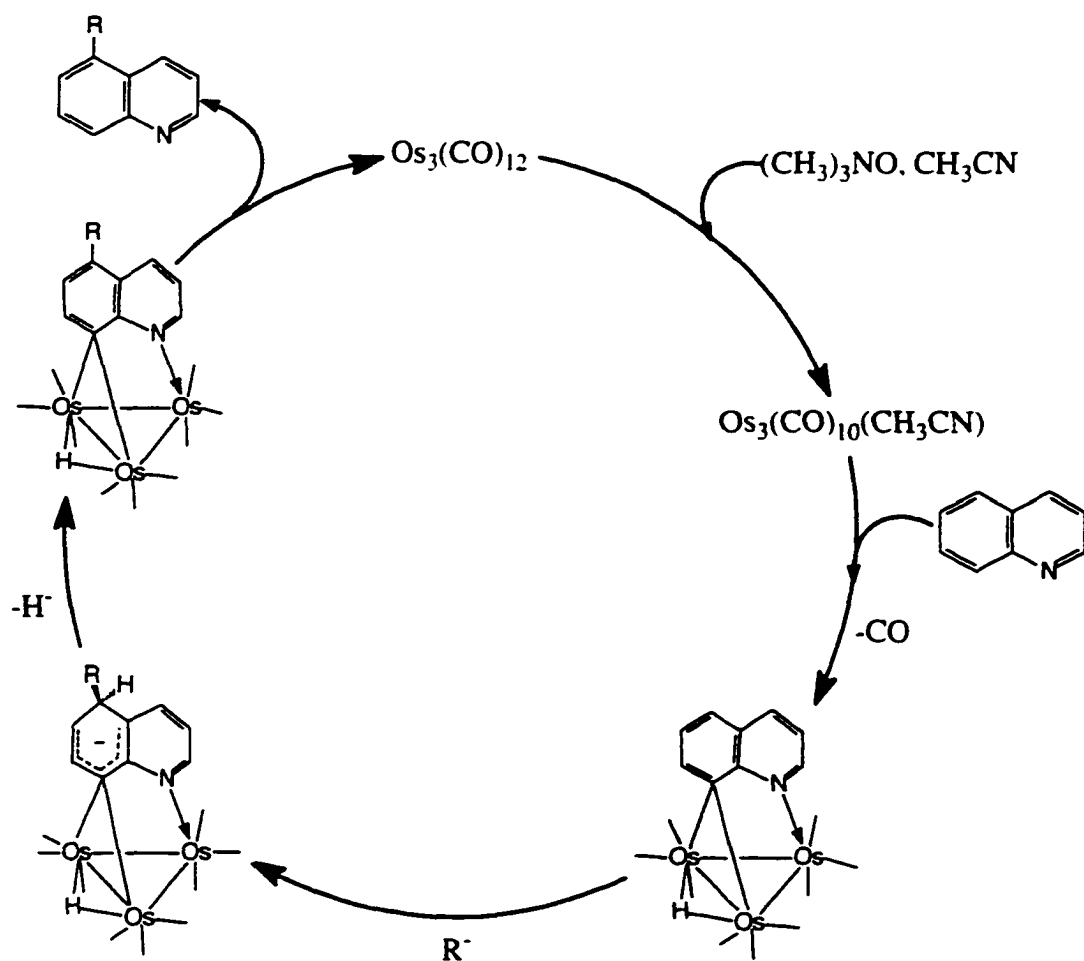
In order for this synthetic methodology to be developed as a useful tool for the synthesis of novel quinoline derivatives, a clean method for cleavage of the quinoline ligand from the cluster is required. For the rearomatized derivatives of structural type **35** the method for cleavage proved to be heating the quinoline cluster complex at 70°C in acetonitrile under an atmosphere of carbon monoxide. This leads to isolation of the free quinoline and formation of Os₃(CO)₁₂ (Equation 3.14). The Os₃(CO)₁₂ precipitates almost quantitatively from the cooled reaction solution while the quinoline can be recovered by evaporation of solvent and filtration through silica if necessary.

Equation 3.14



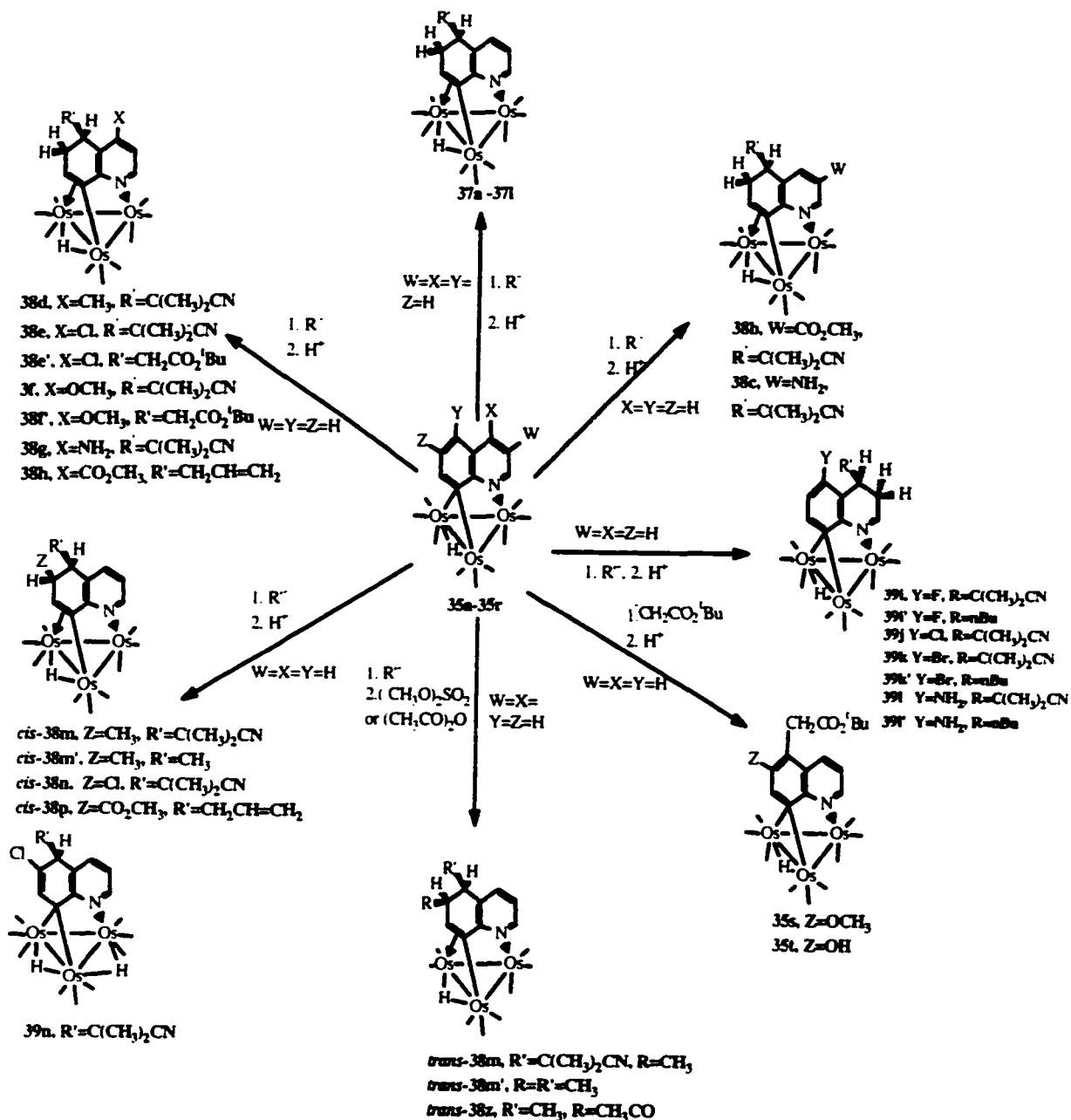
Including the aromatization procedures outlined above, successful cleavage by this method constitutes a stoichiometric cycle for selectively alkylating quinolines at the 5-position (Scheme 3.2).

Scheme 3.2 Complete Stoichiometric Cycle



Unfortunately, this method does not extend to the nucleophilic addition products of structural types **37** or **38**. Although cleavage is observed at elevated pressures of carbon monoxide for **37** & **38**, the reaction is not clean resulting in a mixture of products. Other approaches to cleaving these ligands are currently being explored. A summary of all the chemistry discussed in this chapter is given in Scheme 3.3.

Scheme 3.3 Summary of Reactions of Carbanions with Electron Deficient Quinoline Triosmium Complexes



3.8 Conclusions

The three center two-electron bonding of the C(8) carbon of the quinoline ring with two metal atoms of the Os₃ triangle imparts a significant electron deficiency to C(5) of the quinoline ring making it subject to regiospecific attack by a wide range of carbanions. In sharp contrast to the $\pi\text{-}\eta^6$ -chromium arenes, we do not observe lithiation with CH₃Li or n-BuLi.⁷ Substitution is not observed in the case of the 5-halo quinoline derivatives while for the $\pi\text{-}\eta^6$ -arene complex, substitution is competitive with nucleophilic addition for most nucleophiles with halogen substituted arenes.⁷ Substitution of halogen at the 5-position redirects nucleophilic attack to the 4-position resulting in nucleophilic addition across the 3,4 double bond after acid quench.

These results suggest that the electron deficiency is localized at the 5-position (and presumably the 7-position which is apparently sterically blocked). The failure to observe lithiation even with small relatively hard carbanions probably reflects this concentration of the electron deficiency, whereas in the π -coordinated arenes, the electron withdrawing effect of the metal is distributed among all six carbon atoms. That substitution for halogens is a less accessible pathway for these quinoline derivatives than for $\pi\text{-}\eta^6$ arenes is more difficult to rationalize but may be due to the fact that the direction of electron polarization is along the reaction coordinate for substitution in the case of the $\pi\text{-}\eta^6$ arenes while this is not the case for the $\mu_3\text{-}\eta^2$ quinoline complexes.

It is also noteworthy that these quinoline derivatives react reasonably well with methyl and allyl Grignard reagents while the $\pi\text{-}\eta^6$ arenes do not. This is probably also related to the localization of the electron deficiency, as described above. In addition, this may be a consequence of the fact that the carbonyl ligands on the osmium cluster may

be less subject to competitive nucleophilic attack than the carbonyls in the π - η^6 chromium arenes owing to their higher average infrared stretching frequencies and/or force constants of the C-O carbonyl ligand bonds.¹⁰

The strictly *trans*- addition of the electrophiles (H^+ , $CH_3^+CH_3CO^+$) is a consequence of the planar structure of the intermediate anion (Equation 2.3). What is surprising here is that even with the relatively small methyl group *trans*- addition is >95% by 1H NMR while with hydride as the nucleophile and proton as the electrophile, the stereoselectivity is completely lost, with both *cis*- and *trans*- addition taking place to about the same extent.⁷ These results indicate that the stereoselectivity is steric in origin rather than being directed by prior coordination of the electrophile to the metal core or the carbonyl ligands. That complex (dihydride) **38n** does not convert to **37n** is consistent with this interpretation. In the case of π - η^6 arene complexes quenching with electrophiles other than protons leads primarily to electrophilic alkylation of the carbanion owing to the reversibility of the nucleophilic addition.¹⁴ We see no evidence for reversible addition in the reaction of **35** with nucleophiles although 2:3-fold excesses of the carbanions were sometimes necessary to drive the reaction to completion. Stereoselective *trans*- acylation is observed for π - η^6 arenes with methyl iodide as the electrophile in the presence of carbon monoxide and in this case, interaction with the carbonyl ligands on chromium directs the *trans*- addition.⁷ Topside attack of both nucleophile and electrophile to give overall *cis*- addition is observed in the nucleophilic additions across the 5,6-bond of π - η^6 dihydro-naphthyl chromium tricarbonyls.¹¹

Overall, there are distinct steric and electronic differences between the activation of quinolines by the μ_3 - η^2 bonding mode to triosmium clusters and the well known π - η^6

arene complexes. Of course, none of this chemistry would be possible without the presence of the third metal atom which coordinates the nitrogen lone pair and apparently blocks attack at the 2- position, the normal site of nucleophilic attack in quinolines.¹² Indeed, this chemistry is extendable to a wide range of benzoheterocycles with pyridinyl nitrogens. Thus, the synthetic methodology outlined here is applicable to quinoxaline, benzothiazole 2-methyl benzimidazoles, benzotriazoles and phenanthradines.¹³ This work is currently underway in our laboratories.

3.9 Experimental Section

3.9.1 Material and General Considerations

All reactions were carried out under an atmosphere of nitrogen but were worked up in air. Tetrahydrofuran was distilled from benzophenone ketyl, methylene chloride and acetonitrile from calcium hydride.

Infrared spectra were recorded on a Perkin-Elmer 1600 FT-IR spectrometer and ¹H and ¹³C NMR were recorded on a Varian Unity Plus 400. Elemental analyses were done by Schwarzkopf Microanalytical Labs, Woodside, New York. Chemical shifts are reported down field positive relative to tetramethylsilane and coupling constants are reported only for those resonances relevant to the stereochemistry and while only the multiplicities of resonances with standard couplings are reported.

Dichlorodicyanoquinone and trityl tetrafluoroborate were purchased from Aldrich Chemical and used as received. Trifluoroacetic acid and diisopropylamine were purchased from Aldrich Chemical and distilled from phosphorous pentoxide and calcium hydride respectively before use. The carbanion reagents CH₃Li, n-BuLi, ^tBuLi,

CH_3MgBr . and allylMgBr were purchased from Aldrich and used as received. The carbanion reagents BnLi and PhLi were prepared in ether directly before use by the reaction of the corresponding diorganomercury compound (Strem) with lithium metal (Aesar). The other carbanions were generated by deprotonation of their corresponding neutral precursor with lithium diisopropyl amide which was generated from diisopropyl amine and Li^nBu according to published procedures¹⁴ except for the carbanions resulting from 1,3-dithiane and vinyl bromide which were generated by treatment with $n\text{-BuLi}$ and $^t\text{BuLi}$ respectively, at -78°C .

3.9.2 Preparation of $\text{Os}_3(\text{CO})_9(\mu_3\text{-}\eta^3\text{-C}_9\text{H}_7(\text{R}')\text{N})(\mu\text{-H})$ (37a-237), $\text{Os}_3(\text{CO})_9(\mu_3\text{-}\eta^3\text{-C}_9\text{H}_6(\text{R})(\text{R}')\text{N})(\mu\text{-H})$ (38b, 38c, 38d, 38e, 38e', 38f, 38f', 38h, *cis*-38n, 39n, *cis*-38m, *cis*-38m')

The following procedure was followed for the compounds listed above. 25-200 mg (0.025-0.20 mmol) $\text{Os}_3(\text{CO})_9(\mu_3\text{-}\eta^2\text{-C}_9\text{H}_5(\text{R})\text{N})(\mu\text{-H})$ was dissolved in 5 mL THF and cooled to -78°C , at which time a 1.5-3 molar excess of the appropriate carbanion was added slowly by syringe. The amount of carbanion added was governed by an observable color change from deep green to dark amber or orange. The reaction mixture was warmed to 0°C , stirred for 0.25 to 1h, cooled again to -78°C and quenched with an amount of trifluoroacetic acid, 10% in excess of the amount of carbanion used. The solution generally turned orange-red as it warmed to room temperature. The clear orange-red solution then rotary evaporated, taken up in minimum CH_2Cl_2 , filtered and then purified by thin layer chromatography on 0.1x20x20cm or 0.1x20x40 cm silica gel plates using $\text{CH}_2\text{Cl}_2/\text{hexanes}$ (20-50% CH_2Cl_2 as eluent. In general, one major orange band containing

the nucleophilic addition product was observed in addition to minor amounts of unconsumed starting material, $\text{Os}_3(\text{CO})_{10}(\mu\text{-}\eta^2\text{-C}_9\text{H}_5(\text{R})\text{N})(\mu\text{-H})$ and in the case of *cis*-**38n**, complex **39n** was obtained as a yellow band moving faster than the major product but slower than the starting material. Yields are given along with the analytical and spectroscopic data below.

Compound 37a: Yield for **37a**: 65.9%. Anal. Calcd for $\text{C}_{19}\text{H}_{11}\text{NO}_9\text{Os}_3$: C, 23.58; H, 1.14; N, 1.45%. Found: C, 23.86; H, 0.83; N, 1.38%. IR (ν CO) in hexane: 2117 m, 2078 s, 2046 s, 2024 s, 1989 br, 1968 br. ^1H NMR of **37a** at 400 MHz in CDCl_3 : δ 8.41 (d, H(2)), 7.39 (d, H(4)), 6.84 (t, H(3)), 4.09 (t, H(7)) 2.84 (m, H(5)), 2.28 m & 1.98 m (H(6), 2H),), 1.17(d, CH_3), -16.99 (s, hydride).

Compound 37b: Yield for **37b**: 44.6%. Anal. Calcd for $\text{C}_{22}\text{H}_{17}\text{NO}_9\text{Os}_3$: C, 26.20; H, 1.69; N, 1.36%. Found: C, 26.05; H, 1.67; N, 1.23%. IR (ν CO) in hexane: 2079 s, 2047 s, 2024 s, 1998 w, 1991 br, 1967 w. ^1H NMR of **37b** at 400 MHz in CDCl_3 : δ 8.42 (dd, H(2)), 7.36 (dd, H(4)), 6.82 (t, H(3)), 4.03 (t, H(7)), 2.52 (m, H(5)), 2.31 (m 2H, CH_2 on butyl), 1.50 m (H(6), 2H), 1.29 (m, CH_2 , 4H), 0.86 (t, CH_3) -16.99 (s, hydride).

Compound 37c: Yield for **37c**: 51.6%. Anal. Calcd for $\text{C}_{22}\text{H}_{17}\text{NO}_9\text{Os}_3$: C, 26.16; H, 1.68; N, 1.38%. Found: C, 25.82; H, 1.70; N, 1.32%. IR (ν CO) in hexane: 2102 m, 2078 m, 2057 w, 2048 s, 2023 s, 2003 w, 1989 m, 1969 br. ^1H NMR of **37c** at 400 MHz in CDCl_3 :

δ 8.49 (dd, H(2)), 7.36 (dd, H(4)), 6.82 (t, H(3)), 4.06 (t, H(7)), 2.70 m & 2.16 m (H(6), 2H), 2.28 (d, H(5)), 0.934 (s, 9H, CH₃ on t-Butyl) -16.95 (s, hydride).

Compound **37d**: Yield for **37d**: 48.2%. Anal. Calcd for C₂₅H₁₅NO₉Os₃: C, 22.17; H, 1.36; N, 1.27%. Found: C, 28.17; H, 1.33; N, 1.29%. IR (ν CO) in hexane: 2079 s, 2046 s, 2024 s, 1990 s, 1967 br. ¹H NMR of **37d** at 400 MHz in CDCl₃: δ 8.40 (dd, H(2)), 6.68 (t, H(3)), 6.97 (dd, H(4)), 2.70 (m, H(5)), 2.27 m & 2.12 m (H(6), 2H), 4.03 (t, H(7)), 7.22 (m, 4H), 6.95 (m, 1H), 2.86 (m, CH₂ of benzyl). -16.99 (s, hydride).

Compound **37e**: Yield for **37e**: 66.11%. Anal. Calcd for C₂₄H₁₃NO₉Os₃: C, 27.96; H, 1.26; N, 1.25%. Found: C, 27.55; H, 1.33; N, 1.25%. IR (ν CO) in hexane: 2079 s, 2047 s, 2025 s, 1991 s, 1969 br. ¹H NMR of **37e** at 400 MHz in CDCl₃: δ 8.46 (d, H(2)), 7.09 - 7.32 (m, 5H) 7.03 (d, H(4)), 6.77 (dd, H(3)), 4.02 (m, H(7)), 3.97 (m, H(5)), 2.48 (m, H(6), 2H). -16.99 (s, hydride).

Compound **37f**: Yield for **37f**: 50.8%. Anal. Calcd for C₂₀H₁₁NO₉Os₃: C, 24.52; H, 1.12; N, 1.43%. Found: C, 24.43; H, 1.07; N, 1.42%. IR (ν CO) in hexane: 2101 w, 2079 s, 2047 s, 2024 s, 2001 w, 1991 br, 1969 w. ¹H NMR of **37f** at 400 MHz in CDCl₃: δ 8.45 (dd, H(2)), 7.38 (dd, H(4)), 6.84 (t, H(3)), 5.69 (m, 1H), 5.25 & 5.04 (d, 2H), 4.02 (t, H(7)), 3.42 (m, H(5)), 2.25 (m, H(6), 2H), -17.00 (s, hydride).

Compound **37g**: Yield for **37g**: 48.0%. Anal. Calcd for $C_{24}H_{17}NO_9Os_3$: C, 27.86; H, 1.65; N, 1.35%. Found: C, 27.77; H, 1.81; N, 1.16%. IR (ν CO) in hexane: 2102 w, 2079 s, 2046 s, 2025 s, 1990 br, 1968 w. 1H NMR of **37g** at 400 MHz in $CDCl_3$: Diastereomer 1: δ 8.42 (dd, H(2)), 7.35 (dd, H(4)), 6.82 (t, H(3)), 4.03 (t, H(7)), 2.58 (m, CH_2), 2.21 m (H(6), 2H), 1.72 (m, CH_2), 1.52 (m, H(5)), 1.28 (m, CH_2), 0.978 (t, CH_3) -17.00 (s, hydride). Diastereomer 2: δ 8.40 (dd, H(2)), 7.31 (dd, H(4)), 6.79 (t, H(3)), 3.93 (t, H(7)), 2.53 (m, CH_2), 2.15 (m, H(6), 2H), 1.68 (m, CH_2), 1.49 (m, H(5)), 1.22 (m, CH_2), 0.851 (t, CH_3), -17.10 (s, hydride).

Compound **37h**: Yield for **37h**: 72.1%. Anal. Calcd for $C_{20}H_{10}N_2O_9Os_3$: C, 24.16; H, 1.01; N, 2.42%. Found: C, 24.07; H, 1.22; N, 2.51%. IR (ν CO) in hexane: 2057 w, 2048 s, 2023 s, 2003 w, 1991 m, 1969 br. 1H NMR of **37h** at 400 MHz in $CDCl_3$: δ 8.52 (dd, H(2)), 7.49 (dd, H(4)), 6.92 (t, H(3)), 3.90 (t, H(7)), 3.06 (m, H(5)), 2.39 (m, CH_2), 2.32 (m, H(6), 2H), -17.06 (s, hydride).

Compound **37i**: Yield for **37i**: 69.1%. Anal. Calcd for $C_{22}H_{14}N_2O_9Os_3$: C, 25.90; H, 1.27; N, 2.74%. Found: C, 26.04; H, 1.38; N, 2.50%. IR (ν CO) in hexane: 2050 s, 2025 s, 2003 w, 1991 m, 1969 br, 1957 w. 1H NMR of **37i** at 400 MHz in $CDCl_3$: δ 8.58 (d, H(2)), 7.54 (d, H(4)), 6.91 (t, H(3)), 3.93 (m, H(7)), 2.81 dd & 2.64 dd (H(6), 2H), 2.25 (d, H(5)), 1.42 (s, CH_3), 1.35 (s, CH_3), -17.00 (s, hydride).

Compound **37j**: Yield for **37j**: 72.4%. Anal. Calcd for $C_{22}H_{15}NO_9Os_3S_2$: C, 24.63; H, 1.40; N, 1.31%. Found: C, 24.56; H, 1.34; N, 1.21%. IR (ν CO) in hexane: 2102 m, 2078 m, 2057 w, 2048 s, 2023 s, 2003 w, 1989 m, 1969 br. 1H NMR of **37j** at 400 MHz in $CDCl_3$: δ 8.45 (dd, H(2)), 7.48 (d, H(4)), 6.83 (t, H(3)), 4.04 (t, H(7)), 4.21 (d, 1H), 1.79 (m, H(5)), 2.82(m, 2H), 2.17(tt, H(6), 2H), 2.05 (m, 2H), 2H), -17.00 (s, hydride).

Compound **37k**: Yield for **37k**: 85.8%. Anal. Calcd for $C_{24}H_{19}NO_{11}Os_3$: C, 26.98; H, 1.78; N, 1.31%. Found: C, 27.38; H, 1.55; N, 1.27%. IR (ν CO) in hexane: 2079 s, 2047 s, 2025 s, 1991 m, 1969 br. 1H NMR of **37k** at 400 MHz in $CDCl_3$: δ 8.43 (dd, H(2)), 7.45 (dd, H(4)), 6.82 (t, H(3)), 3.99 (t, H(7)), 3.14 (m, H(5)), 2.45 (dd, H(6), 2H), 2.22 (t, CH_2), 1.39 (s, CH_3 , 9H) -17.04 (s, hydride).

Compound **37l**: Yield for **37l**: 52.6%. Anal. Calcd for $C_{21}H_{13}NO_9Os_3$: C, 25.35; H, 1.31; N, 1.41%. Found: C, 25.31; H, 1.36; N, 1.31%. IR (ν CO) in hexane: 2079 s, 2046 s, 2024 s, 1991 m, 1969 br. 1H NMR of **37l** at 400 MHz in $CDCl_3$: δ 8.42 (dd, H(2)), 7.33 (dd, H(4)), 6.81 (t, H(3)), 5.64 (m, 1H), 5.05 (m, 2H) 4.01 (t, H(7)), 2.65 (m, H(5)), 2.23(m, H(6), 2H), 2.25 (m, CH_2), -17.00 (s, hydride).

Compound **38b** : Yield for **38b**: 50.3%. Anal. Calcd. $C_{24}H_{17}N_2O_{11}Os_3$: C, 26.64; H, 1.57; N, 2.59 %. Found: C, 26.48; H, 1.34; N, 2.57 %. IR (ν CO) in CH_2Cl_2 : 2082 s, 2051 s, 2028 s, 1994 br, 1971 w cm^{-1} . 1H NMR of **38b** at 400 MHz in $CDCl_3$: δ 9.13 (s, H(2)),

8.08 (s, H(4)), 3.49 (s, CH₃ on carboxy), 3.87 (m, H(7)), 2.68 (d, H(5)), 2.83 & 2.22 (dd & q of q, H(6) two protons), 1.39 & 1.37 (s & s CH₃ 6 protons), -17.027 (s, hydride).

Compound **38c**: Yield for **38c**: 60.1%. Anal. Calcd for C₂₂H₁₅N₃O₉Os₃: C, 25.51; H, 1.54; N, 4.05%. Found: C, 27.12; H, 1.87; N, 3.75%. IR (ν CO) in hexane: 2080 m, 2049 s, 2027 s, 2004 m, 1992 s, 1969 w, 1964 w, 1952 w. ¹H NMR of **38c** at 400 MHz in CDCl₃: δ 8.06 (d, H(2)), 7.29 (br, NH₂), 6.73 (s, H(4)), 3.95 (dd, H(7)), 2.71 & 2.25 (m, H(6), 2H), 2.54 (d, H(5)), 1.40 (s, CH₃), 1.33 (s, CH₃), -17.01 (s, hydride).

Compound **38d** : Yield for **38d**: 71.2%. Anal. Calcd. C₂₃H₁₆N₂O₉Os₃: C, 26.60; H, 1.54; N, 2.70 %. Found: C, 26.48; H, 1.49; N, 2.60 %. IR (ν CO) in CH₂Cl₂ : 2080 s, 2050 s, 2026 s, 1990 br, 1968 w, 1954 w cm⁻¹. ¹H NMR of **38d** at 400 MHz in CDCl₃ : δ 8.42 (dd, H(2)), 6.77 (d, H(3)), 3.92 (m, H(7)), 2.97 (dd, H(5)), 2.73 & 2.09 (m & m, H(6) two protons), 2.19 (s, CH₃ on C(4)), 1.46 & 1.42 (s & s CH₃ 6 protons), -17.022 (s, hydride).

Compound **38e'**: Yield for **38e'**: 53.6%. Anal. Calcd for C₂₄H₁₁ClNO₁₁Os₃: C, 26.08; H, 1.81; N, 1.27%. Found: C, 26.12; H, 1.93; N, 1.16%. IR (γ CO) in hexane: 2081 m, 2050 s, 2028 s, 2002 m, 1975 w, 1968 w, 1955 w. ¹H NMR of **38e'** at 400 MHz in CDCl₃: δ 8.31 (d, H(2)), 6.85 (d, H(3)), 3.90 (t, H(7)), 3.45 (m, H(5)), 2.46 (m, CH₂), 2.05 (m, H(6), 2H), 1.44 (s, CH₃, 9H) -17.05 (s, hydride),.

Compound **38e**: Yield for **38e**: 67.1%. Anal. Calcd for $C_{22}H_{13}ClNO_9Os_3$: C, 25.02; H, 1.23; N, 2.65%. Found: C, 24.96; H, 1.15; N, 2.31%. IR (γ CO) in hexane: 2081 s, 2050 s, 2027 s, 1992 br, 1972 w, 1958 w. 1H NMR of **38e** at 400 MHz in $CDCl_3$: δ 8.46 (d, H(2)), 6.94 (d, H(3)), 3.92 (dd, H(7)), 3.17 (m, H(5)), 2.19(m, H(6), 2H), 1.47 (s, CH_3), 1.43 (s, CH_3), -17.02 (s, hydride).

Compound **38f**: Yield for **38f**: 64.0%. Anal. Calcd for $C_{25}H_{21}NO_{12}Os_3$: C, 27.32; H, 2.01; N, 1.27%. Found: C, 27.81; H, 2.20; N, 1.06%. IR (γ CO) in hexane: 2104 m, 2080 s, 2048 s, 2027 s, 1991 br. 1H NMR of **38f** at 400 MHz in $CDCl_3$: δ 8.30 (d, H(2)), 6.32 (d, H(3)), 3.91 (dd, H(7)), 3.82 (s, OCH_3), 3.43 (m, H(5)), 2.02 (dt, H(6), 2H), 2.76 m & 2.35 dd (CH_2 of t-BuAc) 2.12 (s, CH_3 , 9H), -17.06 (s, hydride).

Compound **38f**: Yield for **38f**: 72.0%. Anal. Calcd for $C_{23}H_{16}N_2O_{10}Os_3$: C, 26.28; H, 1.42; N, 2.61%. Found: C, 26.60; H, 1.22; N, 2.54%. IR (γ CO) in hexane: 2104 m, 2088 s, 2048 s, 2028 s, 1990 br. 1H NMR of **38f** at 400 MHz in $CDCl_3$: δ 8.43 (d, H(2)), 6.41 (d, H(3)), 4.00 (dd, H(7)), 3.84 (s, OCH_3), 3.10 (d, H(5)), 2.73 m, -2.18 m, (H(6), 2H), 1.37 (s, CH_3), 1.35 (s, CH_3), -17.06 (s, hydride).

Compound **38h**: Yield for **38h**: 31.1 %. Anal. Calcd for $C_{23}H_{15}N_1O_{11}Os_3$: C, 26.64; H, 1.43; N, 1.33%. Found: C, 26.88; H, 1.53; N, 1.53%. IR (ν CO) in hexane: 2080 s, 2050 s, 2026 s, 1999 m, 1990 br, 1969 w, 1958 w cm^{-1} . 1H NMR of **38h** at 400 MHz in $CDCl_3$: δ 8.52 (d, H(2)), 7.28 (d, H(3)), 5.71 (m, allyl proton), 5.04 (dd, terminal two allyl

protons). 3.92 (m, H(7)), 3.89 (s, CH₃), 3.54 (m, H(5)), 2.48 & 2.29 (m & m, H(6) two protons), 1.93 & 1.95 (t & t, 1st CH₂ on allyl), -17.007 (s, hydride).

Compound 38i: Yield for **38i:** 41.3%. C₂₄H₁₇N₂O₁₁Os₃: C, 26.64; H, 1.57; N, 2.59 %. Found: C, 26.41; H, 1.41; N, 2.46 %.. IR (γ CO) in CH₂Cl₂: 2104 m, 2088 s, 2048 s, 2028 s, 1990 br. ¹H NMR of **38i** at 400 MHz in CDCl₃: δ 8.73 (d, H(2)), 7.10 (d, H(3)), 3.91 (dd, H(7)), 3.81 (dd, H(5)), 2.78 and 2.24 (dd & dd, (H(6), 2H), 1.34 (s, CH₃), 1.31 (s, CH₃), -16.99 (s, hydride).

Compound 39i: Yield for **39i:** 57.2 %. Anal. Calcd for C₂₂H₁₃N₂O₉Os₃F: C, 25.41; H, 1.25; N, 2.69%. Found: C, 25.68; H, 1.39; N, 2.53%. IR (ν CO) in CH₂Cl₂: 2155w, 2125w, 2076 s, 2047 s, 2020 s, 1989 m cm⁻¹. ¹H NMR of **39i** at 400 MHz in CDCl₃: δ 8.50 (dd, H(2)), 8.32 (dd, H(6)), 6.73 (dd, H(7)), 3.48 (d, H(4)), 3.25 (m, H(3) two protons), 1.41 & 1.22 (s & s, methyls), -13.014 (s, hydride).

Compound 39i': Yield for **39i':** 52.3 %. Anal. Calcd for C₂₂H₁₃N₂O₉Os₃F: C, 25.70; H, 1.55; N, 1.36%. Found: C, 25.32; H, 1.42; N, 1.21%. IR (ν CO) in CH₂Cl₂: 2155w, 2125w, 2076 s, 2047 s, 2020 s, 1989 m cm⁻¹. ¹H NMR of **39i'** at 400 MHz in CDCl₃: δ 8.54 (d, H(2)), 8.21 (dd, H(6)), 6.77 (t, H(7)), 3.31 (q, H(4)), 3.04 & 2.83 (dd & dd, H(3) two protons), 1.37 (q, 1st CH₂ on butyl), 1.21 (m, 2nd CH₂ on butyl), 1.11 (m, CH₂), 0.82 (t, terminal CH₃), -13.134 (s, hydride).

Compound 35j: Yield for **35j**: 65.5%. Anal. Calcd $C_{22}H_{13}ClN_2O_9Os_3$. C, 25.02; H, 1.20; N 2.65%. Found: C, 25.15; H, 1.09; N, 2.59%. IR (ν CO) in hexane: 2077 m, 2050 s, 2023 s, 1991 s. 1H NMR of **35j** in $CDCl_3$: δ 8.78 (dd, H(2)), 8.22 (d, H(6)), 6.96 (d, H(7)), 3.68 (d, H(4)), 3.24 (dd, H(3), 2H), 1.47 (s, CH_3), 1.28 (s, CH_3), -12.78 (s, hydride)

Compound 39k: Yield for **39k**: 50.5 %. Anal. Calcd for $C_{22}H_{13}N_2O_9Os_3Br$: C, 24.02; H, 1.18; N, 2.54%. Found: C, 24.56; H, 1.16; N, 2.52%. IR (ν CO) in hexane: 2077 s, 2050 s, 2023 s, 1991 $m\text{ cm}^{-1}$. 1H NMR of **39k** at 400 MHz in $CDCl_3$: δ 8.86 (dd, H(2)), 8.12 (d, H(6)), 7.14 (d, H(7)), 3.31 & 3.20 (dd & dd, H(3) two protons), 1.49 & 1.31 (s & s, methyls), -12.713 (s, hydride).

Compound 39k': Yield for **39k'**: 48.4 %. Anal. Calcd for $C_{22}H_{16}N_1O_9Os_3Br$: C, 24.33; H, 1.29; N, 1.47%. Found: C, 24.45; H, 1.41; N, 1.56%. IR (ν CO) in CH_2Cl_2 : 2155w, 2125w, 2076 s, 2047 s, 2020 s, 1989 $m\text{ cm}^{-1}$. 1H NMR of **39k'** at 400 MHz in $CDCl_3$: δ 8.80 (dd, H(2)), 7.82 (dd, H(6)), 6.81 (d, H(7)), 3.31 (dd, H(4)), 2.39 & 2.24 (m & m, H(3) two protons), 1.60 (m, 1st CH_2 on butyl), 1.42 (q, 2nd CH_2 on butyl), 1.22 (m, CH_2), 0.943 (t, terminal CH_3), -12.974 (s, hydride).

Compound 39l: Yield for **39l**: 51.2%. Anal. Calcd. $C_{22}H_{15}N_3O_9Os_3$: C, 25.51; H, 1.54; N, 4.05 %. Found: C, 25.89; H, 1.69; N, 3.89 %. IR (ν CO) in CH_2Cl_2 : 2078 s, 2049 s, 2021 s, 1984 br, 1944 w cm^{-1} . 1H NMR of **39l** at 400 MHz in $CDCl_3$: δ 8.88 (dd, H(2)),

7.89 (d, H(6)), 6.27 (d, H(7)), 4.88 (s, NH₂), 3.20 (dd, H(4)), 3.15 & 3.01 (dd & d, H(3) two protons), 1.37 & 1.34 (s & s CH₃ 6 protons), -13.778 (s, hydride).

Compound **39l'**: Yield for **39l'**: 53.3%. Anal. Calcd. C₂₂H₁₈N₂O₉Os₃: C, 25.80; H, 1.76; N, 2.73 %. Found: C, 25.59; H, 1.65; N, 2.67 %. IR (ν CO) in CH₂Cl₂: 2076 s, 2047 s, 2021 s, 1988 br, 1942 w cm⁻¹. ¹H NMR of **39l'** at 400 Mz in CDCl₃: δ 8.83 (dd, H(2)), 7.86 (d, H(6)), 6.19 (d, H(7)), 4.65 (s, NH₂), 2.63 (dd, H(4)), 2.95 & 2.85 (dd & d, H(3) two protons), 1.39-1.18 (m, CH₂-CH₂-CH₂ 6 protons), -13.846 (s, hydride).

Compound *cis*-**38m**: Yield for *cis*-**38m**: 71.3%. Anal. Calcd for C₂₃H₁₆N₂O₉Os₃: C, 26.60; H, 1.54; N, 2.70%. Found: C, 26.56; H, 1.53; N, 2.69%. IR (ν CO) in hexane: 2080 s, 2050 s, 2026 s, 1999 m, 1990 br, 1969 w, 1958 w. ¹H NMR of *cis*-**38m** at 400 MHz in CDCl₃: δ 8.55 (d, H(2)), 7.42 (d, H(4)), 6.88 (t, H(3)), 3.64 (d, H(7)), 2.72 (d, H(5), JH(5)-H(6)=4.80 Hz,), 2.59 (m, (H(6), 2H, JH(6)-H(7)=5.95 Hz), 1.64 (d, CH₃, on C(6)), 1.40 (s, CH₃), 1.32 (s, CH₃) -17.03 (s, hydride).

Compound *cis*-**38m'**: Yield for *cis*-**38m'**: 67.1%. Anal. Calcd for C₂₀H₁₃NO₉Os₃: C, 24.49; H, 1.32; N, 1.43%. Found: C, 24.42; H, 1.07; N, 1.43%. IR (ν CO) in hexane: 2078 s, 2047 s, 2024 s, 1990 m, 1968 br. ¹H NMR of *cis*-**38m'** at 400 MHz in CDCl₃: δ 8.39 (dd, H(2)), 7.33 (dd, H(4)), 6.78 (tt, H(3)), 3.52 (d, H(7)), 2.53 (m, H(5) JH(5)-H(6)=4.50 Hz,), 2.37 (m, H(6), JH(6)-H(7)=4.0 Hz), 1.25 (d, CH₃ on C(6)), 1.04 (d, CH₃ on C(5)), -17.02 (s, hydride).

Compound **cis-38n**: Yield for **cis-38n**, 1 eq of acid used ~10% **39n** obtained: 63.0%. Anal. Calcd for $C_{22}H_{13}ClN_2O_9Os_3$: C, 25.02; H, 1.23; N, 2.65%. Found: C, 25.46; H, 1.28; N, 2.19%. IR (ν CO) in hexane: 2102 m, 2083 m, 2076 m, 2051 s, 2030 m, 2018 w, 1995 br. 1H NMR of **cis-38n** at 400 MHz in $CDCl_3$: δ 8.58 (d, H(2)), 7.51 (d, H(4)), 6.96 (t, H(3)), 4.47(t,H(6), JH(5)-H(6)=5.77 Hz)), 3.74 (d, H(7)), 3.02 (d, H(5)), 1.64 (s, CH_3), 1.50 (s, CH_3), -17.26 (s, hydride).

Compound **39n**: Yield for **39n** 10 eq of acid used ~50% **38n** obtained : 36.1%. Anal. Calcd for $C_{22}H_{13}ClN_2O_9Os_3$: C, 25.02; H, 1.25; N, 2.65%. Found: C, 25.41; H, 1.31; N, 2.32%. IR (ν CO) in hexane: 2101 s, 2076 s, 2046 s, 2015 s, 1999 br, 1969 br. 1H NMR of **39n** at 400 MHz in $CDCl_3$: δ 7.49 (d, H(2)), 7.04(d, H(4)), 6.69 (s, H(7)), 5.79 (t, H(3)), 3.52 (s, H(5)), 1.18 (s, CH_3), 0.88 (s, CH_3), -13.51(d, hydride, J Hydride-Hydride=1.6 Hz), -14.52 (d, hydride).

Compound **cis-38p**: Yield for **cis-38p**: 57.2%. Anal. Calcd. $C_{23}H_{15}N_1O_9Os_3$: C, 26.24;H, 1.43; N, 1.33 %. Found: C, 26.16; H, 1.35; N, 1.30 %. IR (ν CO) in CH_2Cl_2 : 2080 s, 2050 s, 2026 s, 1990 br, 1968 w, 1954 w cm^{-1} . 1H NMR of **cis-38p** at 400 MHz in $CDCl_3$: δ 8.43 (d, H(2)), 7.30 (d, H(4)), 6.81 (t, H(3)), 5.61 (m, 2nd H on allyl), 4.97 & 4.78 (m & m. terminal allyl two protons), 4.15 (d, H(7)), 3.82 (s, CH_3 on carboxy), 3.09 (m, 1st allyl proton), 2.99 (m, H(6)),2.27-2.23 (m, H(5) and -1st proton of allyl), -17.085 (s, hydride).

Compound **35s**: Yield for **35s**: 54.1%. Anal. Calcd for $C_{25}H_{19}NO_{12}Os_3$: C, 27.32; H, 1.73; N, 1.27%. Found: C, 27.39; H, 1.75; N, 1.29%. IR (ν CO) in hexane: 2075 s, 2047 s, 2019 s, 1989 br. m. 1H NMR of **35s** at 400 MHz in $CDCl_3$: δ 9.15 (dd, H(2)), 8.36 (s, H(7)), 8.14 (dd, H(4)), 7.08 (tt, H(3)), 3.95 (s, OCH_3 on C(6)), 3.77 (s, CH_2 on C(5)), 1.3 (s, 9H), -11.99 (s, hydride).

Compound **35t**: Yield for **35t**: 35.2%. Anal. Calcd for $C_{24}H_{17}NO_{12}Os_3$: C, 26.56; H, 1.57; N, 1.29%. Found: C, 27.21; H, 1.45; N, 1.25%. IR (ν CO) in hexane: 2075 s, 2048 s, 2019 s, 1989 br. m. 1H NMR of **35t** at 400 MHz in $CDCl_3$: δ 9.16 (dd, H(2)), 8.24 (dd, H(4)), 8.22 (s, H(7)), 7.15 (t, H(3)), 7.81 (s, OH on C(6)), 3.75 (s, CH_2), 1.406 (s, CH_3 , 9H) -12.27 (s, hydride).

3.9.3 Preparation of $Os_3(CO)_9(\mu_3-\eta^3-C_9H_6(6-R)(5-R')N)(\mu-H)$ (*trans*- **38m**, *trans*-**3m'**, *trans* **38z**).

A 50-100 mg (0.05-0.100 mmol) sample of **1a** was dissolved in 5 mL THF, cooled to $-78^\circ C$ and treated with a 2-3 molar excess of $LiC(CH_3)_2CN$ or $LiCH_3$. The reaction solution is warmed to $0^\circ C$, the THF removed by trap distillation and then 5 mL CH_2Cl_2 added after, with a two-fold excess (based on the amount of carbanion used) of dimethylsulfate or acetic anhydride is slowly added by syringe. The reaction mixture was then warmed to room temperature, rotary evaporated, taken up in minimum methylene chloride, filtered and then purified by thin layer chromatography using CH_2Cl_2 /hexanes as eluent. In the case of *trans*- **38m** and *trans*- **38m'**, it was not possible to separate these

products from **37i** and **37a** respectively which were formed (40% of total yield by ^1H NMR) as a result of incomplete electrophilic alkylation of the intermediate anion. The two compounds were separated by preparative HPLC using a reverse-phase C-18 column and 15% water-acetonitrile as the eluting solvent. In the case of **38**, the formation of **37a** was also observed (~10%) but as a distinct orange band on the TLC plate. Isolated yields of *trans*-**38m**, *trans*-**38m'** and **38** are given below with the spectroscopic and analytical data.

Compound *trans*-**38m**: Yield for *trans*-**38m**: 41.1%. Anal. Calcd for $\text{C}_{23}\text{H}_{16}\text{N}_2\text{O}_9\text{Os}_3$: C, 26.61; H, 1.54; N, 2.70%. Found: C, 26.56; H, 1.53; N, 2.69%. IR (ν CO) in hexane: 2080 s, 2050 s, 2026 s, 1999 m, 1990 br, 1969 w, 1958 w. ^1H NMR of *trans*-**38m** at 400 MHz in CDCl_3 : δ 8.60 (dd, H(2)), 7.52 (d, H(4)), 6.90 (t, H(3)), 4.54 (d, H(7)), 2.74 (t, (H(6)) J H(6)-H(7)=8.0 Hz), 2.42 (s, H(5), J H(5)-H(6) = < 1 Hz), 1.05 (d, CH_3 on C(6)), 1.36 (s, CH_3), 1.30 (s, CH_3), -16.51 (s, hydride).

Compound *trans*-**38m'**: Yield for *trans*-**38m'**: 30.1%. Anal. Calcd for $\text{C}_{20}\text{H}_{13}\text{NO}_9\text{Os}_3$: C, 24.49; H, 1.32; N, 1.43%. Found: C, 24.41; H, 1.08; N, 1.41%. IR (ν CO) in hexane: 2078 s, 2024 s, 1990 m, 1967 br. ^1H NMR of *trans*-**38m'** at 400 MHz in CDCl_3 : δ 8.40 (dd, H(2)), 7.47 (dd, H(4)), 6.86 (t, H(3)), 3.74 (d, H(7)), 2.55 (m, H(5), J H(5)-H(6)=11.98 Hz), 1.76 (m, (H(6), J H(6)-H(7)=4.0Hz), 1.24 (t, CH_3 on C(6)), 1.15 (d, CH_3 on C(5)), -17.01 (s, hydride).

Compound **trans-38z**: Yield for **trans-38z**: 56.7%. Anal. Calcd for $C_{21}H_{13}NO_{10}Os_3$: C, 24.95; H, 1.29; N, 1.39%. Found: C, 25.31; H, 1.18; N, 1.27%. IR (ν CO) in hexane: 2080 s, 2049 s, 2026 s, 1991 m, 1967 w. 1H NMR of **trans-38** at 400 MHz in $CDCl_3$: δ 8.42 (d, H(2)), 7.48 (d, H(4)), 6.92 (t, H(3)), 3.60 (d, H(7)), 3.18 (m, H(5), J H(5)-H(6)=12.12 Hz), 2.73 (m, H(6)), J H(6)-H(7)=4.40 Hz), 2.36 (s, $COCH_3$ on C(6)), 1.12 (d, CH_3 on C(5)), -17.12 (s, hydride).

3.9.4 Preparation of $Os_3(CO)_9(\mu_3-\eta^2-C_9H_5(R')N)(\mu-H)$ ($R'=n-Bu$, **35u**; $R'=CH_2CP_2^tBu$, **35v**); Rearomatization of the Nucleophilic Addition Products with Ph_3CBF_4 .

A sample consisting of 50 mg (0.025 mmol) **1a** in 5 mL THF is treated with a two-fold molar excess of $LiR'(R'-n-Bu, CH_2CO_2^tBu)$ at $-78^\circ C$. The reaction solution warmed to $0^\circ C$, and the solvent removed by trap-to-trap distillation. Next, 5 mL CH_2Cl_2 is added and then 2.1 equivalents of $Ph_3C^+ BF_4^-$ (based on **1a**) is added as a solid and the reaction mixture was stirred for 30 min, rotary evaporated and then purified by TLC using CH_2Cl_2 /hexanes (50% CH_2Cl_2) to yield one major band 30-35 mg (55-60%) of $Os_3(CO)_9(\mu_3-C_9H_5(R')N)(\mu-H)(R=n-Bu$ **35u**, $R=CH_2CO_2^tBu$, **35v**). Additional minor bands due to products derived from the trityl cation were also present (Ph_3CH , $Ph_3C-n-Bu$ or $Ph_3C-CH_2CO_2^tBu$).

Compound **35u**: Yield for **35u**: 53.2%. Anal. Calcd for $C_{22}H_{15}NO_9Os_3$: C, 26.21; H, 1.49; N, 1.39%. Found: C, 26.05; H, 1.70; N, 1.27%. IR (ν CO) in hexane: 2077 s, 2047 s, 2019 m, 1990 m. 1H NMR of **35u** at 400 MHz in $CDCl_3$: δ 9.27 (dd, H(2)), 8.49 (d,

H(6)), 8.27 (dd, H(4)), 7.13 (t, H(3)), 7.04 (d, H(7)), 2.78 (t, CH₂ on C(5)), 1.68 (m, -1.45 m, 4H), 0.957 (t, CH₃), -12.29 (s, hydride).

Compound **35v**: Yield for **35v**: 83.4%. Anal. Calcd for C₂₄H₁₇NO₁₁Os₃: C, 26.64; H, 1.66; N, 1.29%. Found: C, 27.64; H, 1.58; N, 1.23%. IR (ν CO) in hexane: 2075 m, 2047 s, 2018 m, 1990 s, 1973 br. ¹H NMR of **35v** at 400 MHz in CDCl₃: δ 9.29 (dd, H(2)), 8.53 (d, H(6)), 8.25 (dd, H(4)), 7.14 (t, H(3)), 7.08 (d, H(7)), 3.75 (s, CH₂ on C(5)), 1.32 (s, 9H), -12.24 (s, hydride).

3.9.5 Preparation of Os₃(CO)₉(μ₃-η²-C₉H₄(5-CH₃)(6-CH₃)N)(μ-H) (**35w**):

Rearomatization with 2,2 dichloro-3,3-dicyanoquinone (DDQ).

50 mg (0.025 mmol) **35m** in 5 mL THF was treated with a two-fold molar excess of LiCH₃ in THF/hexane at -78°C. The reaction mixture was warmed to room temperature and the solvent removed by trap-to-trap distillation. To the reaction residue, 5 mL absolute ethanol was added followed by 1.1 equivalents of DDQ in 1.0 mL absolute ethanol. The reaction mixture was stirred for 20 min, then rotary evaporated, taken up in a minimum amount of CH₂Cl₂, filtered and then purified by TLC using 1:1 CH₂Cl₂/hexane as eluent. In addition to a minor amount of **35m**, one major green band **35w** was isolated, 33 mg (58%).

Compound **35w**: Anal. Calcd for C₂₀H₁₁NO₉Os₃: C, 24.48; H, 1.12; N, 1.43%. Found: C, 24.37; H, 0.97; N, 1.42%. IR (ν CO) in hexane: 2075 s, 2045 s, 2017 m, 1987 br, m.. ¹H

NMR of **35w** at 400 MHz in CDCl₃: δ 9.19 (dd, H(2)), 8.34 (s, H(7)), 8.27 (dd, H(4)), 7.08 (t, H(3)), 2.54 (s, CH₃ on C(5)), 2.24 (s, CH₃ on C(6)), -12.29 (s, hydride).

3.9.6 The Reaction of Os₃(CO)₉(μ_3 - η^3 -C₉H₇(5-CH₃)N) (**37a**) with Diazabicyclononane (DBU)/2,2-dichloro-3,3-dicyanoquinone (DDQ).

To 50.0 mg (0.025 mmol) **37a** in 5 mL CH₂Cl₂ was added 1.1 equivalent DBU by syringe. The solution was stirred for 5 min and then 1.1 equivalent of DDQ in 1.0 mL absolute ethanol was added by syringe. The reaction mixture turned dark green almost immediately and was stirred for 1h, rotary evaporated and then purified by TLC using 1:1 CH₂Cl₂/hexanes as eluent. One major band was isolated 36 mg (67%) which was identified as Os₃(CO)₉(μ_3 - η^2 -C₉H₅(5-CH₃)N)(μ -H) **35x**.

Compound **35x**: Yield for **35x**: 67.3%. Anal. Calcd for C₁₉H₉NO₉Os₃: C, 23.62; H, 0.932; N, 1.45%. Found: C, 23.94; H, 1.00; N, 1.45%. IR (ν CO) in hexane: 2075 s, 2046 s, 2018 m, 1990 br.m. ¹H NMR of **35x** at 400 MHz in CDCl₃: δ , 8.25 (dd, H(2)), 8.19 (dd, H(4)), 7.97 (d, H(7)), 7.18 (d, H(6)), 7.06 (dd, H(3)), 3.15 (s, CH₃ on C(5)), -12.851 (s, hydride).

3.9.7 Cleavage of the Quinoline Ligand from Os₃(CO)₉(μ_3 - η^2 - C₉H₅(5-R)N)(μ -H) (R=H, **35a**; R=n-Bu, **35u**; R=CH₂CO₂^tBu, **35v**)

The following procedure , given here for **35a**, worked equally well for the other complexes of type **35**. A 100 mg (0.10 mmol) is dissolved in 15 mL CH₃CN and degassed with CO. The initially deep green solution turns bright yellow and is stirred at

70°C for 36 h. under a CO atmosphere, during which time a precipitate of Os₃(CO)₁₂ begins to form. The paler yellow solution is cooled to -20°C to complete the precipitation of the carbonyl, filtered, rotary evaporated and extracted with hexane. The residue from the extraction is combined with the initial precipitate to yield 61 mg (75%) of pure (by IR) Os₃(CO)₁₂. Rotary evaporation of the hexane extract yielded 9.2 mg (80%) quinoline which was > 95% pure by ¹H NMR.

3.10 X-ray Structure Determination of *cis*-38m, *trans*-38m, and 39n and 39j.

Crystals of *cis*-38m, *trans*-38m, 39n and 39j for X-ray examination were obtained from saturated solutions of each in hexane/dichloromethane solvent systems at -20°C. Suitable crystals of each were mounted on glass fibers, placed in a goniometer head on the Enraf-Nonius CAD4 diffractometer, and centered optically. Unit cell parameters and an orientation matrix for data collection were obtained by using the centering program in the CAD4 system. For each crystal, the actual scan range was calculated by scan width = scan range + 0.35 tanθ and backgrounds were measured by using the moving-crystal moving-counter technique at the beginning and end of each scan. Two representative reflections were monitored every 2 h as a check on instrument and crystal stability. Lorentz, polarization, and decay corrections were applied, as was an empirical absorption correction based on a series of Ψ scans, for each crystal. The weighting Scheme used during refinement was 1/σ², based on counting statistics.

Each of the structures was solved by the Patterson method using SHELXS-86,¹⁵ which revealed the positions of the metal atoms. All other non-hydrogen atoms were

found by successive difference Fourier syntheses. The expected hydride positions in each were calculated by using the program HYDEX,⁵ hydrogen atoms were included in each structure and were placed in their expected chemical positions using the HFIX command in SHELXL-93.¹⁶ The hydrides were given fixed positions and U's; other hydrogen atoms were included as riding atoms in the final least squares refinements with U's which were related to the atoms ridden upon. All other non-hydrogen atoms were refined anisotropically in *trans-38m*, *39n* and *39j*; however, only the osmium atoms in *cis-38m* could be refined anisotropically due to the poor crystallinity of the sample. In addition, there was dichloromethane solvent present in the lattice of *trans-38m* which could not be modeled precisely.

Scattering factors and anomalous dispersion coefficients were taken from International Tables for X-ray Crystallography.¹⁷ All data processing was carried out on a DEC 3000 AXP computer using the Open MolEN system of programs.¹⁸ Structure solution, refinement and preparation of Figures and Tables for publication were carried out on PC's using SHELXS-86,¹⁵ SHELXL-93¹⁶ and SHELXTL/PC¹⁹ programs.

References

1. Arcia, E.; Kolwaite, D.S.; Rosenberg, E.; Hardcastle, K.I.; Ciurash, J.; Duque, R.; Milone, L.; Gobetto, R.; Osella, D.; Botta, M.; Dastru', W.; Viale, A.; Fiedler, J. *Organometallics*, **1998**, *17*, 415.
2. Kabir, S.E.; Kolwaite, D.S.; Rosenberg, E.; Hardcastle, K.; Cresswell, W.; Grindstaff, J. *Organometallics*, **1995**, *14*, 3611.

3. Bar Din, A.; Bergman, B.; Rosenberg, E.; Smith, R.; Dastru', W.; Viale, A.; Milone, L.; Gobetto, R. *Polyhedron*, **1998**, in press.
4. Bergman, B.; Rosenberg, E.; Smith, R.; *J. Amer. Chem. Soc.*, **1998**, accepted for publication.
5. Orpen, A.G. *J. Chem. Soc., Dalton Trans.*, **1980**, 2509.
6. Clauss, A.D.; Tachikawa, M.; Shapely, J.R.; Pierpont, C.G.; *Inorg. Chem.*, **1981**, 20, 1528.
7. Semmelhack, M.F. in, "Comprehensive Organometallic Chemistry II, eds. Stone, F.G.A.; Abel, E.; Wilkinson, G.; Elsevier Science, Oxford, 1995, Vol. 12, Chap. 9.1, p979.
8. Lavigne, G. in "The Chemistry of Metal Cluster Compounds" eds. Shriver, D.F.; Kaesz, H.D.; Adams, R.D. VCH, New York, 1990, Chap 5.
9. Bovey, F.A. "NMR Data Tables for Organic Chemists," Wiley Interscience, New York 1967.
10. Coleman, J.P.; Hegedus, L.S.; Norton, J.R.; Fink, R.G. "Principles and Applications of Organotransition Metal Chemistry, University Science Books, Mill Valley, Ca, 1987, Chap 3, p96.
11. Semmelhack, M.F.; Sanfert, W.; Keller, L. *J. Amer. Chem. Soc.*, **1980**, 102, 6584.
12. Jones, G.; in "Quinolines," ed. Jones, G., Wiley Interscience, London, **1977**.
13. Kabir, S.E.; Abedin; Bergman, B.; Rosenberg, E.; Hardcastle, K.I.; **1998** Manuscript in preparation.
14. Semmelhack, M.F.; Clark, G.R.; Garcia, D.C.; Harrison, J.J.; Thebtarmonth, Y.; Wuff, W.A.; Yasashita, A.; *Tetrahedron*, **1981**, 37, 3957.

15. Sheldrick, G.M. *Acta Crystallogr.*, **1990**, A46, 467.
16. Sheldrick, G.M. Program for Structure Refinement, University of Goettingen, Germany, **1993**.
17. Wilson, A.J.C.(ed). *International Tables for X-ray Crystallography, Volume C*. Kluwer Academic Publishers, Dordrecht: Tables 6.1.1.4 (pp 500-502) and 4.2.6.8 (pp 219-222), **1992**.
18. Fair, C. Kay. "*MolEN*" Structure Determination System, Enraf-Nonius, Delft, The Netherlands , **1990**.
19. SHELXTL/PC, Siemens Analytical X-ray Instruments, Inc., Madison, WI, USA, **1993**.

Chapter 4

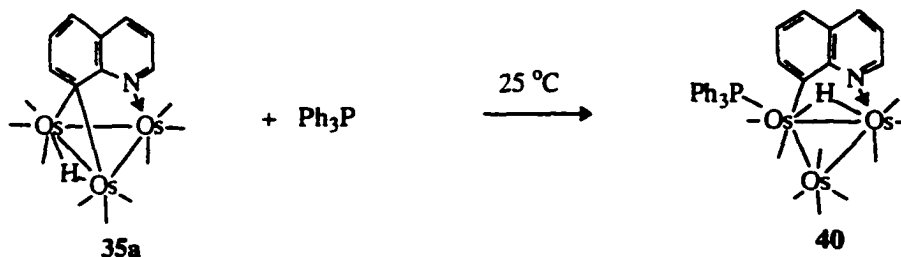
Reaction of $[\text{Os}_3(\text{CO})_9(\mu_3\text{-}\eta^2\text{-C}_9\text{H}_6\text{N})(\mu\text{-H})]$ with Heteroatom Nucleophiles and Protic Acids

4.1 Introduction

Chapter 2 covered the synthesis and reactivity of a novel class of electron deficient triosmium clusters $\text{Os}_3(\text{CO})_9(\mu_3\text{-}\eta^2\text{-C}_9\text{H}_6\text{N})(\mu\text{-H})$ **35a** (and its substituted analogues) from the reaction of quinoline with $\text{Os}_3(\text{CO})_{10}(\text{CH}_3\text{CN})_2$ followed by thermolysis or photolysis of the initially formed decacarbonyl (Scheme 2.5 and Table 2.1).¹⁻³ This type of compound can be synthesized in good yield with a wide range of substituents in the quinoline ring.^{1,4}

The reaction of the electron deficient clusters $\text{Os}_3(\text{CO})_9(\mu_3\text{-}\eta^2\text{-C}_9\text{H}_6\text{N})(\mu\text{-H})$ (**35a**) and $\text{Os}_3(\text{CO})_9(\mu_3\text{-}\eta^2\text{-XC}_9\text{H}_5\text{N})(\mu\text{-H})$ ($\text{X} = 5\text{-NH}_2$, **35l**; 3-NH_2 , **35c**; 6-NH_2 , **35q**; 5-Br , **35k**; 5-CH_3 , **35x**) complexes with soft nucleophiles such as phosphines results in ligand addition at the metal core **40** along with rearrangement (Equation 4.1).^{1,3}

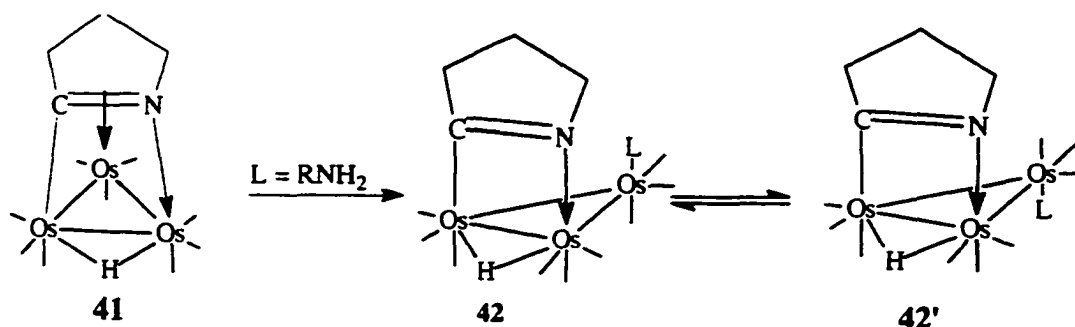
Equation 4.1



On the other hand, reaction with hydride¹ or carbanions⁴ results in nucleophilic attack at the 5-position of the quinoline ring. Subsequent protonation leads to a nucleophilic addition product (Equation 3.1)⁴ and hydride abstraction from the intermediate anion effects overall nucleophilic substitution (Equation 3.11 & Scheme 3.2).⁴ In light of this diverse reactivity, we thought it would be useful to study the reactivity of **35a** with amines and carboxylic acids which are intermediate in nucleophilicity relative to phosphines and carbanions.

We recently completed detailed studies of the reaction of these ligands with the electron precise, but quite reactive μ_3 imidoyl complexes of the type, $\text{Os}_3(\text{CO})_9(\mu_3\text{-}\eta^2\text{-C=N(-CH}_2\text{-)}_3(\mu\text{-H}))$, where coordination was highly selective for primary amines and where the formation of two axially coordinated isomers, $\text{Os}_3(\text{CO})_9(\mu_3\text{-}\eta^2\text{-C=N(-CH}_2\text{-)}_3(\mu\text{-H})\text{L})$ (**42** and **42'**) was observed (Equation 4.2).⁵

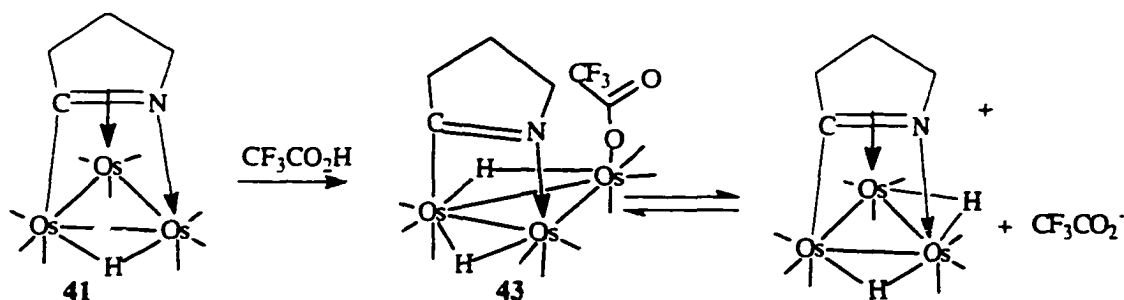
Equation 4.2



The neutral adduct $\text{Os}_3(\text{CO})_9(\mu_3\text{-}\eta^2\text{-C=N(-CH}_2\text{-)}_3(\mu\text{-H})_2(\text{CF}_3\text{CO}_2))$ (**43**), was the main product of the reaction of trifluoroacetic acid with the μ_3 -imidoyl complexes but a small amount of a monoprotonated species was observed to be in equilibrium with the

adduct (Equation 4.3). In the case of non-coordinating anions such as BF_4^- , only simple protonation was observed.^{6,7}

Equation 4.3



We report here the results of studies on the coordination chemistry of ammonia, aliphatic amines, and protic acids with **35a**, in an attempt to define the stereodynamics of its coordination sites and how these differ from those observed in **42** and **43** (Equation 4.2 and 4.3). One of our research goals in developing the chemistry of complexes such as **35a** was to understand the degree of electronic communication between the quinoline ring and the metal core. Our initial efforts in this area have resulted in the synthesis of the compounds $\text{Os}_3(\text{CO})_9(\mu_3-\eta^2-\text{XC}_9\text{H}_5\text{N})(\mu-\text{H})$ ($\text{X} = 5\text{-NH}_2$, **35l**; 3-NH_2 , **35c**; 6-NH_2 , **35q**; 5-Br , **35k**; 5-CH_3 , **35x**), previously discussed in Chapter 2. We report here our initial results of the reactivity that reveal the extraordinary impact of the electron deficient bonding mode of the cluster on the substituent in the 5-position and *vice versa*.

4.2 Results and Discussion

4.2.1 Reactions With Amines

The addition of a large excess (50 fold) of ammonia and various aliphatic amines to

35a results in an instant color change from green to orange and the appearance of two new hydride peaks in the ^1H NMR in the range of -12 to -14 ppm (Table 4.1). The resonance at higher field (isomer I) is invariably in greater intensity (except in the case of NH_3) and the lower field resonance (isomer II) gradually increases in intensity until a final ratio (I/II), in the range of 0.5 to 4.8, is reached which does not change further (Table 4.1).

Table 4.1 Chemical Shifts (ppm) and Isomer Ratios for Amine Adducts of $\text{Os}_3(\text{CO})_9(\mu_3\text{-}\eta^2\text{-C}_9\text{H}_6\text{N})(\mu\text{-H})$, **35a**

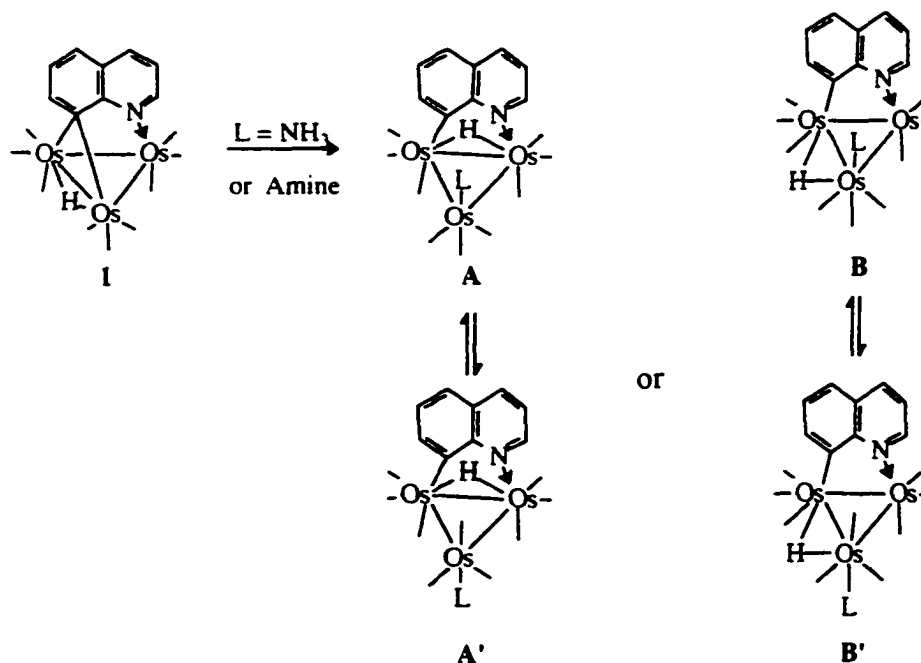
	Isomer I	Isomer II	Solvent	Temperature	I/II
NH_3	-13.65	-13.05	CDCl_3	RT	0.5
	-13.40	-12.70	Acetone	RT	1.3
EtNH_2	-13.66	-13.06	CDCl_3	RT	1.3
	13.43	-12.77	acetone	-40 °C	3.8
Et_2NH^a	-13.80	—	CDCl_3	RT	—
$t\text{-BuNH}_2$	-14.12	-13.56	CDCl_3	-40°C	7.4
$s\text{-BuNH}_2^b$	-13.59/	-12.97/	CDCl_3	-40°C	3.3
	-13.62	-13.00			
$n\text{-BuNH}_2$	-13.39	-12.76	CDCl_3	RT	2.8
$\text{C}_6\text{H}_{11}\text{NH}_2$	-13.61	-13.03	CDCl_3	RT	3.1
	-13.46	-12.81	Acetone	RT	4.8

^a only one resonance observed

^b four hydride resonances observed

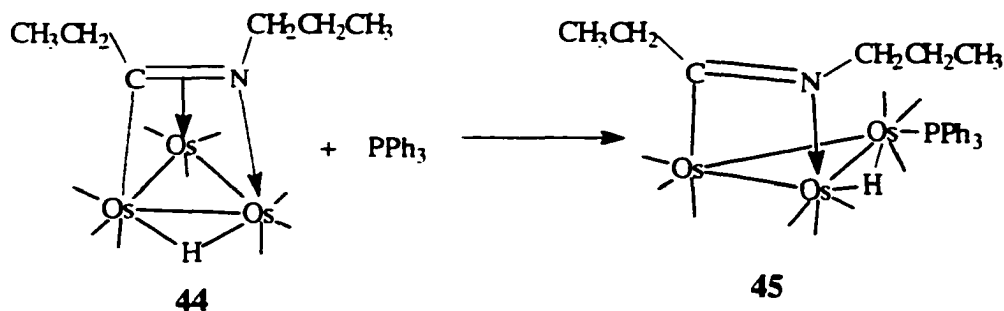
The ^{13}C NMR (CDCl_3 , $-60\text{ }^\circ\text{C}$) of a ^{13}CO enriched sample of **35a** treated with excess ammonia shows two sets of nine carbonyls (I: 187.3, 185.5, 185.6, 180.4, 179.8, 178.8 ($^2J^{13}\text{C}-^1\text{H}=14\text{ Hz}$), 177.3($^2J^{13}\text{C}-^1\text{H}=9\text{ Hz}$), 176.7, 176.2 ppm: II: 187.3, 186.7, 184.6, 182.0, 180.8, 177.8($^2J^{13}\text{C}-^1\text{H}=12.5\text{ Hz}$), 177.5 ($^2J^{13}\text{C}-^1\text{H}=9.6\text{ Hz}$), 176.8, 176.2 ppm). Significantly, the spectrum shows no resonances with ^{13}C satellites that, if present, are indicative of a large *trans*- carbonyl coupling associated with the presence of an $\text{Os}(\text{CO})_4$ group.⁵ The previously reported amine complexes of triosmium clusters, **42** and **42'**, invariably have the amine (or ammonia) in an axial position (Equation 4.2).⁵ Based on these facts alone, we can propose two alternative structures for the set of isomers formed from the interaction of amines with **35a** (Equation 4.4). One set has the hydride and the quinoline ring sharing a common edge while the amine occupies either axial site on the third, unbridged osmium atom (structures **A**, **A'**, Equation 4.4). This structure is directly analogous to that observed related to μ_3 imidoyl complexes, **42** and **42'**, for which solid state structures are available (Equation 4.2).⁵

Equation 4.4



On the other hand, coordination of the amine at the electron deficient Os edge of **35a** could lead to a structure where the quinoline ring and the hydride are on different edges with the amine occupying an axial position on the osmium atom bridged by the hydride but not by the quinoline ring (structures **B**, **B'**, Equation 4.4). This type of structure has been observed in the case of one imido complex **45** bearing ethyl and propyl groups on the imido carbon and nitrogen atoms, respectively (Equation 4.5).⁸ We have also obtained indirect evidence for this structural type as a short-lived intermediate from the selective incorporation of carbon monoxide into **35a**.³ In the case of phosphines reacting with **35a**, such an intermediate is probably the initial product as well but goes on to rearrange as shown above (Equation 4.1).^{1,3}

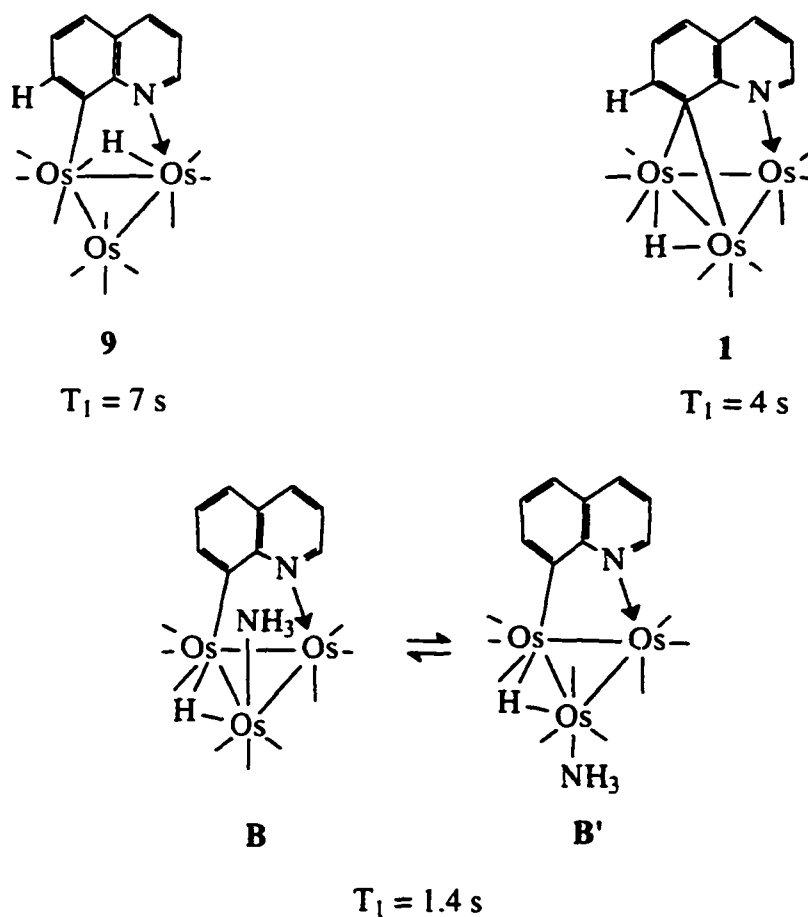
Equation 4.5



The initial formation of one isomer followed by the gradual appearance of a second has been shown to be an intermolecular process for the related μ_3 -imidoyl complexes.⁵ It would appear that this is also the case for **35a** reacting with amines since the overall behavior of **35a** towards amines is so similar.⁵ The question of the structure of the amine adducts of **35a** (A or B) still remains unanswered in the absence of a solid state structure.

The change in longitudinal relaxation time (T_1) of hydrides in metal clusters induced by proximal ligand protons can be used to qualitatively assess the distance between these two types of hydrogens.⁹ Thus, for $\text{Os}_3(\text{CO})_{10}(\mu\text{-}\eta^2\text{-C}_9\text{H}_6\text{N})(\mu\text{-H})$ (**9**) the T_1 of the hydride is 7.0 s while for **35a** it is 4.0 s (Scheme 4.1). We can attribute the shorter relaxation time in **35a** to the proximity of the hydrogen of C(7) to the μ -hydride. If the amine adducts of **35a** have a structure identical to their μ_3 -imidoyl analogs then the T_1 of the μ -hydride would be expected to have a relaxation time similar to **9**. In fact, the T_1 of the ammonia adduct of **35a** is 1.4 s which is consistent with a structure where the ammonia protons are proximal to the hydride; i.e., the structure resulting from addition of the ligand to the carbon bridged edge of the cluster without further rearrangement (structure **B**, Equation 4.4).

Scheme 4.1



This suggested structure is further supported by the ^1H NMR data obtained for the *s*-butyl adduct **35a**. Here, four hydride resonances are observed. This is undoubtedly due to the presence of diastereomers induced by the presence of the chiral center on the *s*-butyl amine. In the structure proposed based on the T_1 measurements (structure **B**, Equation 4.4), the environment on the osmium atom bound to the amine is quite asymmetric owing to the presence of the bridging hydride on one of the two edges of the triangle associated with the amine coordinated osmium atom. In the case of the structure adopted by the μ_3 -imidoyl amine adducts (**42** and **42'** Equation 4.2), the localized environment on the amine bound

nitrogen is more symmetric and indeed only two hydride resonances are observed for the *s*-butyl complex.⁵

Finally, the structure proposed is most consistent with a reversible amine coordination based on the principle of least motion since only the motion of the C(8) carbon pivoting on the coordinated nitrogen is required to reform **35a** from its corresponding amine adduct. This motion is related to the reversible coordination of the C=N bond observed in the μ_3 - to μ - to μ_3 - imidoyl interconversions.⁵

In our previous study of the imidoyl amine adducts, the initially formed isomer has the amine on the same face of the osmium triangle as the pyrrolidine ring (i.e., *syn*-).⁵ This isomer is more favored for the bulkier amines and this also appears to be the trend for the amine complexes of **35a** (Table 4.1). In fact, for the secondary amine Et₂NH only one isomer with a hydride chemical shift similar to the proposed *syn*- isomer is observed (Table 4.1). Our initial thought for the imidoyl series was that the strictly sigma-bond framework of the pyrrolidine ring was less bulky than the carbonyl ligands which have π -electrons.⁵ In light of the isomer ratios observed for the amine complexes of **35a**, this cannot be the case since the quinoline ring also has π -electron density. Yet, the *syn*- isomer is still favored for bulkier ligands and the *anti*- isomer for the least bulky (ammonia). In order to further investigate this point, we measured the effect of temperature and solvent on the isomer ratio for three amine adducts of **35a**. There are two obvious trends in the data (Table 4.2). First, it can be seen that the population of the *syn*- isomer is enhanced in the more polar solvent acetone (Table 4.2). This, of course, is sensible in light of the expected greater polarity of the Os-N bonds with the quinoline and amine relative to the Os-CO bonds. Overall, the ΔH° values

hover around zero, ranging from -3 to +2 kJ/mole. The most significant differences between compounds and between solvents are in the ΔS° (Table 2). Significantly, the ammonia complex is the only one with a negative ΔS° . This indicates that solvation, not steric effects, can account for the observed differences in the isomer ratios. Apparently, the more polar *syn*-isomers lead to more disordered solute-solvent interactions and this effect is enhanced by the presence of non-polar substituents on the amine. That the larger cyclohexyl group shows a less positive ΔS° than the ethyl group is difficult to rationalize but may relate to the mobility of this ligand in the adduct.

Table 4.2 ΔH° (kJ/mol) and ΔS° (J/mol K) for Amine Adducts of $\text{Os}_3(\text{CO})_9(\mu_3\text{-}\eta^2\text{-C}_9\text{H}_6\text{N})(\mu\text{-H})$ 35a

	K(I/II) 233K	K(I/II) 298K	ΔH° (kJ/mol)	ΔS° (J/mol K)	Solvent
NH ₃	0.55	0.49	-0.85±0.19	-0.844±0.77	CDCl ₃
NH ₃	1.55	1.33	-2.15±0.75	-4.38±2.9	Acetone
NH ₂ Et	1.22	1.34	3.35±0.48	13.9±1.8	CDCl ₃
NH ₂ Et	4.0	3.85	2.20±0.74	19.7±2.9	Acetone
C ₆ H ₁₁ NH ₂	3.45	4.07	-0.95±0.54	6.76±2.2	CDCl ₃
C ₆ H ₁₁ NH ₂	5.12	4.81 (extr.)	-1.44±0.27	8.21±1.1	Acetone

^a Values and errors obtained by taking the least squares fit to the function $\ln I/II = \Delta H^\circ / T - \Delta S^\circ / R$ for at least ten temperatures between 233 and 298 K.

The trends in the equilibrium constants for the formation of amine complexes with 35a follow the trends observed for the related μ_3 imidoyl species, *n*-Bu>*s*-Bu>*t*-Bu. The

absolute values for the equilibrium constants for **35a** however, are much greater being 44.4, 2.7, and 0.39; and 1.25, 0.37, and 0.005 for **35a** and the μ_3 -imidoyls respectively.⁵ This undoubtedly reflects the greater electron deficiency for the $46e^-$ cluster relative to the reactive but electron-precise μ_3 -imidoyls.

The reaction of **35l** with *n*-BuNH₂ in both CD₂Cl₂ and CD₃OD showed no sign of complex formation even in the presence of a 100-fold excess of *n*-BuNH₂. This can be attributed to the electron donating ability of the amino group which funnels electron density down to the electron deficient C(8)-Os₂ bonding framework by conventional benzenoid resonance.

The 3- and 6- amino derivatives **35c** and **35q** do coordinate *n*-BuNH₂, as in **35a**. The formation constants are of the same order of magnitude as for **35a**, with **35q** showing a significantly larger formation constant than **35c** or **35a** (Table 4.3). As for **35a**, isomer I, presumably the more polar isomer is favored with the equilibrium ratios of I/II being two to three times larger than for **35a** (Table 4.3). One might have expected the K_f for **35q** to be less than that of **35c** since the electron donating amino group is on the carbocyclic ring, albeit in the *meta* position. Clearly, the magnitude of K_f and the I/II ratio depend on a subtle combination of factors which cannot be delineated at this time. The one firm conclusion that can be drawn from these studies is the profound influence that substitution at the 5- position of the quinoline ring has on the electron density at the metal core. This is born out by our studies of the Os₃(CO)₉(μ_3 - η^2 -(5-Br)C₉H₅N)(μ -H)⁴ (**35k**) where the electron withdrawing bromine in the 5- position gives the largest K_f of all the derivatives of **35a** investigated so far. In the case of Os₃(CO)₉(μ_3 - η^2 -(5-CH₃)C₉H₅N)(μ -H)⁴ (**35x**), where there is only a weakly

electron donating group in the 5 - position amine complex formation was also not observed even in the presence of a large excess of n-BuNH₂.

Table 4.3 Equilibrium Constants and Isomer Ratios for n-BuNH₂ Complexes of Electron Deficient Quinoline Complexes

Compound	K _{FORM}	I/II	δ hydride I(II)	Solvent
35a	44.4	2.8	-13.39(-12.76)	CDCl ₃
35c	53.9	7.3	-13.42(-12.81)	CD ₂ Cl ₂
35q	66.7	4.6	-13.42(-12.79)	CD ₂ Cl ₂
35k	94.5	1.2	-13.47(-12.90)	CDCl ₃

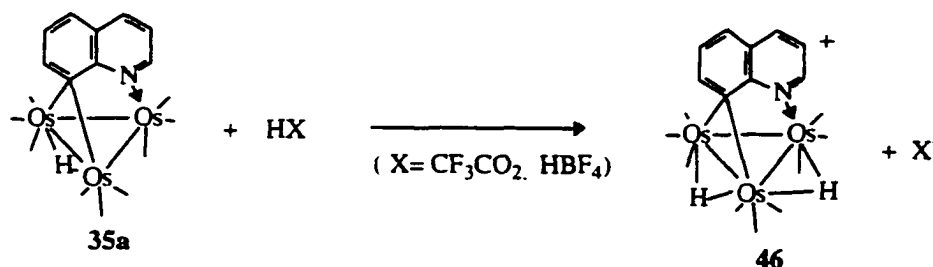
^a ± 10 % at 22 °C

4.2.2 Reactions with Protic Acids

In order to further probe the electron distribution in 35a, 35l, 35c, 35k, 35q, and 35x we investigated their reactions with the acids CF₃CO₂H and HBF₄. Addition of a six-fold excess of CF₃CO₂H to a CD₂Cl₂ solution of 35a results in complete conversion to a deep orange solution which exhibits two hydride resonances at -13.66 and -11.61 ppm in a 1:1 ratio. The aromatic resonances are all shifted downfield with respect to 35a. An equilibrium constant for protonation was calculated from a titration of 35a with CF₃CO₂H (Table 4.4). The ¹³C-NMR (CD₂Cl₂) of a ¹³CO sample of 35a in the presence of the same excess gives a ¹³C NMR in the carbonyl region showing nine resonances at 180.65, 175.20, 172.50, 172.45, 171.01, 167.93, 166.52, 159.84, and 159.99 ppm. The two resonances at 159.84 and 158.99 ppm appear as doublets of doublets in the proton coupled spectrum (²J ¹³C-¹H=13.74,

4.58 and 13.73, 6.10 Hz respectively) while the two at 180.65 and 172.45 ppm appear as doublets ($^2J^{13}\text{C}-^1\text{H}=9.15$ and 7.63 Hz). Protonation with the non-coordinating acid, HBF_4 yields the virtually identical ^1H (Table 4) and ^{13}C NMR (CD_2Cl_2) data (180.61, 175.78, 172.92, 172.36, 171.43, 168.13, 166.71, 159.94, 158.85 ppm with an identical coupling pattern). These data are consistent with simple protonation to give a dihydride cation (Equation 4.6) as opposed to acid adduct formation (Equation 4.3). The equilibrium constant for formation of the cation is considerably larger for the stronger acid, HBF_4 (Table 4.4). The observation of well resolved carbonyl- hydride couplings indicates that the protonated species is rigid on the NMR time scale while the hydrides in the related cationic μ_3 - imidoyl species are fluxional at ambient temperatures.

Equation 4.6



The protonation of **35a** with aliquots of $\text{CF}_3\text{CO}_2\text{H}$ reveals that the 5-amino derivative is considerably more basic at the metal core than **35a** (Table 4.4). After the first aliquot (slightly in excess of 1 equivalent) is added, **35i** is completely converted to the dihydride cation and the resonance at 5.60 ppm attributable to the amino resonance is no longer observed. Instead, a broad resonance at 7.82 ppm is observed which is attributable to a partially averaged signal of the $\text{CF}_3\text{CO}_2\text{H}$ and the amino group of **35i**. The $\text{CF}_3\text{CO}_2\text{H}$ proton

resonance is observed at 8.00 ppm in the presence of **35a**. As more $\text{CF}_3\text{CO}_2\text{H}$ is added to the solution of **35l**, the acid amine resonance shifts to lower fields and sharpens somewhat indicating more rapid exchange between the amine and the acid. Significantly, the amine resonances for **35c** and **35q** are found at considerably higher fields than for **35l** at 4.14 and 4.79 ppm, respectively. On treatment with $\text{CF}_3\text{CO}_2\text{H}$, the same overall behavior as for **35l** is observed for **35c** and **35q** except that the partially averaged acid/amine resonance is found between **35c** and **35q** ppm, suggesting a higher degree of amino protonation. The protonation equilibrium values (Table 4.4) obtained from these experiments are consistent with **35l** having the greatest influence on the electron density at the metal core. A Hammett plot of the equilibrium data using standard values of σ^{10} yields a reasonably good straight line with a correlation coefficient of 0.93 and ρ value of -0.13 (Figure 4.1).

4.3 Conclusions

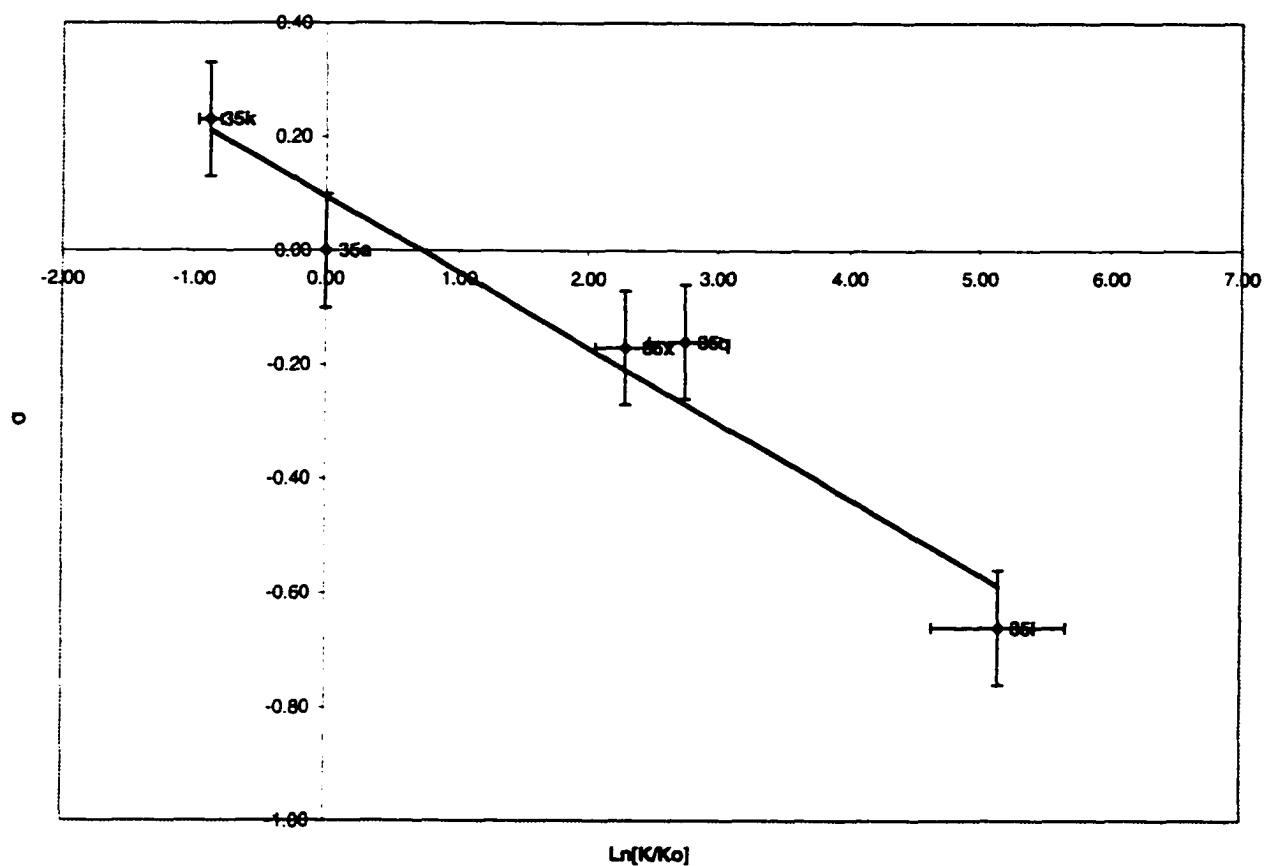
The electron deficient $\mu_3\text{-}\eta^2$ -quinoline triosmium clusters exhibit behavior towards amines similar to the related $\mu_3\text{-}\eta^2$ pyrrolidine triosmium clusters.⁵ Both show initial formation of a single isomer which then equilibrates to a mixture of two complexes. The equilibrium constants in both series depend on the steric bulk of the amine with the overall magnitudes being much greater for the quinoline series. Based on the NMR evidence accumulated to date, the actual structure of the amine-quinoline adducts is different from that of the imidoyls. However, definitive conclusions about the actual structures must await solid state structural determinations which have been difficult to obtain owing to the instability of the adducts as crystalline solids.

Table 4.4 Protonation Equilibria for Electron Deficient Triosmium Clusters^a

Compound	K_{eq}	Acid	δ hydrides	Solvent
35a	0.12	CF ₃ CO ₂ H	-13.66	CDCl ₃
			-11.61	
35a	12.2	HBF ₄	-13.70	CDCl ₃
			-11.65	
35l	20.8	CF ₃ CO ₂ H	-14.35	CDCl ₃
			-12.60	
35c	0.72	CF ₃ CO ₂ H	-13.81	CDCl ₃
			-11.73	
35q	1.88	CF ₃ CO ₂ H	-13.72	CDCl ₃
			-11.70	
35k	0.05	CF ₃ CO ₂ H	-13.78	CDCl ₃
			-11.50	
35x	1.19	CF ₃ CO ₂ H	-14.00	CDCl ₃
			-12.15	

^a Measured by ¹H NMR \pm 10% at 22°C

Figure 4.1 Hammett, σ vs ρ Plot of the Protonation Equilibria for Compounds 35a, 35l, 35c, 35q, 35k, and 35x Reacting with $\text{CF}_3\text{CO}_2\text{H}$ (error bars for the σ values are from reference [10] and are $\pm 10\%$ for K_{eq} values).



In sharp contrast to the $\mu_3\text{-}\eta^2$ -imidoyl clusters, the $\mu_3\text{-}\eta^2$ -quinoline clusters do not form acid adducts but simply undergo protonation in the presence of $\text{CF}_3\text{CO}_2\text{H}$.

The most interesting aspect of these studies is the profound influence that substituents in the 5- position have on the electronic properties of the metal core. That the simple free energy relationship normally applied to organic reactions can be used to rationalize the relationship between substitution on the carbocyclic ring and protonation at the metal core is reassuring in that the relatively complex interactions (from an orbital point of view) between an organic moiety and two metal atoms can be understood in terms of a traditional physical organic chemistry model. The isomer I and II populations and the somewhat higher value of K_f for the 6- amino quinoline derivative, are less well understood, but seem to be dominated by solvation effects, at least from the data gathered so far. Unlike the p-bound metal arene complexes which undergo nucleophilic attack at the ring with heteroatom nucleophiles, the trismium clusters show coordination to the metal core, but at the ring with carbanions. This amphiphilic behavior could prove very useful.

4.4 Experimental Section

4.4.1 Materials and General Considerations

Synthesis of compounds **35a**¹, **35c**, **35k**¹¹, **35l**¹¹, **35q**, and **35x**⁴ were previously discussed in Chapter 2. Methylene chloride was distilled from calcium hydride before use. Acetone- d_6 , methylene chloride- d_2 , and methanol- d_4 were purchased from Aldrich in single sample ampules and used as received. Chloroform- d_1 was dried over molecular sieves before use. NMR spectra were recorded on Jeol EX-400 or Varian Unity Plus 400 NMR

spectrometers. Samples for T_1 measurement were previously degassed by three freeze thaw cycles. The non selective inversion recovery pulse sequence was used to obtain T_1 values. Infrared spectra were recorded on a Perkin-Elmer 1600 spectrometer and elemental analyses were performed by Schwarzkopf Microanalytical Laboratories, Woodside, New York.

4.5 Evaluation of Isomer Ratios and Equilibrium Constants

Compounds **35a** or **35l**, **35c**, **35k**, **35q**, and **35x** were weighed directly into flame dried NMR tubes in 9-11 mg samples (~ 0.01 mmol). 0.60 mL of the NMR solvent was then added by syringe, followed by syringe addition of 2-20 μL of the amine or acid. The NMR tube was then capped and shaken and the proton or ^{13}C NMR monitored for at least 24 h after which time no further changes in the spectra were observed. The isomer ratios and equilibrium constants were evaluated by integration of the appropriate resonances. For formation constants, the equilibrium expression was:

$$K_f(\text{L/mol}) = \frac{[\text{cluster-amine adduct}]}{[\text{cluster}] [\text{amine}]}$$

In most cases the equilibrium constant was evaluated at several concentrations of added amine and an average value is reported in Table 3. For the protonation equilibrium, the expression used was:

$$K_p = \frac{[\text{cluster H}^+] [\text{X}^-]}{[\text{cluster}] [\text{HX}]}$$

Again, the value of the equilibrium constant was evaluated at several acid concentrations in most cases.

References for Chapter 4

1. E. Rosenberg, S.E. Kabir, D.S. Kolwaite, K.I. Hardcastle, W. Cresswell, J. Grindstaff. *Organometallics*, **14** (1995), 3611.
2. E. Rosenberg, D.S. Kolwaite, S.E. Kabir, K.I. Hardcastle, T. McPhillips, R. Duque, M. Day. *Organometallics*, **15**, (1996), 1979.
3. E. Rosenberg, D.S. Kolwaite, E. Arcia, K.I. Hardcastle, J. Ciurash, R. Duque, R. Gobetto, L. Milone, D. Osella, M. Botta, W. Dastru`, A. Viale, Ian Fiedler. *Organometallics*, **16** (1997), accepted for publication.
4. E. Rosenberg, B. Bergman, K.I. Hardcastle, Mondana Visi, Joana Ciurash. *Organometallics*, (1997), submitted.
5. E. Rosenberg, S. E. Kabir, M. Day, E. Wolf, T. McPhillips, K.I. Hardcastle. *Organometallics*, **14** (1995), 721.
6. E. Rosenberg, K.I. Hardcastle, S.E. Kabir, L. Milone, R. Gobetto, M. Botta, N. Nishimura, M. Yin. *Organometallics*, **14** (1995), 3068.
7. E. Rosenberg, M. Day, D. Espitia, S.E. Kabir, M. Day, K.I. Hardcastle, M. Irving. *J. Cluster Sci.*, **5** (1994), 481.
8. E. Rosenberg, K.I. Hardcastle, S.E. Kabir, R. Gobetto, L. Milone, D. Osella. *Organometallics*, **10** (1991), 3550.
9. S. Aime, R. Gobetto, to be published.
10. L.P. Hammett. *Physical Organic Chemistry*, 2nd Ed., McGraw-Hill, New York, 1970.
11. L. Bradford, T.J. Elliot, F.M. Rowe. *J. Amer. Chem. Soc.*, **69** (1947), 437.

Chapter 5

Unresolved Problems and Future Work

5.1 Reaction of $\text{Os}_3(\text{CO})_9(\mu_3\text{-}\eta^2\text{-C}_9\text{H}_5(4\text{-Cl})\text{N})(\mu\text{-H})$ **35e** with Excess Lithium *t*-Butyl Acetate to Form Complex (**53**).

In the reaction of $\text{Os}_3(\text{CO})_9(\mu_3\text{-}\eta^2\text{-C}_9\text{H}_5(4\text{-Cl})\text{N})(\mu\text{-H})$ **35e** with lithium *t*-butyl acetate at -78°C in a solution of THF an unusual rearrangement of the *t*-BuOAc fragment is observed upon addition of excess nucleophile. Addition of the nucleophile (enolate anion) at C(5) forms the expected carbon-carbon bond to generate the anionic complex **47** as shown in Scheme 5.1. The normal addition was isolated after protonation of the anionic complex yielding $\sigma\text{-}\pi\text{-vinyl Os}_3(\text{CO})_9(\mu_3\text{-}\eta^2) (\text{C}_9\text{H}_5(4\text{-Cl})(5\text{-}^t\text{BuOAc})(\mu\text{-H})$ complex **38e'** discussed in Chapter 3 (Scheme 3.2). Next, a secondary attack by excess of the enolate anion gives carbon alkylation to the ester, resulting in the tetrahedral-intermediate **48**, which then releases *t*-butoxide. Upon protonation of **49** followed by liberation of isobutylene gas (formation of isobutylene gas is the driving force for the

reaction via the Le Chatelier's principle) complex **50** is produced. Complex **50** then undergoes a decarbonylation reaction resulting in the acetyl complex **53**.¹

Initially the one and two dimensional ¹H NMR studies of complex **53** were inconclusive requiring us to analyze a solid state structure to determine the exact structure. The solid state structure of **53** is given in Figure 5.1, with the selected bond distances and angles given in table 5.1.

The overall structure of **53** is very similar to the previously reported σ - π -vinyl complex $[\text{Os}_3(\text{CO})_9(\mu_3\text{-}\eta^2\text{-C}_9\text{H}_8\text{N})(\mu\text{-H})]$ (formed from the H-/H+ addition to **35a**), and complexes **37e** (section 3.1.1), *cis*-**38m** (section 3.3.2), and *trans*-**38m** (section (3.3.3)). The structure of **46** consists of an isosceles triangle between the osmium atoms with the metal-metal bond lengths between 2.77-2.88 (Å). The hydride was located using the program HYDEX.² The hydride is tucked below the plane of the metal triangle. This calculated position for the hydride is confirmed by the positions of carbonyl groups CO(13) and CO(33).

The bond lengths in the heteroaromatic ring are all in the range of 1.33-1.40(Å) indicating that the bonds have remained delocalized. However, the saturated carbocyclic shows some ring puckering as a result of the lengthened sigma bonds in the ring system. The C(5)-C(6) bond at 1.52(Å) is clearly a single bond, while the C(6)-C(7) and C(7)-C(8) bond lengths 1.46(Å) and 1.44(Å) respectively indicate shortened π -bonds.

The assignment of the sigma (σ)-interaction between Os(3)-C(8) of length 2.10 (Å) and the pi (π) interaction between Os(1)-C(7) (2.43 Å) and Os(1)-C(8) 2.23 (Å) is consistent with previous studies of σ - π interactions on triosmium clusters.³

In order to prove this theory we must perform two alkylation reactions on isolated σ - π -vinyl addition products Os₃(CO)₉(μ_3 - η^2) (C₉H₅(4-Cl)(5-^tBuOAc)N)(μ -H) **38e'** and Os₃(CO)₉(μ_3 - η^2) (C₉H₆(5-^tBuOAc)N)(μ -H) **37k** with the Li-^tBuOAc nucleophile to try induce the **54** rearrangement complex intentionally. Addition of 1-2 molar excess of Li-^tBuOAc will be added at -78°C to a THF solution containing complex **37k** or **38e'**. Then the solution will be warmed to room temperature for 1h, followed by protonation with CF₃CO₂H at -78°C. These experiments are currently being carried out in the Rosenberg laboratory.

Figure 5.1 Solid State Structure for $\text{Os}_3(\text{CO})_9(\mu_3\text{-}\eta^3\text{-C}_9\text{H}_6(4\text{-Cl})\text{N})(\mu\text{-H})$ 53
Showing the Calculated Positions of the Hydride.

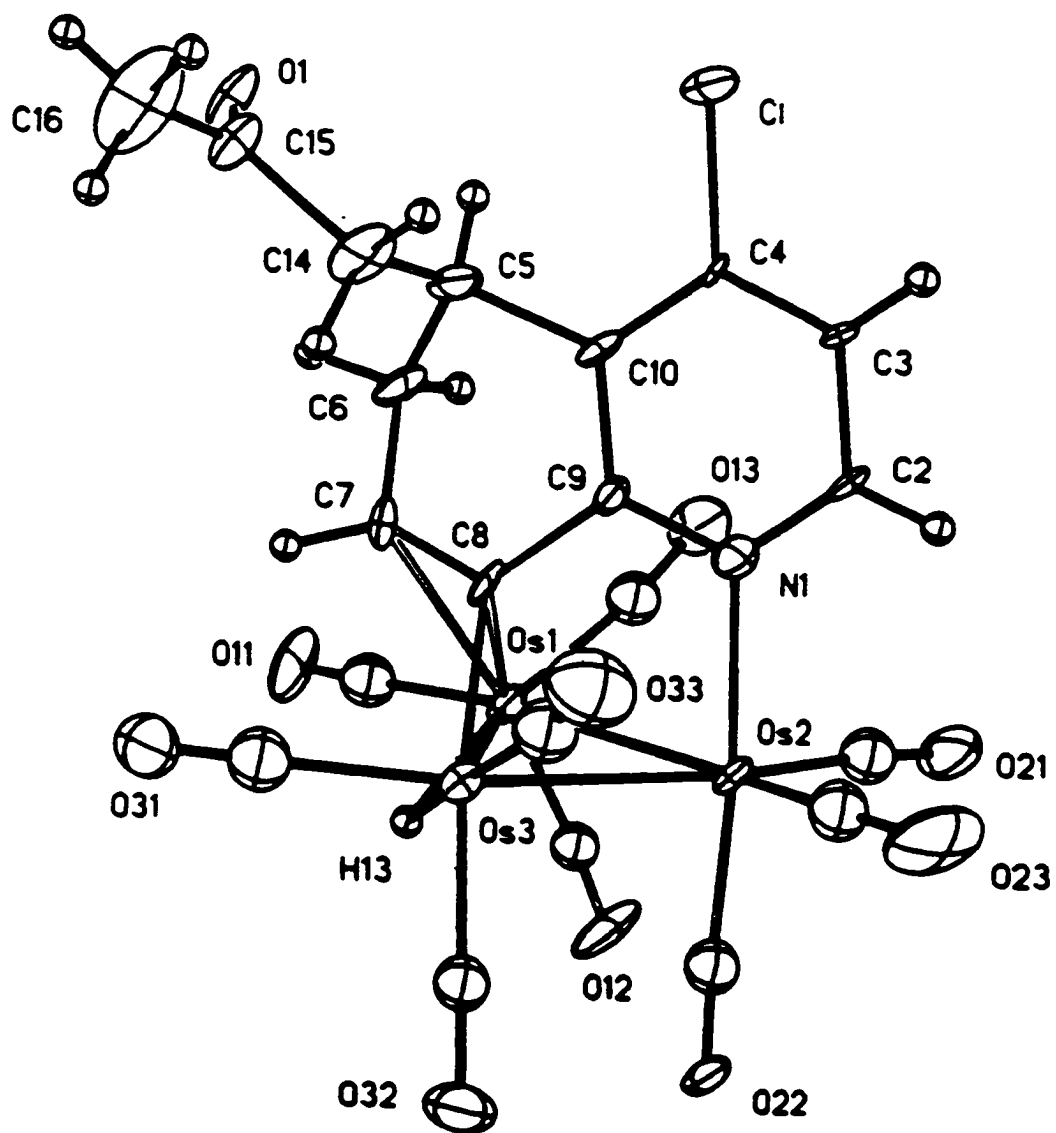
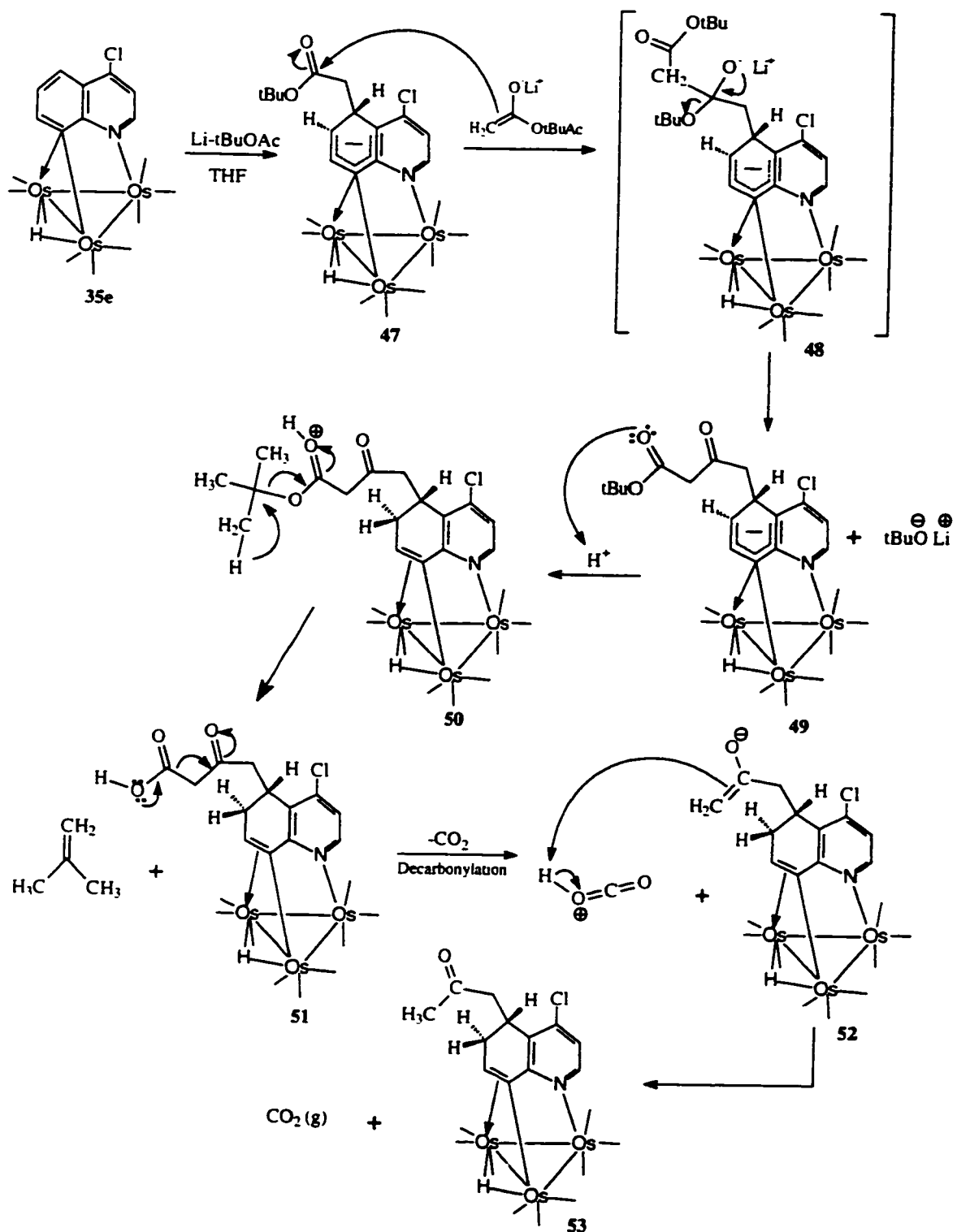


Table 5.1 Selected Bond Distances (Å) and Angles (°) for Complex 53

Distances			
Os(1)-Os(2)	2.88 (2)	O(1)-C(15)	1.18 (3)
Os(2)-Os(3)	2.77 (2)	C(5)-C(10)	1.41 (3)
Os(3)-Os(8)	2.10 (2)	C(2)-C(3)	1.40 (3)
Os(1)-Os(3)	2.85 (2)	C(3)-C(4)	1.37 (3)
Os(1)-C(8)	2.23 (2)	C(4)-C(10)	1.36 (3)
Os(2)-N(1)	2.17 (2)	C(5)-C(6)	1.52 (3)
N(1)-C(2)	1.33 (2)	C(6)-C(7)	1.46 (3)
C(5)-C(14)	1.47 (3)	C(7)-C(8)	1.44 (3)
C(14)-C(15)	1.60 (4)	C(8)-C(9)	1.48 (2)
C(15)-C(16)	1.43 (3)	Os(3)-C(8)	2.10 (2)
C-O ^b	1.17 (3)	Os-CO ^b	1.89 (3)
Angles			
Os(3)-Os(2)-Os(1)	60.62 (4)	C(8)-C(7)-Os(1)	64.6 (11)
Os(3)-Os(1)-Os(2)	57.78 (4)	N(1)-Os(2)-Os(3)	86.10 (4)
C(8)-Os(1)-Os(2)	71.20 (5)	C(7)-C(6)-C(5)	114 (2)
C(8)-Os(3)-Os(2)	75.20 (5)	C(7)-C(8)-C(9)	115 (2)
C(8)-Os(3)-Os(1)	50.6 (5)	Os(3)-C(8)-Os(1)	82.6 (7)
Os(2)-Os(3)-Os(1)	61.61(4)	Os-C-O ^b	174 (3)

^a Numbers in parentheses are average standard deviations.

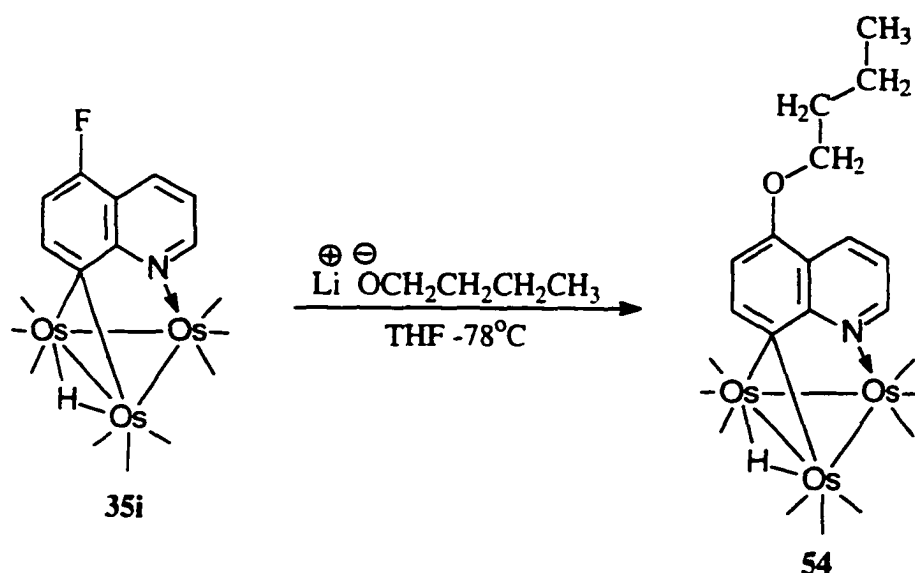
^b Average values.



5.2 Reaction of $\text{Os}_3(\text{CO})_9(\mu_3\text{-}\eta^2\text{-C}_9\text{H}_5(5\text{-F})\text{N})(\mu\text{-H})$ **35i** with Lithium n-Butoxide.

When the 5-fluoro quinoline complex **35i** is reacted with lithium n-butoxide substitution for the fluoro group is observed. This is the only example of a nucleophilic substitution reaction observed on these electron deficient ($\mu_3\text{-}\eta^2$) metal bound quinoline complexes. Attempts to substitute the fluoro (and other halogens) with carbon nucleophiles resulted in addition across the C(3)-C(4) bond as discussed in section 3.4.

Equation 5.1

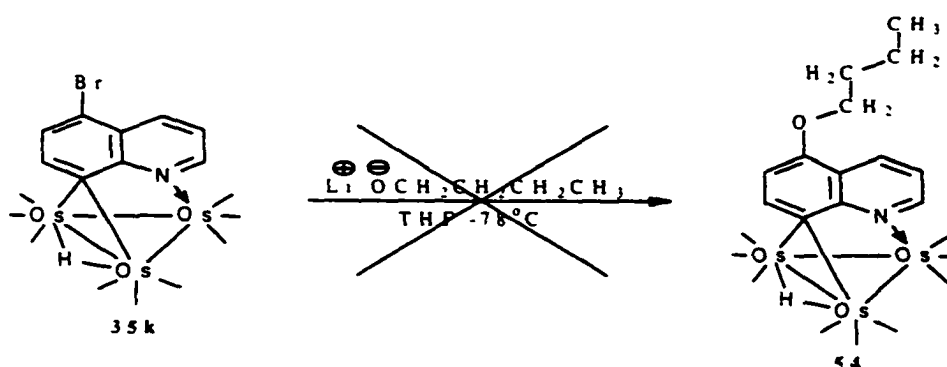


Initial ^1H NMR eluted to a aromatic structure with the carbon alkylation on the n-butyl group at the 5- position. The presence of the heteroatom oxygen forming the ether linkages wasn't obvious via NMR techniques. Fortunately we were able to obtain X-ray quality crystals for solid state work to be performed.

The structure of **54** is very similar to complex **35a** previously reported, and **35n** in section 2.2.1. The structure of **54** consists of an isosceles triangle with three

approximately equal Os-Os bonds (table 5.2) with the metal-metal bond lengths between 2.76-2.78 (Å). The hydride was located using the program HYDEX. The hydride is tucked below the plane of the metal triangle. This calculated position for the hydride is confirmed by the positions of carbonyl groups CO(13) and CO(33). The planar quinoline ligand sits perpendicular to the metal triangle, Os(1)-C(8) and Os(3)-C(8) bonds are almost symmetrical (2.29 and 2.24 (Å)) suggesting a three center-two electron bond with carbon C(8). The bond lengths in the quinoline ring system range from (1.30-1.47 Å) indicating a completely delocalized ring system.

Equation 5.2



Attempts to react $\text{Os}_3(\text{CO})_9(\mu_3-\eta^2)\text{-(C}_9\text{H}_5(5\text{-Br)N})(\mu\text{-H})$ **35k** with Lithium n-butoxide were unsuccessful (Equation 5.2). This seems consistent with the π -arene complexes which undergo addition / elimination reactions with heteroatom nucleophiles at a much faster rate with fluoro than bromo substituents.⁵ Attempts reproduce the n-butoxide nucleophilic substitution reaction on **35i** are currently being carried out to better determine the percentage yield, but are slowed from the limited supply of 5-fluoro quinoline ligand to prepare complex **35i**.

Figure 5.2 Solid State Structure for $54 \text{ Os}_3(\text{CO})_9(\mu_3\text{-}\eta^2\text{-C}_9\text{H}_5(5\text{-O}^t\text{Bu})\text{N})(\mu\text{-H})$

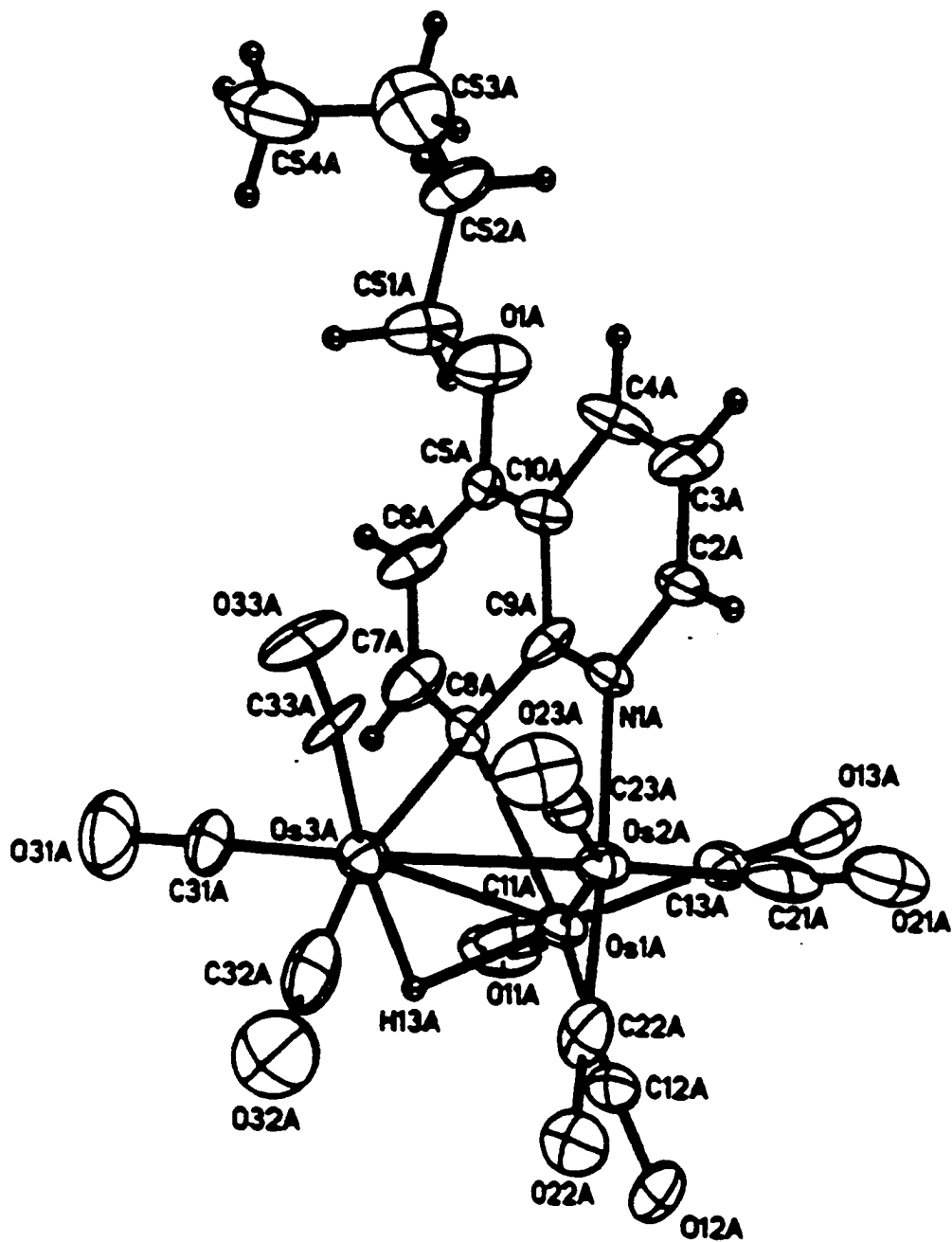


Table 5.2 Selected Bond Distances (Å) and Angles (°) for Complex 54

Distances			
Os(1)-Os(3)	2.76 (13)	N(1)-C(2)	1.40 (2)
Os(2)-N(1)	2.13 (10)	N(1)-C(9)	1.30 (2)
Os(1)-Os(3)	2.76 (10)	C(2)-C(3)	1.35 (2)
Os(1)-C(8)	2.29 (12)	C(3)-C(4)	1.44 (2)
Os(1)-Os(2)	2.78 (14)	C(5)-C(6)	1.37 (2)
Os(2)-Os(3)	2.78 (13)	C(6)-C(7)	1.37 (2)
Os(3)-C(8)	2.24 (11)	C(7)-C(8)	1.39 (2)
O(1)-C(5)	1.38 (2)	O(1)-C(51)	1.44 (2)
C(8)-C(9)	1.47 (2)	C(51)-C(52)	1.58 (2)
C(52)-C(53)	1.38 (3)	C(53)-C(54)	1.52 (5)
Os-CO ^b	1.17 (3)	Os-CO ^b	1.85 (3)
Angles			
Os(3)-Os(1)-Os(2)	60.21 (3)	C(5)-C(6)-C(7)	110.4 (11)
Os(1)-Os(3)-Os(2)	60.05 (3)	C(6)-C(5)-O(1)	115.9 (12)
Os(3)-C(8)-Os(1)	75.1 (4)	C(8)-Os(1)-Os(3)	51.6 (4)
C(8)-Os(3)-Os(2)	78.8 (3)	Os(1)-Os(2)-Os(3)	59.74 (3)
N(1)-Os(2)-Os(3)	82.9 (4)	N(1)-Os(2)-Os(1)	82.9 (4)
C(5)-O(1)-C(51)	119.2 (11)	C(8)-Os(3)-Os(1)	78.8 (3)
Os-C-O	174.2 (8)		

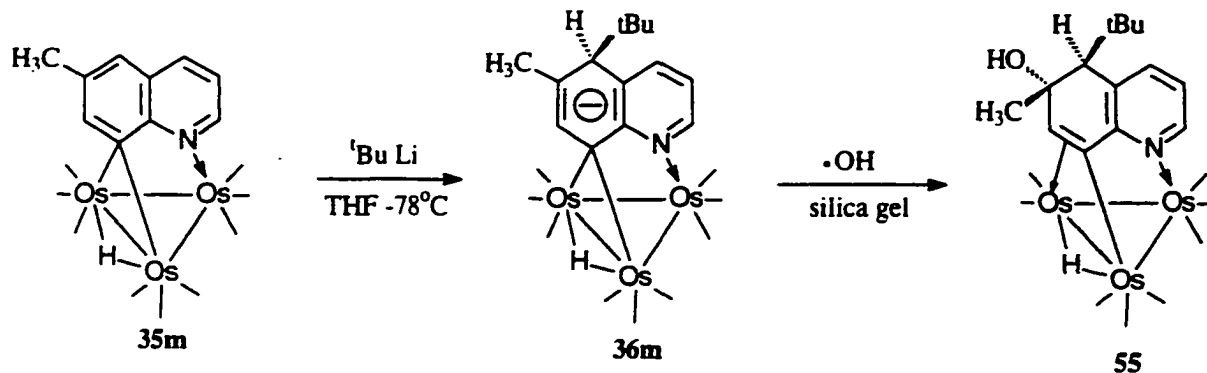
^a Numbers in parentheses are average standard deviations.

^b Average values.

5.3 Carbon C(6) Hydroxylation of Complex 35m: Preparation of the Phenolic Complex $\text{Os}_3(\text{CO})_9(\mu_3\text{-}\eta^3\text{-C}_9\text{H}_6(5\text{-}^t\text{Bu})(6\text{-CH}_3)(6\text{-OH})\text{N})(\mu\text{-H})$ 55

When complex **35m** the 6-methyl substituted quinoline complex is reacted with *t*-butyl lithium at -70°C in a solution of THF, the anionic complex **36m** with the new carbon-carbon bond at C(5) is formed as previously discussed in chapter 3. When this anionic complex **36m** is applied directly to a silica gel thin layer chromatography plate, it undergoes a hydroxylation reaction to generate the phenolic complex **55** (Equation 5.3).

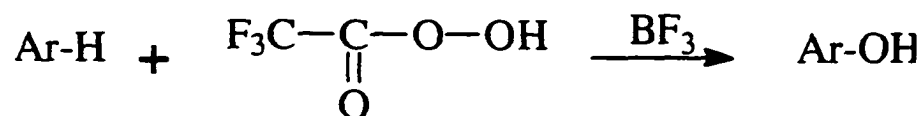
Equation 5.3



This procedure provides an excellent method for direct hydroxylation of the anionic complex **36m** at carbon C(6) in a simple one step procedure. One possible mechanism of reaction involves a reaction with an oxygen electrophile. However, oxygen electrophiles are very uncommon, since oxygen does not bear a positive charge very well.⁶ There have only been a few reports of direct hydroxylation by an electrophilic process.⁶ One notable reaction that can be mentioned is shown in Equation 5.4, use trifluoroacetic acid and boron trifluoride to hydroxylate an aryl system.⁶ In

general, poor yields are obtained, partly because introduction of an OH group activates the ring to further attack. Quinone formation is common.

Equation 5.4



A proposed reaction to validate this hypothesis, would involve reacting the intermediate anion complex **36m** with trifluoroperacetic acid and boron trifluoride to hydroxylate at carbon C(6).

Another possible explanation for the formation of **55** involves a radical pathway by reaction of **36m** with free hydroxyl radicals generated from the silica gel surface. A reaction to test if indeed this is the mechanism, uses Fenton's Reagent (a good source of hydroxyl radicals) to hydroxylate complex **36m**.⁶ If this proves successful other radical sources should be tried, such as bubbling oxygen through the reaction solution of **36m** to generate the quinone complex.

A solid state structural investigation of complex **55** was carried out to confirm the conformation of the structure proposed from the ¹H NMR data. The solid state structure of **55** is shown in Figure 5.3, with selected bond lengths and angles given in table 5.3. Again, the overall structure is very similar to the previously reported σ - π -vinyl complex [Os₃(CO)₉(μ_3 - η^2 -C₉H₈N)(μ -H)] (formed from the H-/H+ addition to **35a**), and complexes **37e** (section 3.1.1), *cis*-**38m** (section 3.3.2), and *trans*-**38m** (section (3.3.3), and **53**. The structure of **55** consists of an isosceles triangle between the osmium atoms with the metal-metal bond lengths between 2.80-2.90 (Å). The hydride

was located using the program HYDEX.² The hydride is tucked below the plane of the metal triangle. This calculated position for the hydride is confirmed by the positions of carbonyl groups CO(13) and CO(33).

The bond lengths in the heteroaromatic ring are all in the range of 1.32-1.41(Å) indicating that the bonds have remained delocalized. However, the saturated carbocyclic shows some ring puckering as a result of the lengthened sigma bonds in the ring system. The C(5)-C(6) bond at 1.60 (Å) is clearly a single bond, while the C(6)-C(7) and C(7)-C(8) bond lengths 1.52(Å) and 1.39(Å) respectively indicate shortened π -bonds. The assignment of the sigma (σ)-interaction between Os(1)-C(8) of length 2.13 (Å) and the pi (π) interaction between Os(3)-C(7) (2.40(Å) and Os(3)-C(8) 2.26 (Å) is consistent with previous studies of σ - π interactions on triosmium clusters.³

Work is currently underway to see if this hydroxylation procedure can be extended to include other complexes, to determine the limitations of the system (for example if the presence of the activating groups at C(5) and C(6) are necessary).

Figure 5.3 Solid State Structure for $\text{Os}_3(\text{CO})_9(\mu_3\text{-}\eta^3\text{-C}_9\text{H}_5(5\text{-}^t\text{Bu})(6\text{-CH}_3)(6\text{-OH})\text{N})(\mu\text{-H})$ 55 Showing the Calculated Positions of the Hydride.

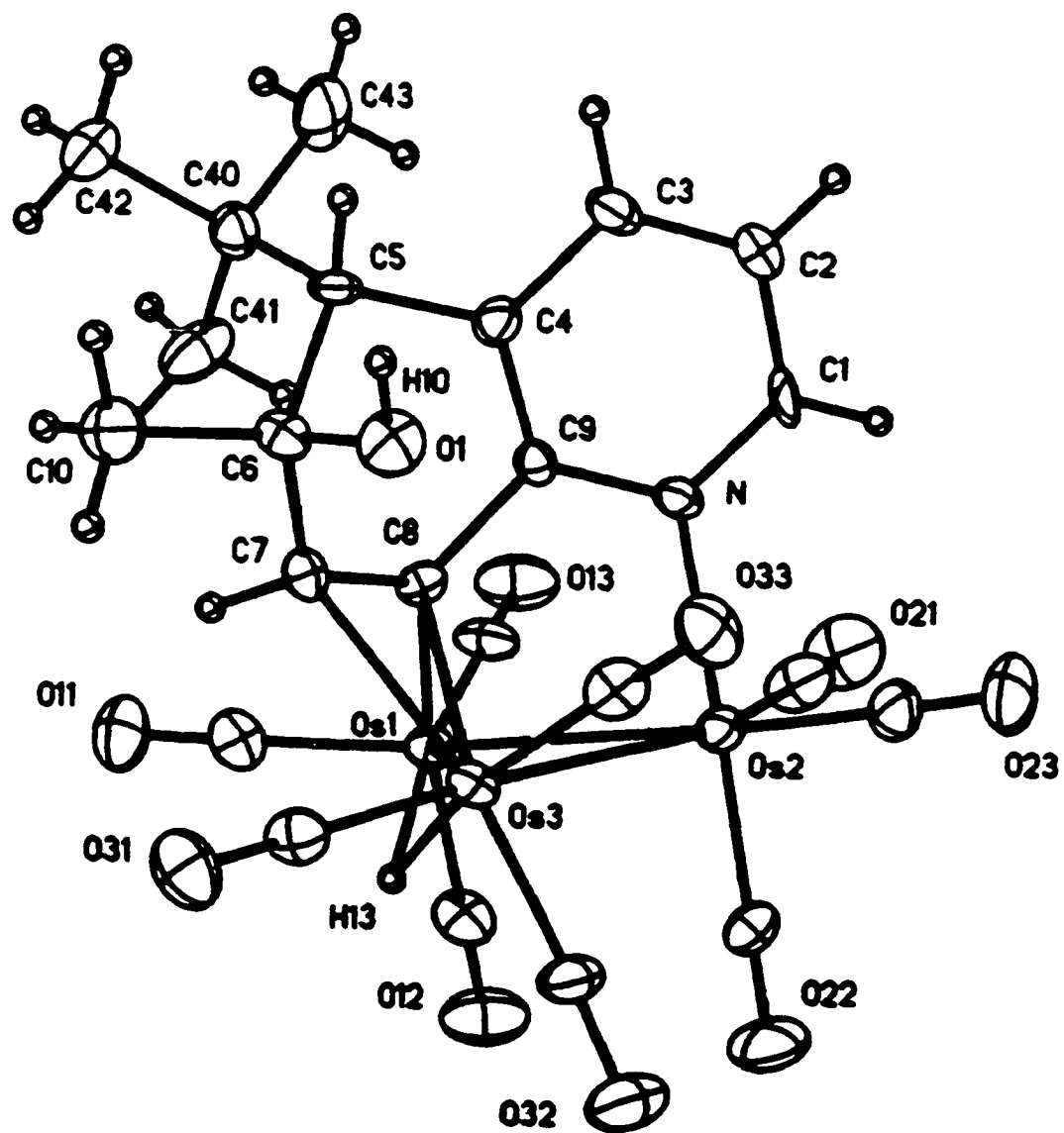


Table 5.3 Selected Bond Distances (Å) and Angles (°) for Complex 55

Distances			
Os(1)-Os(2)	2.80 (6)	C(4)-C(5)	1.54 (3)
Os(2)-Os(3)	2.90 (6)	C(5)-C(10)	1.41 (3)
Os(3)-Os(8)	2.26 (8)	C(1)-C(2)	1.39 (3)
Os(1)-Os(3)	2.84 (5)	C(2)-C(3)	1.37 (3)
Os(3)-C(7)	2.40 (4)	C(3)-C(4)	1.41 (3)
Os(2)-N(1)	2.17 (6)	C(4)-C(9)	1.38 (3)
N(1)-C(1)	1.32 (2)	C(5)-C(6)	1.60 (3)
N(1)-C(9)	1.35 (2)	C(6)-C(7)	1.52 (3)
C(7)-C(8)	1.39 (3)	C(8)-C(9)	1.48 (2)
C-O ^b	1.14 (3)	Os-CO ^b	1.89 (3)
Angles			
Os(2)-Os(1)-Os(3)	61.86 (4)	C(7)-C(8)-Os(3)	121.4 (7)
Os(1)-Os(3)-Os(2)	58.50 (4)	N(1)-Os(2)-Os(3)	86.10 (4)
Os(1)-C(8)-Os(3)	80.60 (2)	C(7)-C(6)-C(5)	108.4 (7)
C(8)-Os(1)-Os(3)	51.60 (2)	C(7)-C(8)-C(9)	114.0 (7)
C(8)-Os(3)-Os(1)	50.6 (5)	C(7)-C(8)-Os(3)	78.6 (7)
C(7)-Os(3)-Os(2)	104.8(4)	Os-C-O ^b	177 (3)

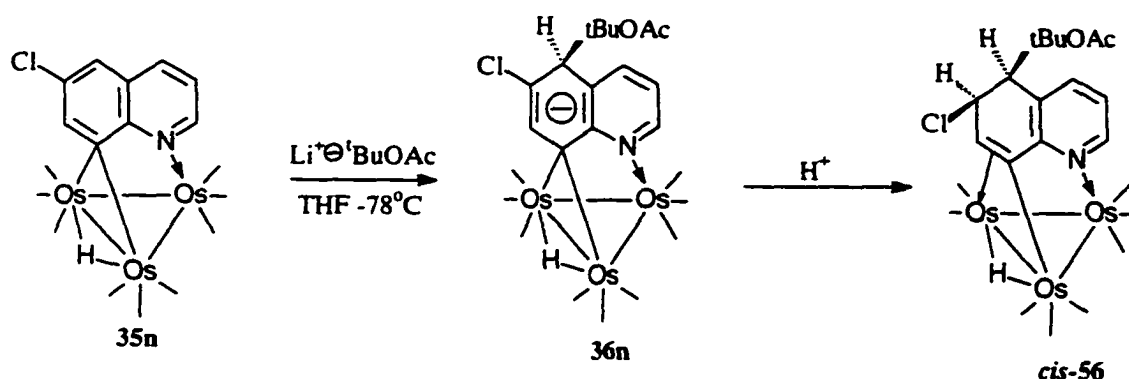
^a Numbers in parentheses are average standard deviations.

^b Average values.

5.4 The Restricted σ - π -Vinyl Interchange on Complex $\text{Os}_3(\text{CO})_9(\mu_3\text{-}\eta^3\text{-C}_9\text{H}_5(5\text{-CH}_2\text{CO}_2^t\text{Bu})(6\text{-Cl})\text{N})(\mu\text{-H})$ *cis*-56

When complex **35n** is with lithium t-butyl acetate at -78°C in a solution of THF a new carbon-carbon bond is formed at carbon C(5) and after protonation complex *cis*-**56** is isolated in a 64.6% yield (Equation 5.5).

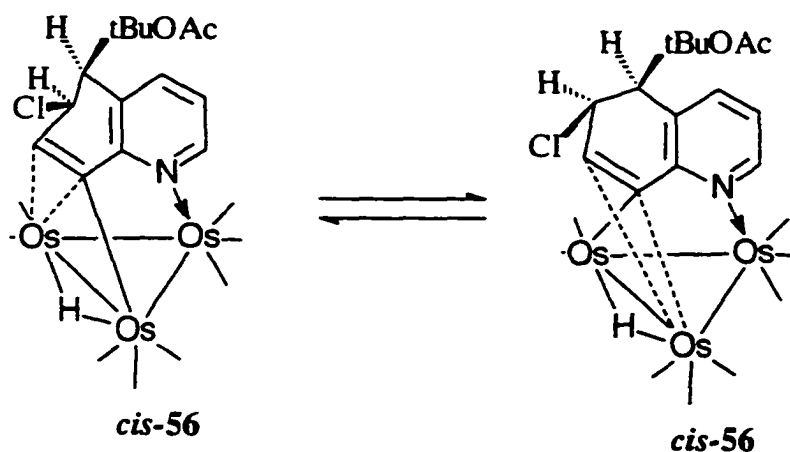
Equation 5.4



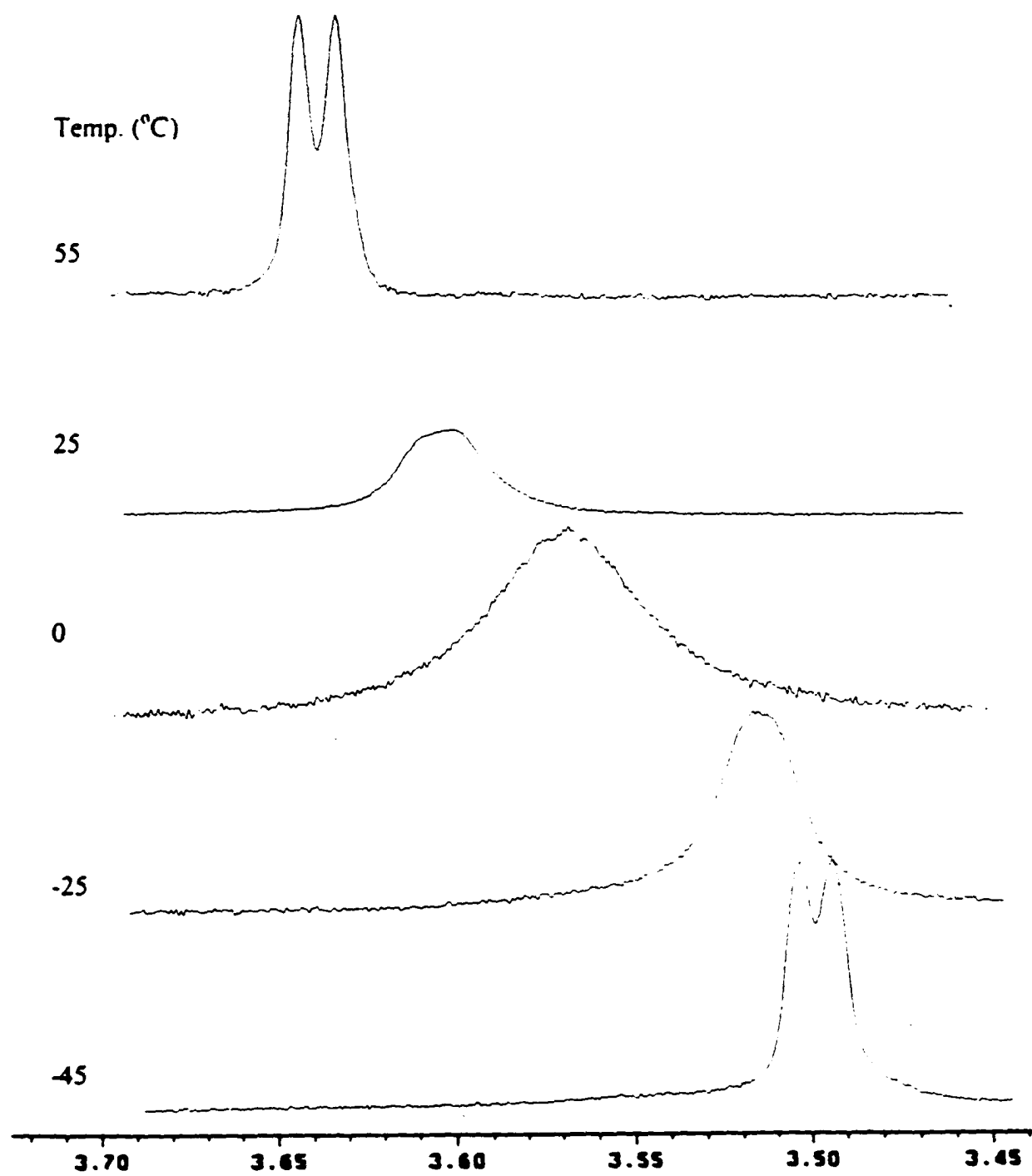
Upon examining the ^1H NMR spectra of complex **49** ($\mu_3\text{-}\eta^3\text{-C}_9\text{H}_5(5\text{-}^t\text{BuOAc})(6\text{-Cl})\text{N})(\mu\text{-H})$ it was discovered that the H(7) proton resonance was broadened. Broadening on spectra in σ - π -vinyl systems usually indicates some type of fluxional interchange occurring (at a slower rate relative to the NMR time scale) between the ligand and the cluster attached at carbon C(8) (Scheme 5.2).

We therefore attempted to study this system using variable temperature ^1H NMR collecting a series of spectra at temperatures ranging from -45 - 55°C shown in Figure 5.4. At the high temperature limit we observed a doublet for the H(7) proton resonance at 3.65ppm. Upon cooling the sample, this H(7) peak broadened, and then at the lower limit

Scheme 5.2



-45°C was again observed as a doublet a 3.51 ppm. The change in chemical shift and the sharpening, broadening, and resharping of the resonances indicates the presence of an undetectable isomer of *cis-56* which is probably the result of conformational change in the ring. Apparently this change must strongly influence the shift of H(7). The monosubstituted complexes appear to be much more fluxional as would be expected from the less steric crowding across the C(5)-C(6) bond. The exact nature of the difference between the two isomers remains unclear and a thorough study of related complexes is currently underway.

Figure 5.4 Variable Temperature ^1H NMR Spectra for Proton H(7) in *cis*-56

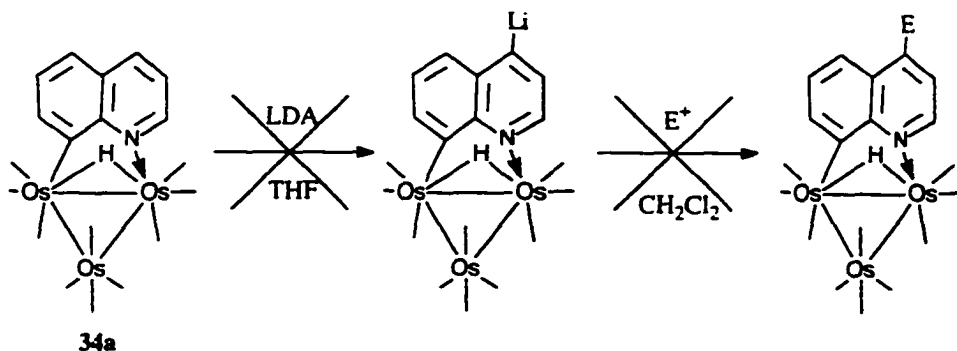
5.5 Attempted Two Step Lithiation Followed by Electrophile Trapping

After examining the $(\mu_3-\eta^2)$ electron deficient quinoline triosmium carbonyl systems reactivity towards nucleophiles (discussed in chapters 2-4) we were interested in whether these systems could be lithiated, and then trapped with an appropriate electrophile. We learned from our survey of nucleophiles that this selective proton abstraction would require high kinetic basicity and very low nucleophilic reactivity. The large range of successful carbon nucleophiles (including n-butyl lithium) made lithium diisopropylamide (LDA) the best choice.

The first complex selected was the normal 48-electron complex **34a** $\text{Os}_3(\text{CO})_{10}(\mu_2-\eta^2-\text{C}_9\text{H}_6\text{N})(\mu-\text{H})$. This electron precise system was similar in reactivity to free quinoline (with the nitrogen protected), and it was thought that carbon C(4) would be the site of lithiation.

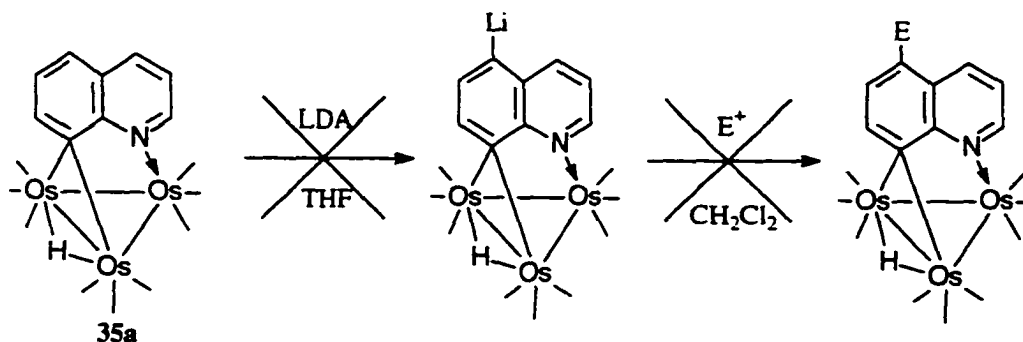
When one equivalent of LDA was added at -78°C to the yellow THF solution containing **34a**, a red color change was observed (Equation 5.6). This color change hinted to possible lithiation. Next, a trap to trap distillation of the THF solvent followed by replacing with a fresh methylene chloride solvent. However, upon addition of the electrophile (D^+ , CH_3I , $(\text{CH}_3\text{O})_2\text{SO}_2$) the solution returned to the original yellow color. After purifying the product the ^1H NMR revealed it to be **34a** the starting material.

Equation 5.6



Next, the electron deficient complex 35a was reacted using the same procedure, unfortunately negative results were also obtained (Equation 5.7). As with metal π -arenes (section 1.7) there are very few examples where lithiation / electrophilic trap process has been shown to be synthetically useful.²

Equation 5.7

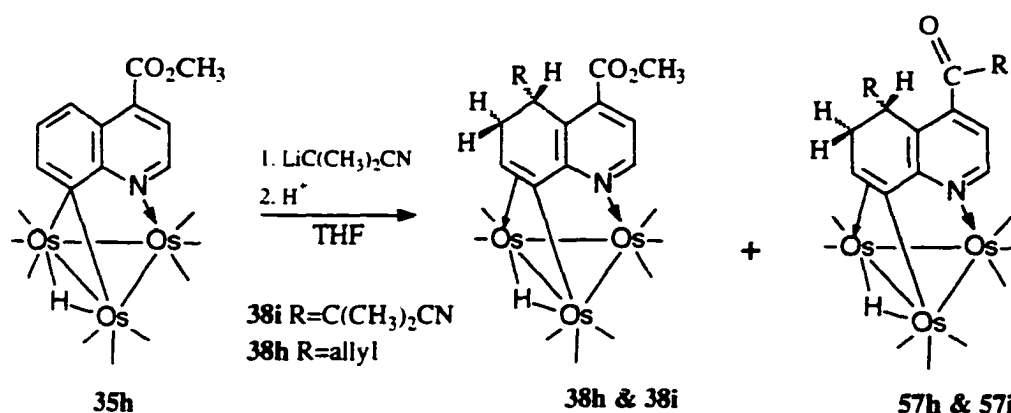


The questions to be answered did lithiation occur successfully? And / or was electrophile alkylating in a reversible process? Or did the LDA coordinate to the metal core reversibly (as other amines were shown to do in chapter 4), and then exchange with a CO group formed from the decomposition of some complex? The answers to these questions will hopefully be found from the studies on these system that are currently being carried out in by Rosenberg research group.

5.6 Double alkylation at Carbon C(5) and the Ester Carbon on C(4): Reaction of 35h with Excess Carbanion

The 4-carboxymethyl derivative, **35h**, reacts cleanly with allyl magnesium, and Li-C(CH₃)₂CN to give the expected nucleophilic addition product Os₃(CO)₉(μ₃-η³)(C₉H₆(4-CO₂CH₃)(5-allyl)N)(μ-H) **38h** and **38i** Os₃(CO)₉(μ₃-η³)-(C₉H₆(4-CO₂CH₃)(5-C(CH₃)₂CN)N)(μ-H) as shown in Equation 5.8.

Equation 5.8



It is significant that in the cases of the 3- and 4- carboxymethyl derivatives, attack at the ester carbonyl does not represent a competitive pathway since the **38h & 38i** are obtained in moderate yields. Attack at the carbomethoxy group is only observed when an excess of carbanion is used, resulting in the additional products **57h & 57i** alkylated at ester carbonyl.

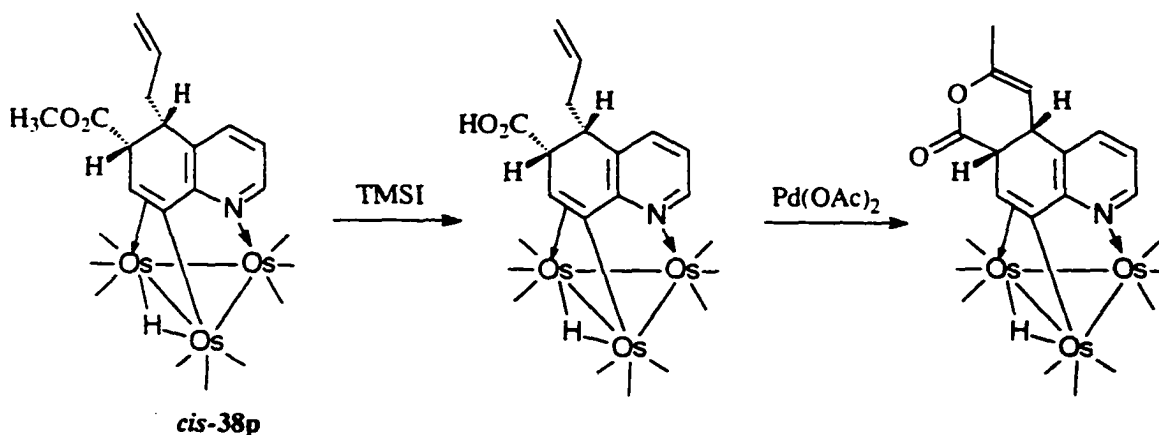
So far we only observed these products from alkylating **35h**. Complexes **38h** and **38i** are thought to alkylate at the more electron deficient heterocyclic ring to yield complexes **57i** and **57h**. Currently the Rosenberg group is attempting to react the isolated

complexes **38h** and **38i** with a 1-1.5 molar equivalent of the appropriate carbanion to show that this alkylation procedure can be done in a stepwise manner.

These complexes being doubly alkylated may prove useful for the functionalization of tri- and tetra-cyclic lactones and lactams across the C(4)-C(5) carbon bond.

Some targeted ring synthesis that were attempted and are being pursued further are as follows: Using a palladium-catalyzed cyclization across the C(5)-C(6) bond of the quinoline. Starting from isolated complex $\text{Os}_3(\text{CO})_9(\mu_3-\eta^3)(\text{C}_9\text{H}_6(5\text{-allyl})(6\text{-CO}_2\text{CH}_3)(\mu\text{-H}))$ *cis-38p* and reacting with iodotrimethylsilane (TMSI) to generate the free acid. Then the cyclization is carried out catalyzed by $\text{Pd}(\text{OAc})_2$ as shown in Equation 5.9 resulting in the formation of the lactone. If the ring strain become too severe in these reduced systems, it may be necessary to aromatize prior to ring closing. This same procedure can be used to cyclize lactones across C(4)-C(5).⁸

Equation 5.9



Another system is the lactam system, starting with amino complexes and again involving the palladium(II)-catalyzed cyclization across C(4)-C(5) and C(5)-C(6) positions of the quinoline.⁹

Indeed, this chemistry is extendable to a wide range of benzoheterocycles with pyridinyl nitrogens. Thus, the synthetic methodology outlined here is applicable to quinoxaline, benzothiazole, 2-methyl-benzimidozoles, benzotriazoles and phenanthridines.

5.7 Experimental Section

5.7.1 Material and General Considerations

All reactions were carried out under an atmosphere of nitrogen but were worked up in air. Tetrahydrofuran was distilled from benzophenone ketyl, methylene chloride and acetonitrile from calcium hydride.

Infrared spectra were recorded on a Perkin-Elmer 1600 FT-IR spectrometer and ¹H and ¹³C NMR were recorded on a Varian Unity Plus 400. Elemental analyses were done by Schwarzkopf Microanalytical Labs, Woodside, New York. Chemical shifts are reported down field positive relative to tetramethylsilane and coupling constants are reported only for those resonances relevant to the stereochemistry and while only the multiplicities of resonances with standard couplings are reported.

The preparation and characterization of compounds **34a**, **35a**, **35e**, **35h**, **35i**, **35m**, and **35n** were previously reported in chapter 2, and **38h** and **38i** in Chapter 3.

Trifluoroacetic acid and diisopropylamine were purchased from Aldrich Chemical and distilled from phosphorous pentoxide and calcium hydride respectively before use. The carbanion reagents Li ⁿBu, Li ^tBu, and allylMgBr were purchased from Aldrich and used as received. The other carbanions Li-(C(CH₃)₂CN), Li-^tBuOAc were generated by deprotonation of their corresponding neutral precursor with lithium diisopropyl amide which was generated from diisopropyl amine and n-BuLi according to published procedures at -78°C.³ The electrophiles (CH₃O)₂SO₄, CH₃I, were purchased from Aldrich Chemical Co. and distilled from phosphorous pentoxide.

5.8 Preparation of Complexes 53-57i

The following procedure was followed for the compounds listed above. 50 mg (0.050 mmol) Os₃(CO)₉(μ₃-η²-C₉H₅(R)N)(μ-H) was dissolved in 5 mL THF and cooled to -78°C, at which time a 1.1-1.5 molar excess of the appropriate carbanion was added slowly by syringe, except for the case of 57h and 57i where a 5 molar excess was used. The amount of carbanion added was governed by an observable color change from deep green to dark amber or orange. The reaction mixture was warmed to 0°C, stirred for 0.25 to 1h, cooled again to -78°C and quenched with an amount of trifluoroacetic acid, 10% in excess of the amount of carbanion used. The solution generally turned orange-red as it warmed to room temperature. In cases where electrophiles were used a trap to trap distillation of the THF solvent, followed by replacing the solvent with fresh CH₂Cl₂. The clear orange-red solution then rotary evaporated, taken up in minimum CH₂Cl₂, filtered and then purified by thin layer chromatography on 0.1x20x20cm or 0.1x20x40cm silica gel plates using CH₂Cl₂/hexanes (20-50% CH₂Cl₂ as eluent. In general, one major

orange band containing the nucleophilic addition product was observed in addition to minor amounts of unconsumed starting material. $\text{Os}_3(\text{CO})_{10}(\mu\text{-}\eta^2\text{-C}_9\text{H}_5(\text{R})\text{N})(\mu\text{-H})$. Yields are given along with the analytical and spectroscopic data below.

5.9 Analytical and Spectroscopic Data

Compound 53: Yield for **53:** %. Anal. calcd. for $\text{C}_{21}\text{H}_{12}\text{N}_1\text{O}_{10}\text{Os}_3$: C, 24.14; H, 1.15; N, 1.33%. Found: C, 24.26; H, 1.03; N, 1.31%. IR (ν_{CO}) in CH_2Cl_2 : 2079s, 2055s, 2024s, 2008m, 1998s, 1972m, 1959m, 1949m cm^{-1} . ^1H NMR of **46** at 400 MHz in CDCl_3 : δ 8.314 (d, H(2)), 6.85 (d, H(3)), 3.82 (q, H(7)), 3.52 (m, H(5)), 2.80 (q, H(6)), 2.54 (dd, H(6)), 2.43 & 2.05 (dd & tt, CH_2 two protons), -17.039 (s, hydride).

Compound 54: Yield for **54:** 36.7 %. Anal. calcd. for $\text{C}_{22}\text{H}_{14}\text{N}_1\text{O}_{10}\text{Os}_3$: C, 25.33 H, 1.34; N, 1.34%. Found: C, 25.06; H, 1.43; N, 1.38%. IR (ν_{CO}) in CH_2Cl_2 : 2076s, 2050s, 2026s, 1996s, 1980m, 1962w, 1948w cm^{-1} . ^1H NMR of **47** at 400 MHz in CDCl_3 : δ 9.21 (d, H(2)), 8.46 (d, H(6)), 8.42 (dd, H(4)), 7.05 (t, H(3)), 6.95 (d, H(7)), 4.17 (t, 1st CH_2 on butyl), 1.84 (m, CH_2 two protons), 1.54 (m, CH_2), 1.02 (t, terminal CH_3), -12.607 (s, hydride).

Compound 55: Yield for **55:** 75.0 %. Anal. calcd. for $\text{C}_{23}\text{H}_{19}\text{N}_1\text{O}_{10}\text{Os}_3$: C, 26.54; H, 1.82; N, 1.34%. Found: C, 26.54; H, 1.47; N, 1.12%. IR (ν_{CO}) in CH_2Cl_2 : 2156w, 2126w, 2080s, 2048s, 2023s, 2006m, 1983w, 1952w cm^{-1} . ^1H NMR of **48** at 400 MHz in CDCl_3 : δ 8.42 (d, H(2)), 7.33 (d, H(4)), 6.78 (7, H(3)), 3.65 (s, H(7)), 2.48 (s, H(5)), 1.713 (s, CH_3), 1.21 (s, OH), 0.989 (s, t-butyl), -17.371 (s, hydride).

Compound **cis-56**: Yield for **cis-56**: 73.1 %. Anal. calcd. for $C_{21}H_{12}N_1O_{10}Os_3$: C, 24.14; H, 1.15; N, 1.33%. Found: C, 24.26; H, 1.03; N, 1.31%. IR (γ CO) in CH_2Cl_2 : 2079s, 2055s, 2024s, 2008m, 1998s, 1972m, 1959m, 1949m cm^{-1} . 1H NMR (Temp.= 25°C) of **cis-49** at 400 MHz in $CDCl_3$: δ 8.45 (dd, H(2)), 7.58 (dd, H(4)), 6.85 (t, H(3)), 4.33 (t, H(6)), 3.61 (br, H(7)), 3.32 & 2.93 (m & dd, CH_2 two protons), 2.46 (q, H(5)), 1.35 (s, t-butyl), -17.335 (s, hydride).

Compound **57i**: Yield for **57i**: %. Anal. calcd. for $C_{21}H_{12}N_1O_{10}Os_3$: C, 24.14; H, 1.15; N, 1.33%. Found: C, 24.26; H, 1.03; N, 1.31%. IR (γ CO) in CH_2Cl_2 : 2079s, 2055s, 2024s, 2008m, 1998s, 1972m, 1959m, 1949m cm^{-1} . 1H NMR of **50** at 400 MHz in $CDCl_3$: δ 8.76 (d, H(2)), 7.15 (d, H(3)), 3.89 (m, H(7)), 3.37 (d, H(5)), 2.72 & 2.37 (dd & dd, H(6) two protons), 1.68 (d, methyl on C(4)), 1.33 (d, methyls on C(5)), -17.012 (s, hydride).

Compound **57h**: Yield for **57h**: %. Anal. calcd. for $C_{21}H_{12}N_1O_{10}Os_3$: C, 24.14; H, 1.15; N, 1.33%. Found: C, 24.26; H, 1.03; N, 1.31%. IR (γ CO) in CH_2Cl_2 : 2079s, 2055s, 2024s, 2008m, 1998s, 1972m, 1959m, 1949m cm^{-1} . 1H NMR of **57h** at 400 MHz in $CDCl_3$: δ 8.34 (d, H(2)), 6.72 (d, H(3)), 5.49-5.71 (m, middle proton on allyls 2 total), 5.21-4.71 (m, terminal allyl protons 4 total), 3.87 (m, H(7)), 3.59 (m, H(5)), 2.77 (dd, H(6)), 2.50-2.25 (m, 1^{st} CH_2 on allyl 4 total), 1.86 (tt, H(6)), -17.073 (s, hydride).

5.10 X-ray Structure Determination of 53-55.

Crystals of 53-55 for X-ray examination were obtained from saturated solutions of each in hexane/dichloromethane solvent systems at -20°C. Suitable crystals of each were mounted on glass fibers, placed in a goniometer head on the Enraf-Nonius CAD4 diffractometer, and centered optically. Unit cell parameters and an orientation matrix for data collection were obtained by using the centering program in the CAD4 system. For each crystal, the actual scan range was calculated by scan width = scan range + 0.35 tan θ and backgrounds were measured by using the moving-crystal moving-counter technique at the beginning and end of each scan. Two representative reflections were monitored every 2 h as a check on instrument and crystal stability. Lorentz, polarization, and decay corrections were applied, as was an empirical absorption correction based on a series of Ψ scans, for each crystal. The weighting Scheme used during refinement was $1/\sigma^2$, based on counting statistics.

Each of the structures was solved by the Patterson method using SHELXS-86,¹¹ which revealed the positions of the metal atoms. All other non-hydrogen atoms were found by successive difference Fourier syntheses. The expected hydride positions in each were calculated by using the program HYDEX,² hydrogen atoms were included in each structure and were placed in their expected chemical positions using the HFIX command in SHELXL-93.¹² The hydrides were given fixed positions and U's; other hydrogen atoms were included as riding atoms in the final least squares refinements with U's which were related to the atoms ridden upon. All other non-hydrogen atoms were refined anisotropically in *trans*-38m, 39n and 39j; however, only the osmium atoms in *cis*-38m could be refined anisotropically due to the poor crystallinity of the sample. In

addition, there was dichloromethane solvent present in the lattice of *trans*-**38m** which could not be modeled precisely.

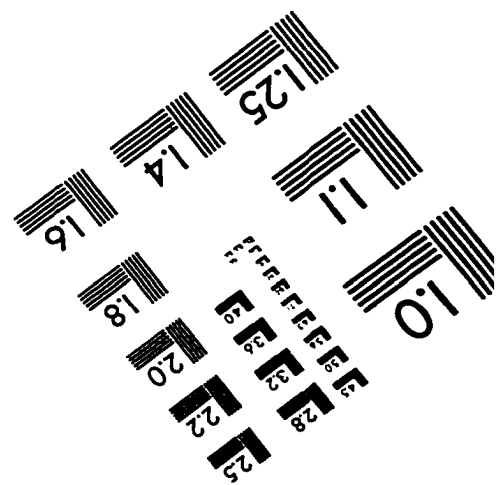
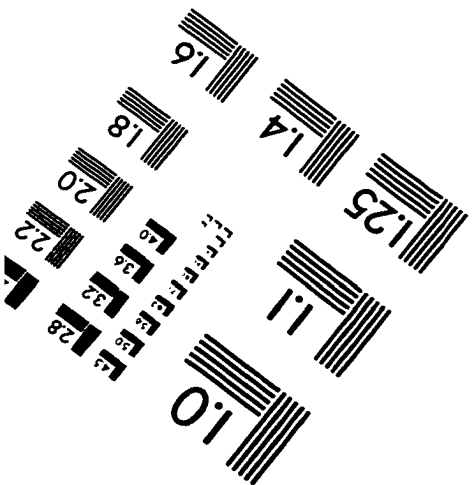
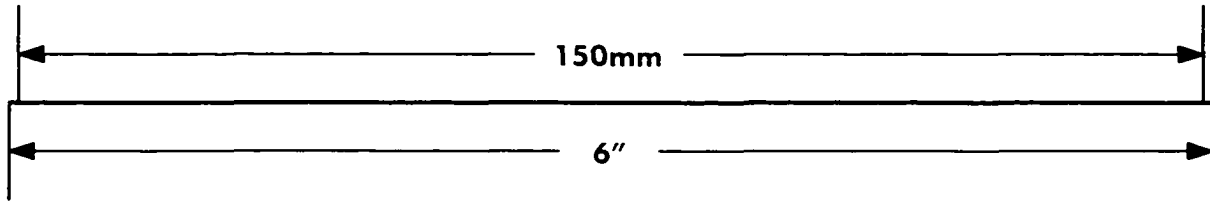
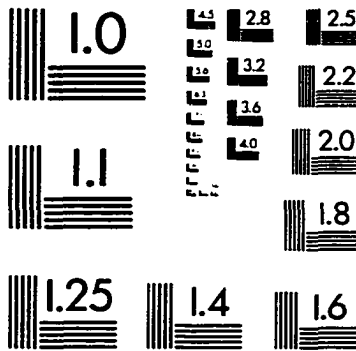
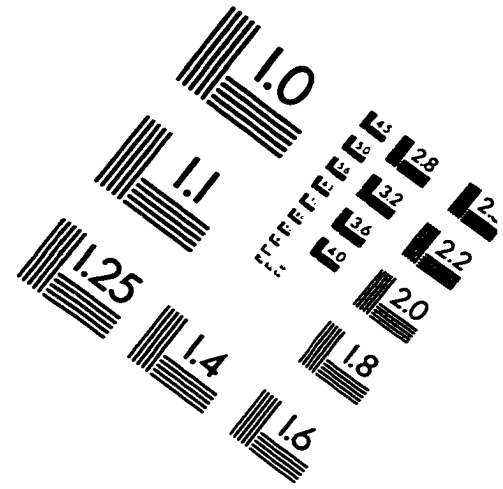
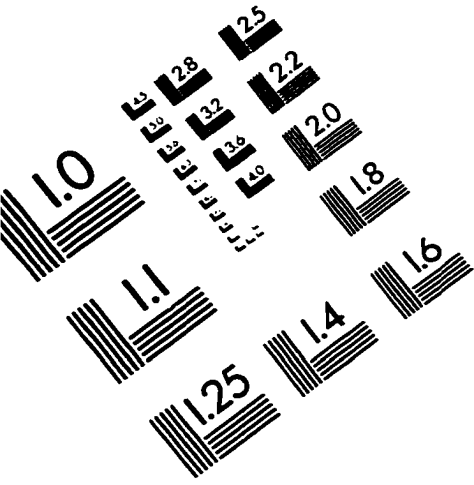
Scattering factors and anomalous dispersion coefficients were taken from International Tables for X-ray Crystallography.¹³ All data processing was carried out on a DEC 3000 AXP computer using the Open MolEN system of programs.¹⁴ Structure solution, refinement and preparation of Figures and tables for publication were carried out on PC's using SHELXS-86,¹¹ SHELXL-93¹² and SHELXTL/PC¹⁵ programs.

5.11 References for Chapter 5

1. Smith, M.B.: "*Organic Synthesis*", McGraw-Hill Inc., New York, **1994**, p13, 636, and 939.
2. Orpen, A.G. *J. Chem. Soc., Dalton Trans.*, **1980**, 2509.
3. Arcia, E.; Kolwaite, D.S.; Rosenberg, E.; Hardcastle, K.I.; Ciurash, J.; Duque, R.; Milone, L.; Gobetto, R.; Osella, D.; Botta, M.; Dastru', W.; Viale, A.; Fiedler, J. *Organometallics*, **1998**, *17*, 415.
4. Kabir, S.E.; Kolwaite, D.S.; Rosenberg, E.; Hardcastle, K.; Cresswell, W.; Grindstaff, J. *Organometallics*, **1995**, *14*, 3611.
5. Semmelhack, M.F. in, "Comprehensive Organometallic Chemistry II, eds. Stone, F.G.A.; Abel, E.; Wilkinson, G.; Elsevier Science, Oxford, 1995, Vol. 12, Chap. 9.1, p979.
6. March, J.; "*Advanced Organic Chemistry -Reactions Mechanisms and Structure 2nd ed.*", John Wiley and Sons, New York, **1992**, p553.

7. Bergman, B.; Rosenberg, E.; Smith, R.; *J. Amer. Chem. Soc.*, **1998**, accepted for publication.
8. Larock, R.; Hightower, T.; *J. Org. Chem.*, **1993**, 58, 5298.
9. Larock, R.; Hightower, T.; Hasvold, L.; Peterson, K.; *J. Org. Chem.*, **1996**, 561 3584.
10. Bar Din, A.; Bergman, B.; Rosenberg, E.; Smith, R.; Dastru, W.; Viale, A.; Milone, L.; Gobetto, R. *Polyhedron*, **1998**, in press.
11. Sheldrick, G.M. *Acta Crystallogr.*, **1990**, A46, 467.
12. Sheldrick, G.M. Program for Structure Refinement, University of Goettingen, Germany, **1993**.
13. Wilson, A.J.C.(ed). *International Tables for X-ray Crystallography, Volume C*. Kluwer Academic Publishers, Dordrecht: Tables 6.1.1.4 (pp 500-502) and 4.2.6.8 (pp 219-222), **1992**.
14. Fair, C. Kay. "MolEN" Structure Determination System, Enraf-Nonius, Delft, The Netherlands . **1990**.
15. SHELXTL/PC, Siemens Analytical X-ray Instruments, Inc., Madison, WI, USA, **1993**.

IMAGE EVALUATION TEST TARGET (QA-3)



APPLIED IMAGE . Inc
 1653 East Main Street
 Rochester, NY 14609 USA
 Phone: 716/482-0300
 Fax: 716/288-5989

© 1993, Applied Image, Inc., All Rights Reserved